EG&G Idaho, Inc.

FORM EG&G-398
(Rev. 05-79)

INTERIM REPORT

Accession No. _____

Report No. EGG-TFBP-5218

Contract Program or Project Title:

Thermal Fuels Behavior Program

Subject of this Document:

Power-Cooling-Mismatch Test Series, Test PCM-7, Quick Look Report

Type of Document:

Quick Look Report

Author(s):

D. T. Sparks, N. T. LeFebre

Date of Document:

August 1980

Responsible NRC Individual and NRC Office or Division:

M. L. Picklesimer

This document was prepared primarily for preliminary or internal use. It has not received full review and approval. Since there may be substantive changes, this document should not be considered final.

EG&G Idaho, Inc.
Idaho Falls, Idaho 83401

Prepared for the
U.S. Nuclear Regulatory Commission
Washington, D.C.
Under DOE Contract No. DE-AC07-76ID01570
NRC FIN No.
A 6041

INTERIM REPORT

8009100412

EGG-TFBP-5218
August 1980

POWER-COOLING-MISMATCH TEST SERIES
TEST PCM-7
QUICK LOOK REPORT

By

D. T. Sparks
N. T. LeFebre

Approved:

RR Hobbins
for R. K. McCardell, Manager
PBF Experiment Specification and Analysis Branch

RR Hobbins
for P. E. MacDonald, Manager
LWR Fuel Research Division

Thermal Fuels Behavior Program
EG&G Idaho, Inc.

CONTENTS

FIGURES

TABLES

SUMMARY

The Power-Cooling-Mismatch (PCM) Test PCM-7 was performed as part of the Thermal Fuels Behavior Program conducted by EG&G Idaho, Inc., for the U. S. Nuclear Regulatory Commission. This test was one of a series of PCM tests designed to characterize the behavior of light water reactor type fuel rods operating under power-coolant imbalance conditions. The primary objective of Test PCM-7 was to subject a nine-rod fuel bundle to stable film boiling conditions to investigate the potential for film boiling and rod failure propagation by allowing the test bundle to remain in film boiling for a period of time. The applicability of the previously established PCM single-rod data base to multiple-rod geometries was of fundamental interest.

Test PCM-7 incorporated nine pressurized water reactor (PWR) type fuel rods with active fuel lengths of 0.914 m arranged in a 3 x 3 bundle geometry. The test fuel rods were clad with zircaloy-4 and held in position by a series of grid spacers which provided a lattice spacing typical of commercial 15 x 15 PWR fuel bundle assemblies. In this configuration, the environment of the central fuel rod is similar to that expected in a commercial power reactor lattice during PCM conditions.

The test was conducted in three phases; a self powered neutron detector (SPND) calibration phase, a power calibration-conditioning phase, and a post boiling transition phase. During the latter test phase, at least seven of the nine test rods were subjected to high temperature film boiling operation, with measured cladding temperatures of 1025 to 1300 K (peak). The indicated time of high temperature operation ranged from 230 s to a maximum of 1740 s. The estimated time of rod failure was about 1104 s after the first indication of high temperature film boiling operation.

Preliminary interpretation of the Test PCM-7 results does not suggest film boiling propagation within the cluster. Evaluation of rod failure propagation will require posttest examination. Both onset of boiling

transition and quench conditions for Test PCM-7 compare favorably with previous single rod and cluster PCM results. The thermal-hydraulic conditions to initiate film boiling were indistinguishable from the conditions required to quench the fuel rods. This observation suggests that onset of boiling transition and film boiling destabilization proceed along similar paths, with little or no hysteresis.

1. INTRODUCTION

A Power-Cooling-Mismatch Test series is being conducted in the Power Burst Facility (PBF) for the U. S. Nuclear Regulatory Commission to provide modeling and damage information for a spectrum of power-cooling imbalance events. Data from the test series will be used to help evaluate conservatisms in the current thermal margin criteria, and help assess the potential for rod-to-rod interactions during high temperature film boiling operation.

Test PCM-7 was the final experiment in the Power-Cooling-Mismatch Test Series. The specific objectives of the test were to evaluate the potential for film boiling and rod failure propagation within a nine-rod cluster geometry. The testing also provided an opportunity to compare the conditions at onset of boiling transition and quench with previous PCM test results.[1]

The Test PCM-7 fuel assembly consisted of nine unirradiated Pressurized Water Reactor (PWR) type fuel rods arranged in a 3 x 3 lattice and situated in a common zircaloy flow shroud. The test rods active fuel lengths were 0.914 m. The rods were held in position by a series of five grid spacers with rod-to-rod spacings typical of a commercial 15 x 15 PWR fuel bundle. The rods were backfilled with helium to a cold pressure of 2.58 MPa. Nominal UO_2 fuel enrichments were 93, 35, and 20 wt% U-235 for the center, side and corner rods, respectively.

Test PCM-7 was conducted in three primary phases. The first phase, the SPND calibration phase, included 2.5 hours of low power operation to provide data for a calibration of the test train self powered neutron detectors in the PBF. The second phase, the power calibration and conditioning phase, included 30 hours of nuclear operation with individual test rod peak powers up to 57 kW/m, to provide heat balance information and allow pellet cracking and relocation in the fuel rods. The third phase, the boiling transition phase, consisted of two flow reduction and one power increase PCM transients. The flow reduction transients provided the

conditions at the onset of film boiling at test peak rod powers of about 53 kW/m. The final transient, initiated by a power increase from 30 to 55 kW/m peak rod power, provided information on the onset of film boiling, the potential for rod-to-rod film boiling and failure propagation, and rod-to-rod interactions. The final transient was terminated by a flow increase to allow evaluation of quench and rewet in the cluster. The testing was completed on July 11, 1980.

A detailed description of the experiment configuration and conduct is presented in Section 2. Preliminary test results are described in Section 3. A summary of the Test PCM-7 results and observations is contained in Section 4. Appendix A contains on-line data plots (unqualified) of the important parameters for the final boiling transition testing phase.

2. EXPERIMENT DESCRIPTION

Test PCM-7 was conducted to provide film boiling and rod failure propagation information in a small cluster geometry. The experiment also provided comparison data for evaluation of the current thermal margin licensing criteria, and a comparison with previous single rod and cluster film boiling results. This section describes the experiment configuration and test conduct for Test PCM-7.

2.1 Experiment Configuration

The Test PCM-7 fuel rods were similar in construction to commercial PWR fuel rods, except for the active fuel length (0.914 m) and fuel enrichments. Nominal fuel pellet enrichments of 93, 35, and 20 wt% U-235 for the center, side and corner rods, respectively, were chosen to provide a relatively flat rod-to-rod power distribution. The nine test rods were arranged in a 3 x 3 array with an assembly pitch typical of a 15 x 15 PWR fuel bundle. Nominal design characteristics of the test fuel rods are listed in Table 1.

The nine fuel rods were positioned in a Zircaloy-4 shroud and held in place by a series of five grid spacers. The grid spacers were positioned along the fuel rod length as indicated in Figure 1. The axial spacing between the third and fourth spacers (from the bottom) was designed to eliminate spacer influence on the hot region of the fuel rods. The distance between the third and fourth spacers was 58.9 cm. The rods were nchored at the lower end and free at the top to allow for axial expansion. Above the fuel rods and shroud was an upper plenum region which contained a fragment screen to inhibit fuel and cladding washout in the event of rod breakup. An orifice plate in the lower assembly was positioned to provide the required flow split between the flow shroud and bypass region (the area between the flow shroud and in-pile flow tube). The lower plenum region contained a catch basket to constrain fuel and cladding pieces in the event of test rod breakup.

TABLE 1. NOMINAL DESIGN CHARACTERISTICS OF
PWR-TYPE FUEL RODS FOR TEST PCM-7

Rod Parameter	Value		
Cladding outside diameter (mm)	10.72		
Cladding inside diameter (mm)	9.50		
Wall thickness (mm)	0.61		
Fuel material	UO_2		
Pellet enrichment (wt% U-235)	93.15 (center rod)	34.87 (side rods)	19.87 (corner rods)
Cladding material	Zircaloy-4		
Fuel density (g/cm^3)	10.14 (center rod)	10.22 (side rods)	10.23 (corner rods)
Pellet diameter (mm)	9.30		
Pellet shape	Dished		
Pellet length (mm)	15.5		
Fuel stack length (mm)	914.4		
Plenum length (mm)	50.3		
Plenum spring	Cr-V alloy		
Fill gas	helium		
Internal pressure (MPa)	2.585		

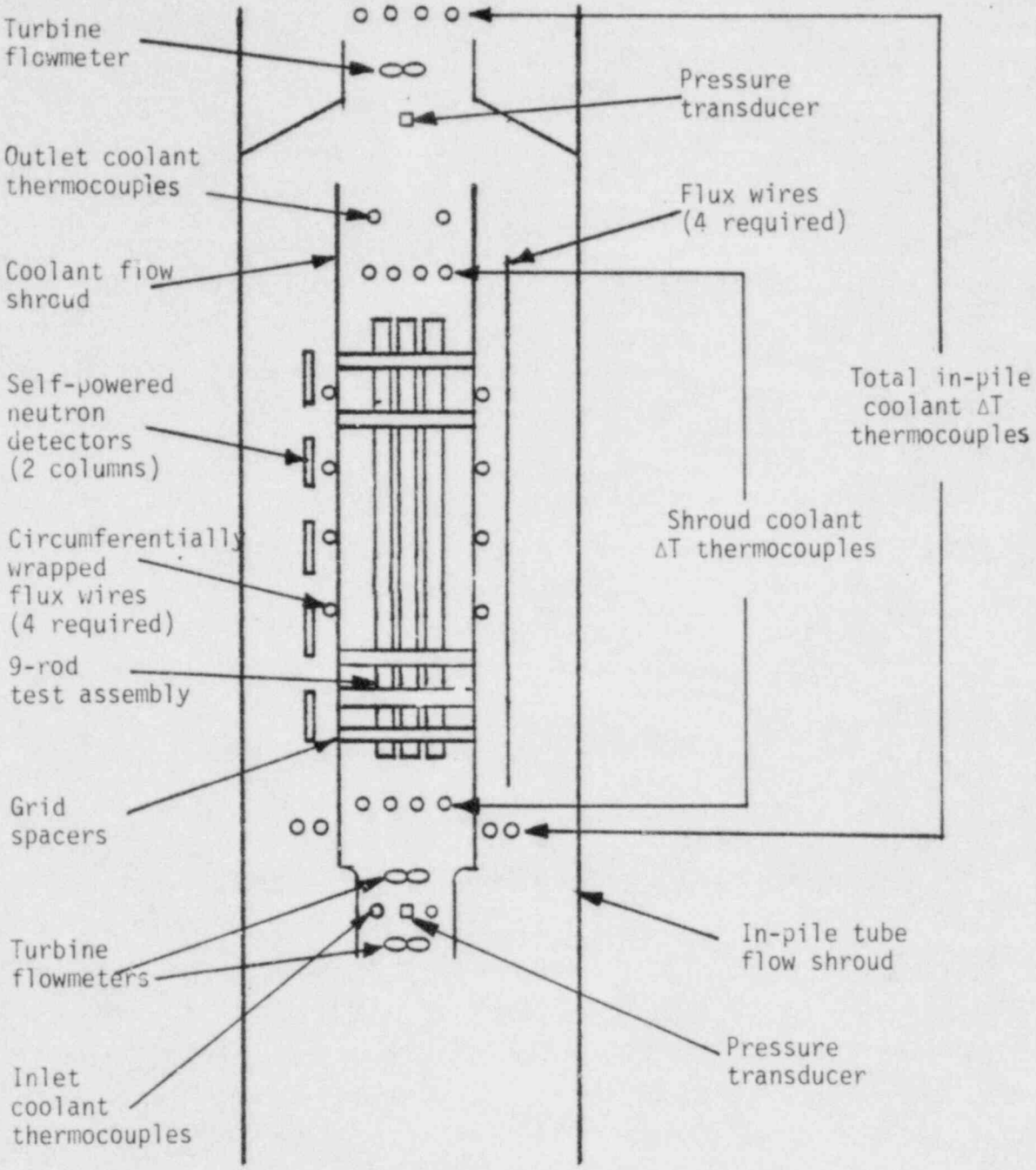

Figure 1. Schematic of the Test PCM-7 test train assembly showing the relative positions of the fuel rods and test train instrumentation.

The instrumentation associated with the fuel rod cluster and test train are shown in Figures 1 and 2. The test train instrumentation measured the coolant temperature, pressure, flow rate, and local neutron flux. The fuel rods were instrumented in the following manner: Rods 207-1, 207-5 and 207-6 were instrumented for the measurement of internal gas pressure [by means of pressure transducers (PXDs)], fuel centerline temperature, cladding elongation [by means of linear variable differential transformers (LVDTs)], and cladding surface temperatures (Rod 207-5 also contained a thermocouple for measurement of the plenum gas temperature); Rods 207-7 and 207-8 were instrumented to measure cladding elongation; and Rods 207-2, 207-3, 207-4 and 207-9 were instrumented for cladding surface temperature measurements.

2.2 Test Conduct

Nuclear operation for Test PCM-7 included three primary test phases; an SPND calibration phase, a power calibration-conditioning phase, and a boiling transition phase. Details of each test phase are presented in this section.

2.2.1 SPND Calibration

The objective of the SPND calibration was to provide an in-situ calibration of the relative sensitivities of the two self powered neutron detector columns (5 each). The 2.5 hour calibration was performed at hot (~600 K) pressurized (15.4 MPa) conditions and constant test rod power of 14 kW/m. Following 2.5 hours at constant power, the reactor was shut down and two of the cobalt-aluminum flux wires positioned axially on the outside of the flow shroud were removed. The SPND current from each detector will be integrated and compared to the flux wire results to determine the relative neutron sensitivity of each SPND. The power and coolant conditions during the SPND calibration are shown in Figure 3. Figure 4 illustrates the axial power profile determined from the Co-Al flux wire scans during the SPND calibration phase. The normalized, uncorrected SPND

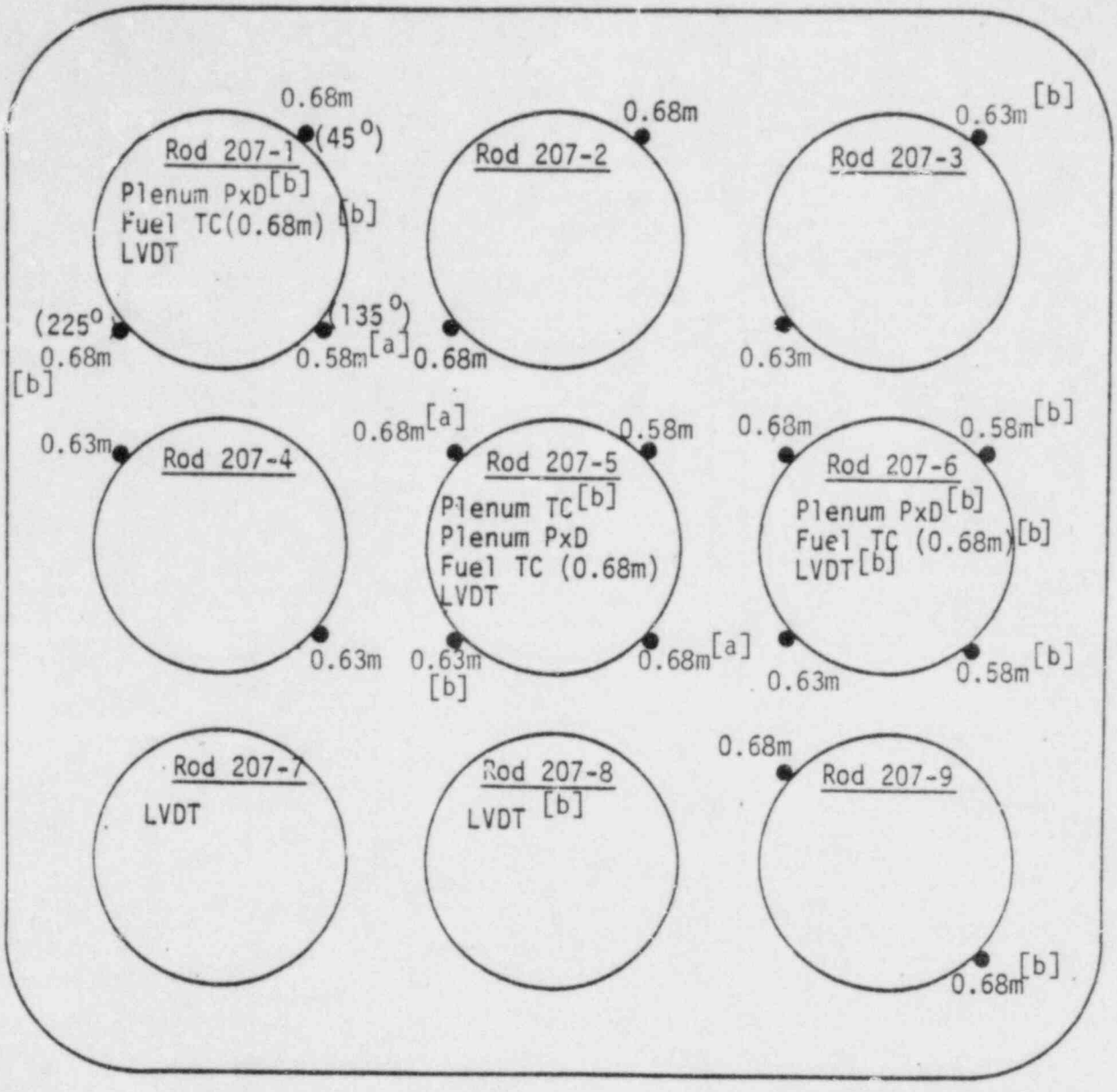

[a] Indicates location of the small diameter (0.71 mm) thermocouples

[b] Instrument failed

Figure 2. Schematic of Test PCM-7 nine-rod cluster, showing the locations of the fuel rod instrumentation with respect to the bottom of the fuel stack.

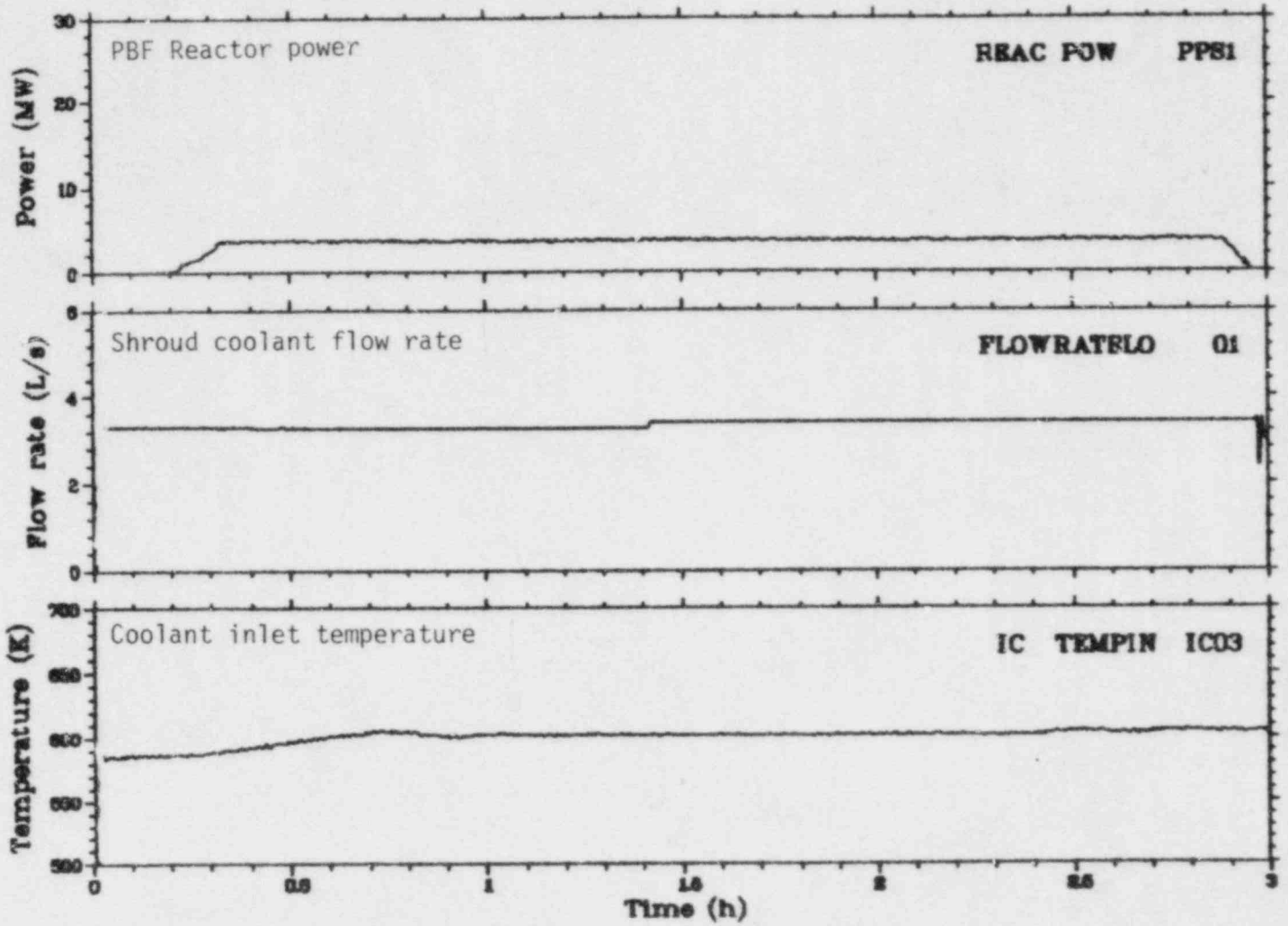

Figure 3. Reactor power and test train coolant conditions during Test PCM-7 SPND calibration phase.

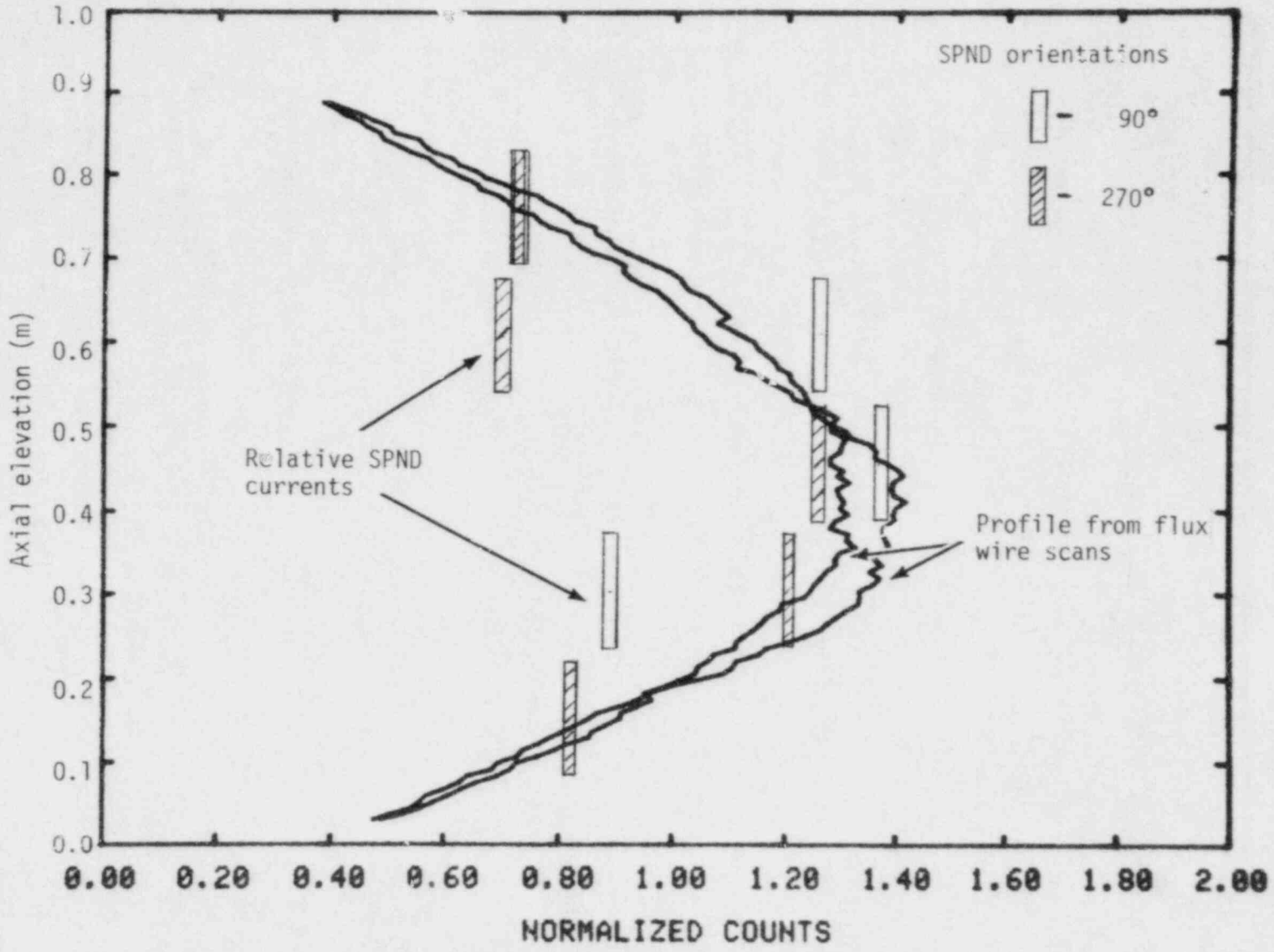

Figure 4. Relative SPND currents (uncorrected) and axial power profile determined from flux wire scans for SPND calibration test phase.

values are also shown for the nine operable SPNDs. By correcting the relative sensitivity of each SPND to the correct axial power profile, the SPNDs can be used to determine the instantaneous power profile during Test PCM-7.

2.2.2 Power Calibration-Conditioning

The objectives of the power calibration-conditioning test phase were to relate the overall cluster power generation to reactor core power and the SPNDs output, and to allow pellet cracking and relocation in the rods. An overall heat balance of the cluster was obtained using measured coolant inlet conditions (pressure and temperature), inlet coolant volumetric flow rate, and temperature rise across the assembly. Since two-phase coolant conditions were expected at the flow shroud exit during portions of Test PCM-7, approximately 70% of the inlet coolant was bypassed around the shroud and recombined with the shroud exit water to yield a subcooled coolant mixture in the upper plenum region. Measurement of recombined flow and temperature rise in conjuction with shroud flow and temperature rise measurements under subcooled conditions, provided an intercalibration of bundle powers between the two methods. A calorimetric heat balance of the cluster was thereby obtained during the entire Test PCM-7 operation. The power and coolant conditions during the power calibration and conditioning phase are shown in Figure 5.

Table 2 presents a summary of power and coolant conditions at representative levels during the Test PCM-7 power calibration-conditioning phase. Since the flowmeter to measure the recombined coolant flow rate at the outlet of the test assembly (see Figure 1) failed early in the testing, an intercalibration of shroud and assembly bundle powers required the use of a flowmeter in the IPT inlet piping (IC FLOW IN IC-01). Since some leakage occurred between the inlet flowmeter location and the inlet to the test assembly, a correction to the assembly powers was applied. The basis for the correction was at least squares linear regression of powers determined from the shroud instrumentation (flow rate and coolant

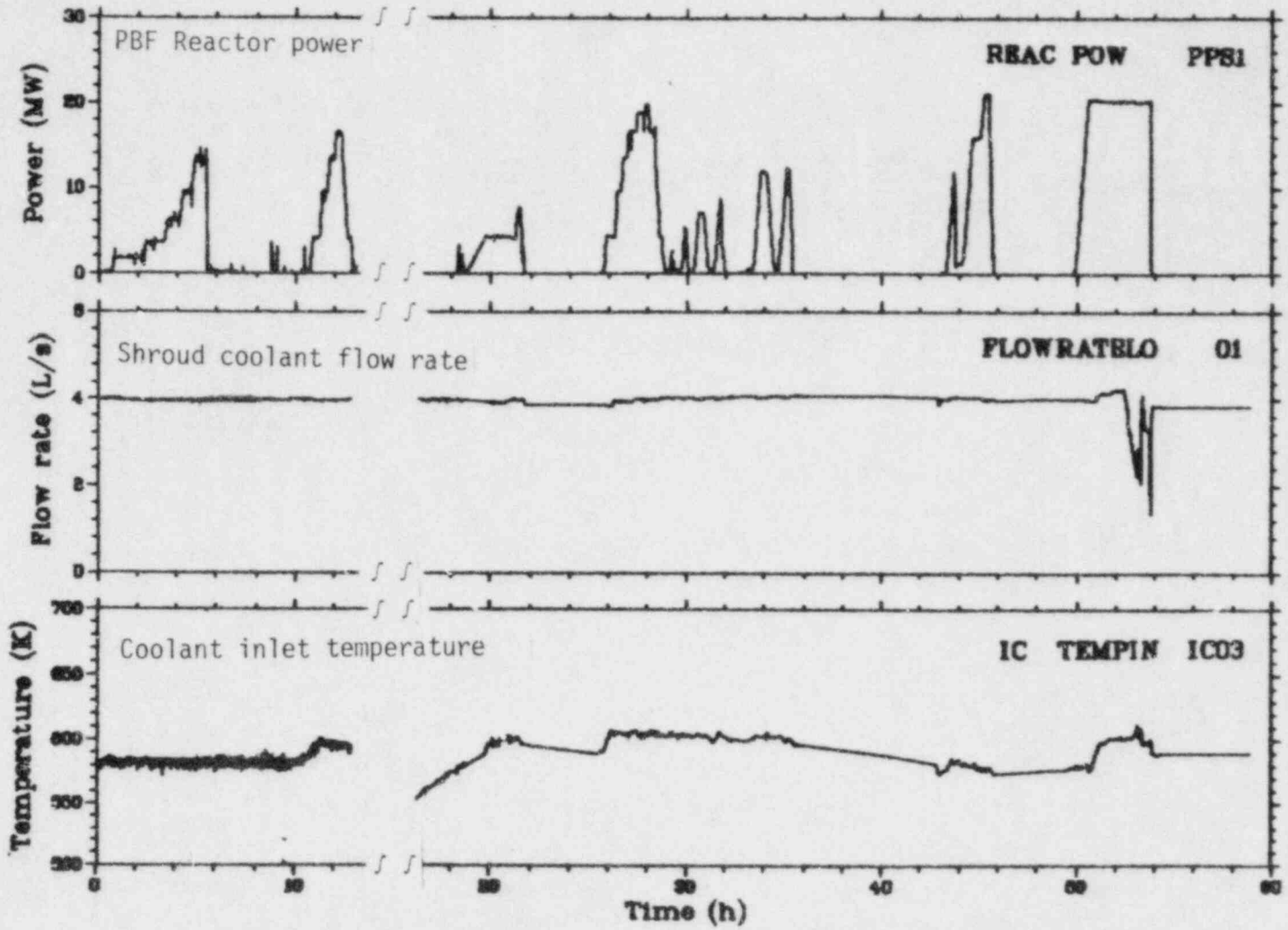

Figure 5. Reactor power and test train coolant conditions during Test PCM-7 power calibration-conditioning phase.

TABLE 2. REPRESENTATIVE POWER AND COOLANT CONDITIONS DURING TEST PCM-7 POWER CALIBRATION CONDITION PHASE

Reactor Power (MW)	Coolant Inlet Temperature (K)	Shroud Flow Rate (L/s)	IPT Inlet Flow Rate (L/s)	"Shroud" Test Rod Peak Power[a] (kW/m)	"IPT Inlet" Test Rod Peak Power[b] (kW/m)
1.63	580	4.02	15.47	6.34	6.07
3.57	581	3.99	15.40	12.88	13.47
6.24	580	3.98	15.30	21.42	21.59
9.36	580	3.98	15.34	30.71	31.25
12.88	580	3.97	15.31	40.77	41.72
4.06	589	4.00	15.33	13.62	13.56
9.39	597	3.99	15.38	29.74	30.92
13.15	590	3.99	15.31	37.82	39.15
16.24	594	3.98	15.33	48.19	48.59
9.74	593	4.00	15.42	30.32	30.92
7.69	600	3.98	15.19	26.42	26.18
4.26	594	3.86	14.63	14.90	13.52
8.52	604	3.94	15.03	29.28	26.45
13.09	604	3.97	15.08	42.64	41.44
16.35	603	3.96	15.00	48.75	49.57
18.53	604	4.01	15.24	c	55.40
19.51	603	4.00	15.18	c	57.06
16.32	604	4.01	15.22	45.99	48.89
8.64	602	4.02	15.29	29.03	26.84
11.66	601	4.05	15.29	37.19	35.25
20.78	585	3.99	14.81	58.80	57.78

a. Weighted individual rod power at peak elevation determined from shroud coolant flow rate and shroud coolant temperature rise. (1.36 peak to average power profile assumed).

b. Weighted individual peak rod power at peak elevation determined from IPT inlet flow rate and overall assembly coolant temperature rise. Value corrected for leakage by regression with "shroud" power: Test rod power = -0.1082 + 0.8544 (uncorrected "IPT Inlet" power).

c. Shroud coolant temperature rise not useable due to saturated outlet coolant conditions.

temperature rise) with powers determined using the inlet (IPT) flowmeter and overall assembly temperature rise. The methods used to calorimetrically determine the Test PCM-7 fuel rod powers are documented in Reference 1.

2.2.3 Boiling Transition Testing

The objectives of the boiling transition testing were to evaluate the potential for film boiling and rod failure propagation in a small cluster geometry. Additionally, data on the conditions at the onset of boiling transition and quench were obtained for direct comparison with previous PCM test results. The final boiling transition test phase was preceded by two scoping flow reductions at constant power (53 kW/m) to determine the coolant flow rate at the onset of boiling transition. The flow rate was then established at the lower value observed to initiate film boiling, and the power increased from 30 to 55 kW/m (~4 kW/m per minute ramp) to initiate the final boiling transition test phase.

During the two scoping flow reductions, boiling transition was induced by small incremental flow reductions (~3%) at constant test rod power (~53 kW/m). The power was decreased to rewet the rods after indication of boiling transition. Boiling transition was detected on the center fuel rod (Rod 207-5) at a shroud coolant volumetric flow rate of 1.1 and 1.3 L/s (597 and 689 kg/s$\cdot$m^2 coolant mass flux) during the first and second scoping flow reductions, respectively. Figure 6 shows the power and inlet coolant conditions during the scoping flow reduction cycles.

The primary fuel rod response information from Test PCM-7 was obtained during the final boiling transition cycle. The shroud coolant flow rate was established at 1.1 L/s (576 kg/s$\cdot$m^2 mass flux) at an inlet temperature of 602 K and system pressure of 15.3 MPa. The test rod peak power (weighted) was then increased from 30 to 55 kW/m at a rate of 4.0 kW/m per minute to induce boiling transition. Power was held constant during the remainder of the transient. The test rods were allowed to remain in high temperature film boiling for several minutes beyond detection of fuel rod failure. The "borderline" film boiling conditions and the extended high temperature operation will allow evaluation of film

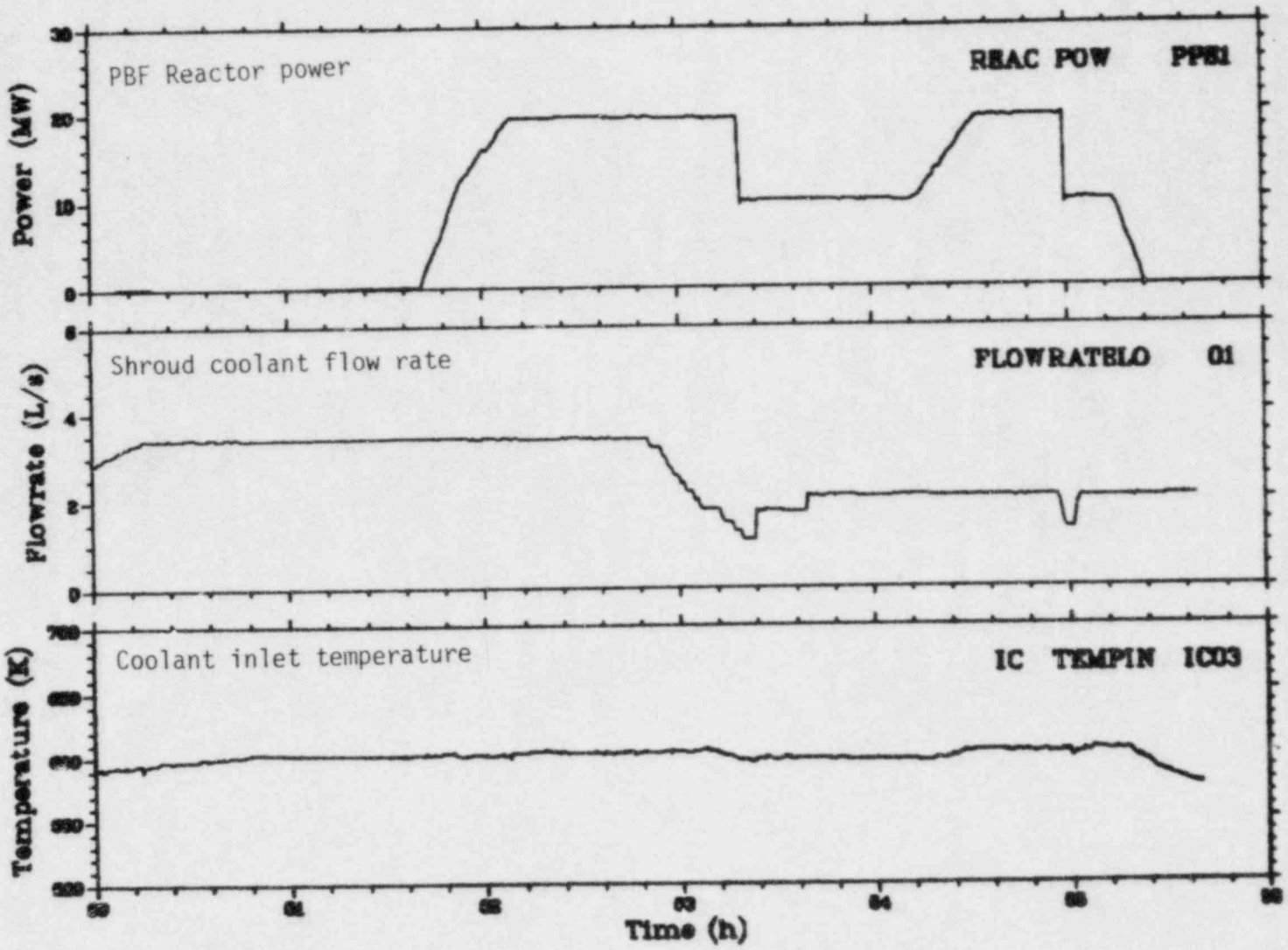

Figure 6. Reactor power and test train coolant conditions during Test PCM-7 scoping flow reduction cycles.

boiling and fuel rod failure propagation from on-line data analysis and posttest metallurgical examination. The coolant flow rate was increased to rewet the fuel rods and provide information on quench from film boiling conditions. The test conditions during the final boiling transition test phase are depicted in Figure 7, where zero time is an arbitrary reference time corresponding to the first indication of boiling transition in the cluster.

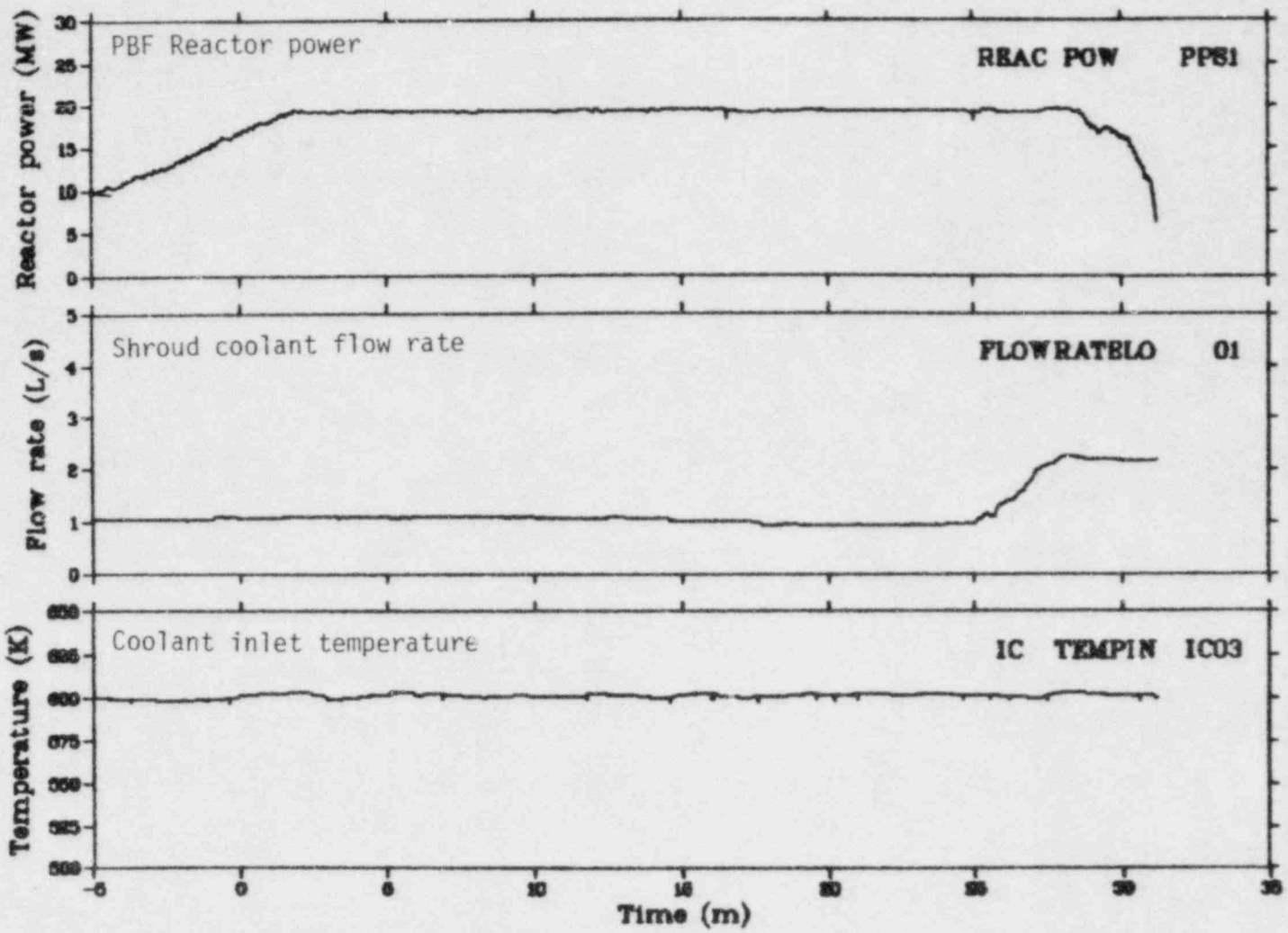

Figure 7. Reactor power and test train coolant conditions during Test PCM-7 final boiling transition test phase.

3. TEST RESULTS

The preliminary results from Test PCM-7 are presented in this section. Primary emphasis is placed on the conditions at onset of boiling transition and quench, the potential for rod-to-rod interactions, and the fuel rod behavior during the final boiling transition testing phase. A comparison of Test PCM-7 results with previous PCM test results is also presented.

3.1 Boiling Transition

The conditions at onset of boiling transition and the fuel rod behavior during the post-boiling transition phase of Test PCM-7 are described in this section. Boiling transition was detectable by means of cladding thermocouples, which indicate high temperature thermal excursions resulting from film boiling, and linear variable differential transformers (LVDTs) which measure fuel rod displacement resulting from high temperature thermal expansion.

3.1.1 Conditions at Onset of Boiling Transition

Boiling transition was first detected within the nine-rod bundle during the two scoping flow reduction cycles. Film boiling was induced by small incremental flow reductions (~3%) at constant test rod power. During the first scoping flow reduction, boiling transition was detected on the center rod (Rod 207-5). The rod remained in film boiling approximately 30 s and attained a maximum measured cladding surface temperature of 880 K. During the second scoping flow reduction, two rods (Rods 207-2 and 207-5) experienced boiling transition. For both cycles, power was rapidly reduced to terminate the transient. The fuel rod peak powers and bundle coolant mass flux at onset of boiling transition for the two scoping flow reductions are summarized in Table 3.

The final boiling transition cycle was initiated by increasing the PBF driver core power and thus test rod power. The test rod peak power

TABLE 3. SUMMARY OF BOILING TRANSITION (BT) RESULTS FOR TEST PCM-7 SCOPING CYCLES

Fuel Rod	Fuel Rod Peak Power at BT (kW/m)	Bundle Coolant Mass Flux at Onset of BT ($kg/s \cdot m^2$)	Total Time In Film Boiling (s)	Maximum Indicated Cladding Surface Temperature (K)
Scoping #1				
207-5	52.38	597	30	878
Scoping #2				
207-2	52.66	700	30	700
207-5	52.42	689	63	1010

(weighted) was increased from 30 to 55 kW/m at a rate of 4.0 kW/m per minute. The bundle coolant flow rate was held constant during the power increase at approximately 1.1 L/s (576 kg/s·m^2 coolant mass flux). A nominal system pressure of 15.4 MPa and coolant inlet temperature of ~602 K were maintained during the transient. Approximately 9 minutes after the first indication of boiling transition, the coolant flow rate was reduced in ~3% increments to a final value of 0.95 L/s. The flow was subsequently increased to rewet the fuel rods and conclude the experiment.

During the final boiling transition cycle, the center rod (207-5) was the first within the bundle to commence film boiling operation. The bundle was allowed to continue high temperature operation for about 24 minutes after the first indication of film boiling. At least seven of the nine rods attained film boiling during the transient. Rod failure was detected by the fission product detection system (FPDS) about 22.6 minutes after the first indication of film boiling. By estimating the inherent delay between rod failure and detection of failure by the FPDS (about 4.2 minutes), the time of rod failure was estimated to be 18.4 minutes after the first indication of film boiling. A summary of the film boiling history for Test PCM-7 is shown in Figure 8.

Figures 9, 10, 11, and 12 illustrate the measured temperatures at three elevations during the film boiling phase of Test PCM-7. The high temperature thermal excursions are indicative of local film boiling operation. The first indication of film boiling within the test bundle was at the 0.68-m elevation on center Rod 207-5, followed by periods of film boiling on six other rods at the various measurement elevations.

A composite of the fuel rod displacement measurements obtained during Test PCM-7 is presented in Figure 13. During periods of fuel rod heatup caused by high temperature operation, the rods thermally elongate as indicated by the cladding displacement curves. Fuel Rods 207-1 and 207-5 experienced 0.13% and 0.21% cladding elongation, respectively. Essentially no change in length was detected on Rod 207-7 by the LVDT. This suggests

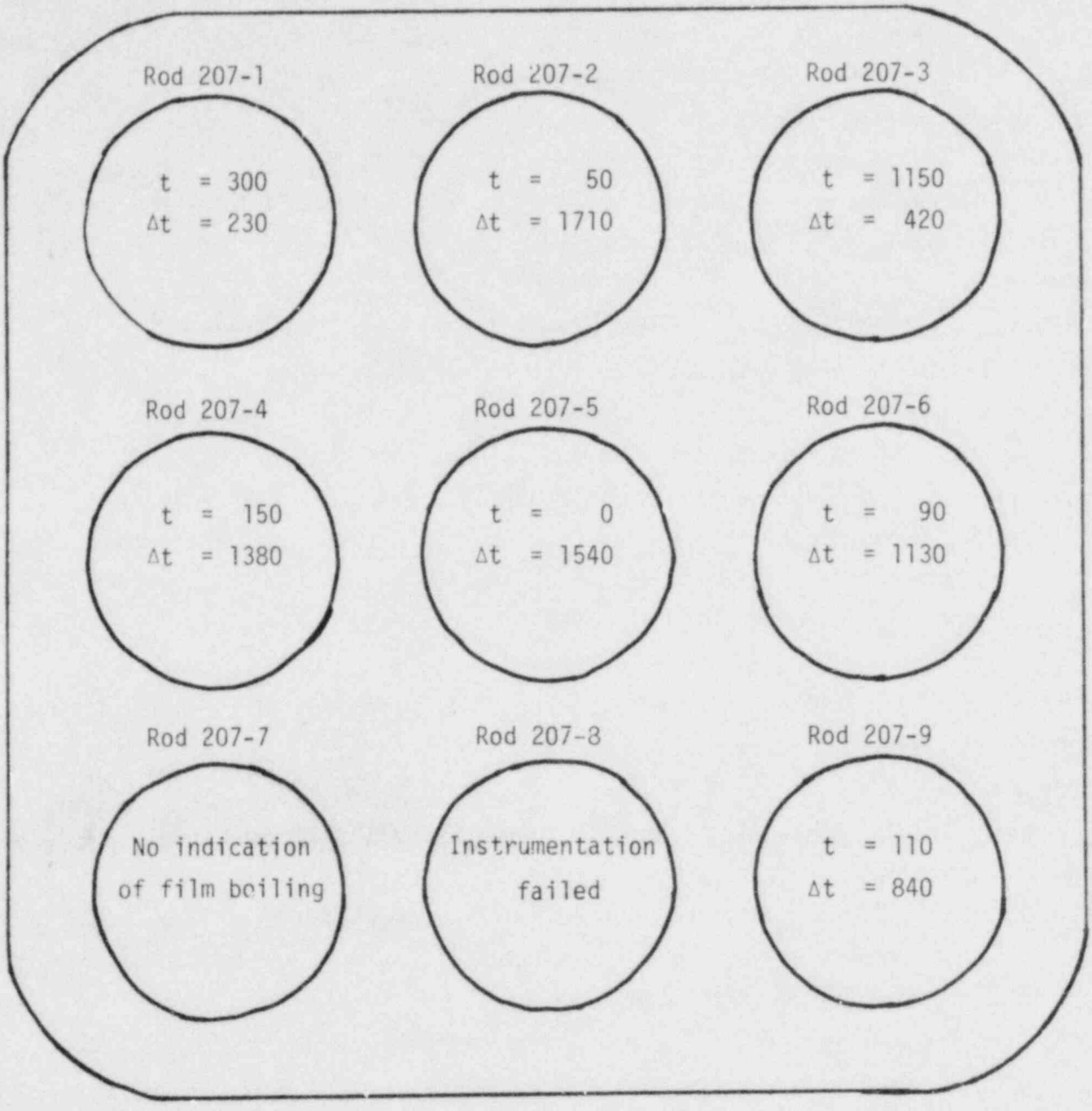

t = time (s) at first indication of film boiling

Δt = total period (s) of film boiling

Figure 8. Summary of Test PCM-7 film boiling times during final boiling transition test phase. Time = 0 corresponds to the first indication of boiling transition (Rod 207-5) on July 11, 1980, at 16:41:45.

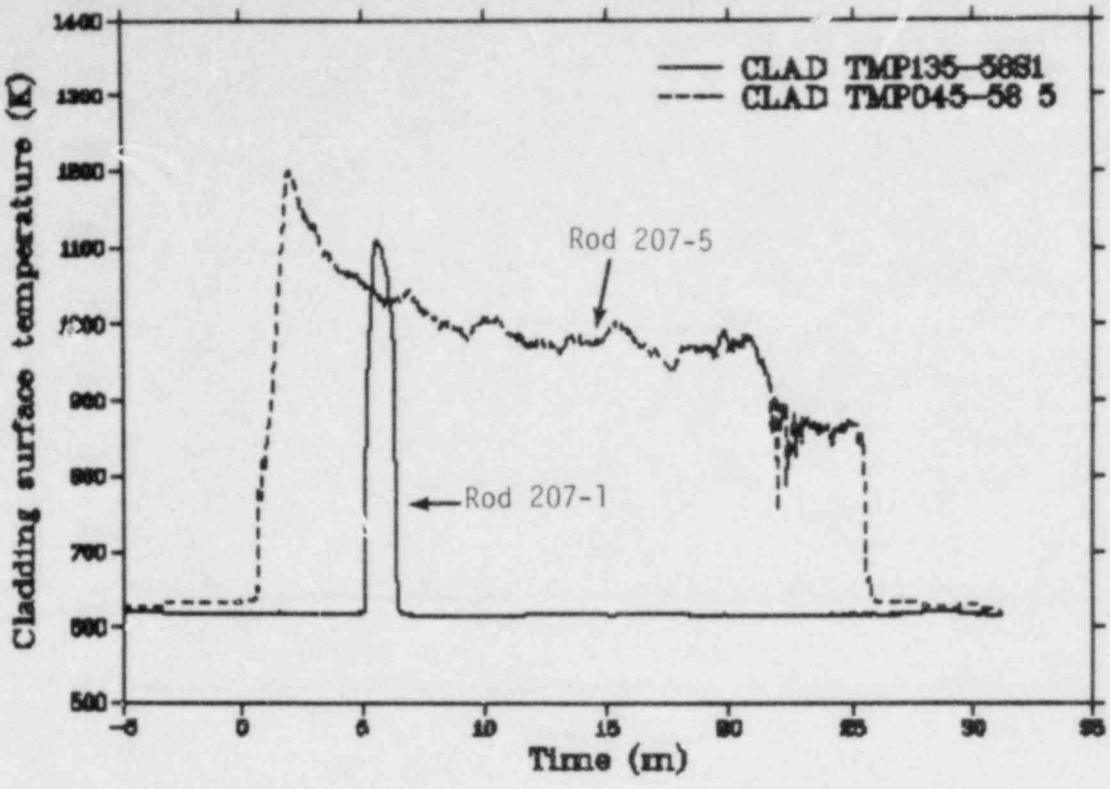

Figure 9. Measured cladding temperature history at the 0.58-m elevation (from bottom of fuel stack) during final boiling transition test phase - Rods 207-1 and -5.

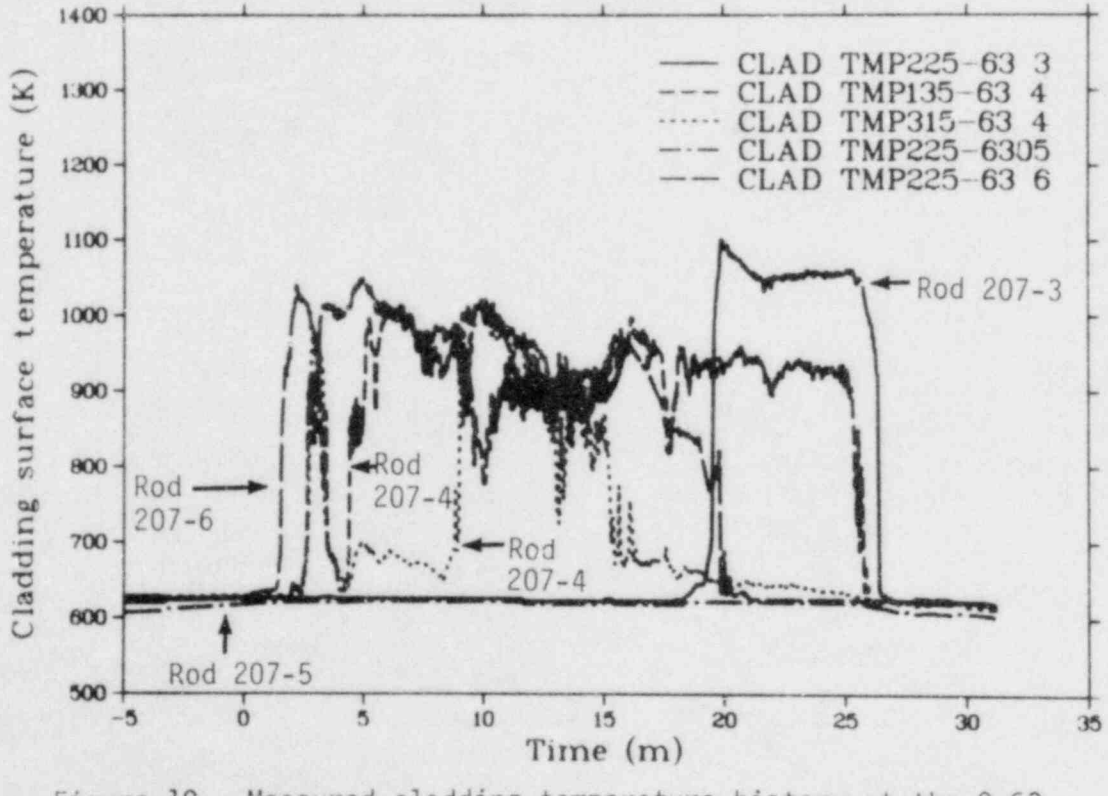

Figure 10. Measured cladding temperature history at the 0.63-m elevation (from bottom of fuel stack) during final boiling transition test phase - Rods 207-3, -4, -5, and -6.

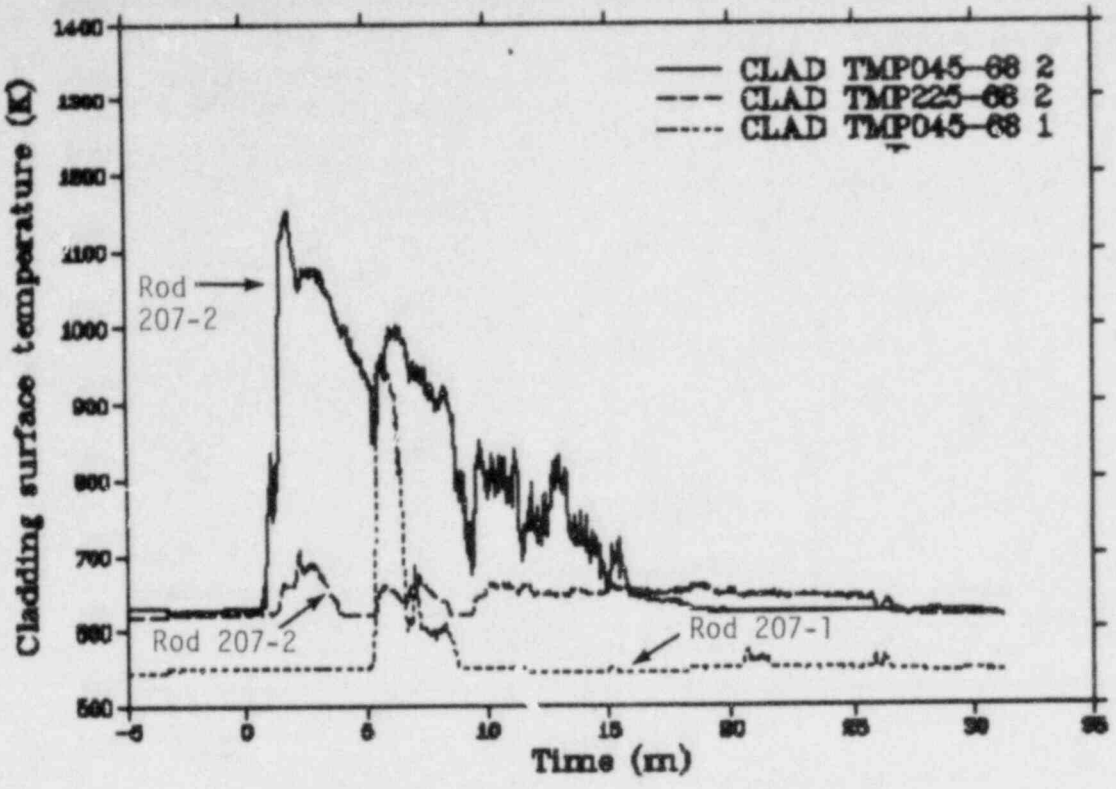

Figure 11. Measured cladding temperature history at the 0.68-m elevation (from bottom of fuel stack) during final boiling transition test phase - Rods 207-1 and -2.

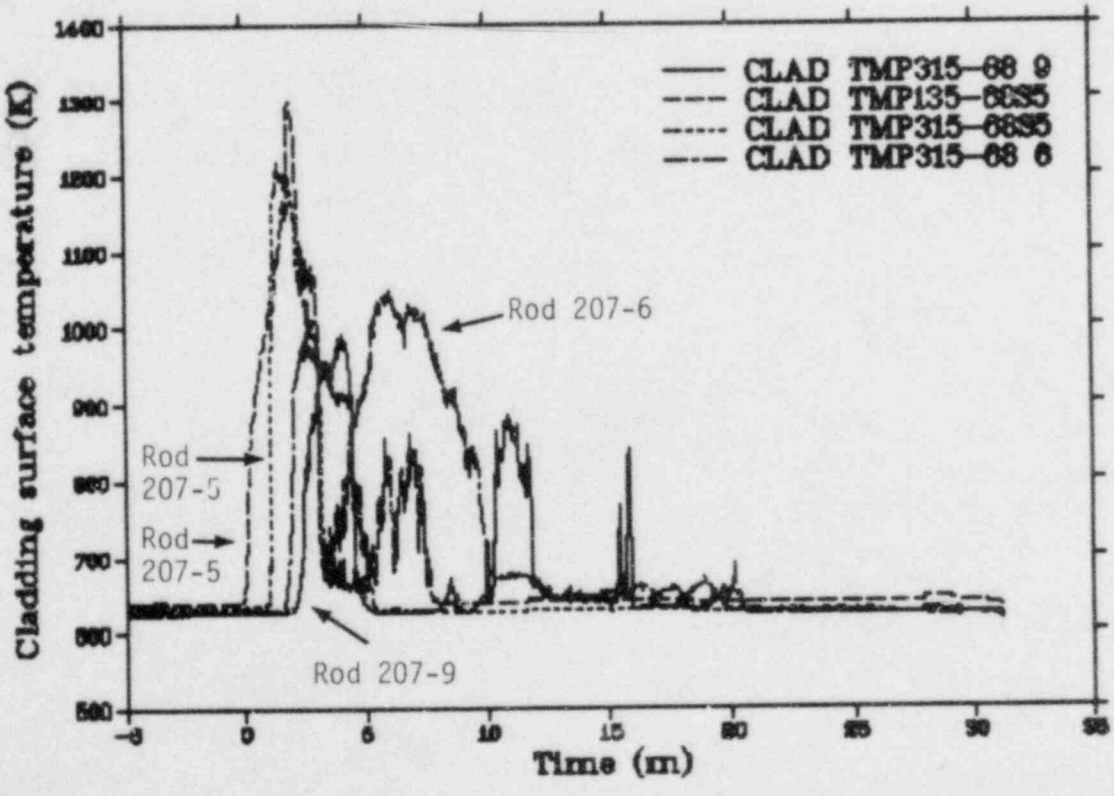

Figure 12. Measured cladding temperature history at the 0.68-m elevation (from bottom of fuel stack) during final boiling transition test phase - Rods 207-5, -6, and -9.

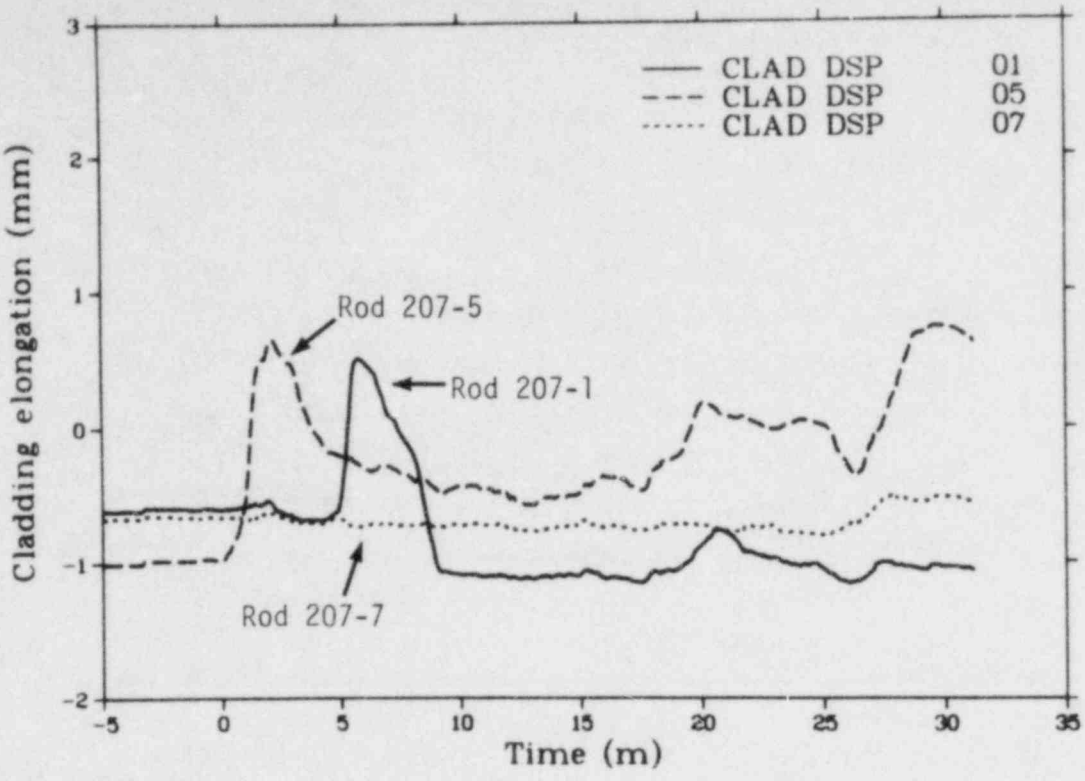

Figure 13. Measured cladding axial displacement during final boiling transition testing showing film boiling response on Rods 207-5 and 207-1, and no film boiling indication on Rod 207-7.

either no boiling transition occurred on Rod 207-7, or that a low temperature thermal excursion over a small axial extent resulted in a negligible increase in rod length.

Table 4 summarizes the data presented in Figures 9 through 13. The peak rod power and the bundle coolant mass flux at the onset of boiling transition are also tabulated for each rod. Rod 207-5 was at a peak rod power of 48.3 kW/m when it first attained film boiling. The majority of the other test rods were at peak rod powers between 53-54 kW/m when boiling transition occurred.

3.1.2 Fuel Rod Behavior

Figure 14 illustrates the approximate film boiling history of the instrumented rods and shows the corresponding PBF power and shroud volumetric flow rate during the final post-boiling transition phase of Test PCM-7. The areas bounded by the differing symbols illustrate approximate elevations and associated times of film boiling operation of the fuel rods. One of the nine rods (Rod 207-7) is not believed to have experienced film boiling based on the LVDT data obtained. The instrumentation capable of detecting film boiling on Rod 207-8 failed prior to the final boiling transition cycle. Therefore, only the seven fuel rods known to have experienced film boiling are illustrated. During the power increase from 10 to 19.5 MW (core power), center Rod 207-5 attained boiling transition and remained in film boiling for approximately 1540 s. While reactor power continued to increase (to 19.5 MW), side Rods 207-2 and 207-6, and corner Rod 207-9 also surpassed boiling transition (~50-110 s). Rods 207-6 and 207-9 operated in film boiling for approximately 1130 and 840 s, respectively. At approximately 120 s, the PBF driver core power reached a maximum of 19.5 MW (55 kW/m weighted test rod peak power). After this time, Rods 207-4, 207-1, and 207-3 commenced film boiling operation. Rod 207-1 operated in film boiling a brief period of time (~230 s) and then rewet. Approximately 1,440 s after the transient was initiated, the coolant flow rate was increased from 0.95 to 2.25 L/s. During the flow increase, all film boiling operation was terminated and the fuel rods rewet.

TABLE 4. SUMMARY OF POST BOILING TRANSITION (BT) RESULTS FOR TEST PCM-7

Fuel Rod	Boiling Transition Occurrence	Fuel Rod Peak Power at BT (kW/m)	Bundle Coolant Mass Flux at Onset of BT ($kg/s \cdot m^2$)	Total Time In Film Boiling (s)	Maximum Indicated Cladding Surface Temperature (K)	Elevation of Maximum Indicated Cladding Temperature (m)	Cladding Elongation After DNB (%)
207-1	yes	55.2	576	230	1120	0.58	0.13
207-2	yes	53.4	597	1710	1155	0.68	a
207-3	yes	53.2	509	420	1100	0.63	a
207-4	yes	52.8	585	1360	1025	0.63	a
207-5	yes	48.3	576	1540	1300	0.68	0.21
207-6	yes	53.3	597	1130	1050	0.63 and 0.68	b
207-7	no	--	--	0	a	a	0
207-8	unknown	--	--	--	a	a	b
207-9	yes	54.0	589	840	1085	0.68	a

a. Fuel rod not instrumented for this measurement.

b. Instrument failed.

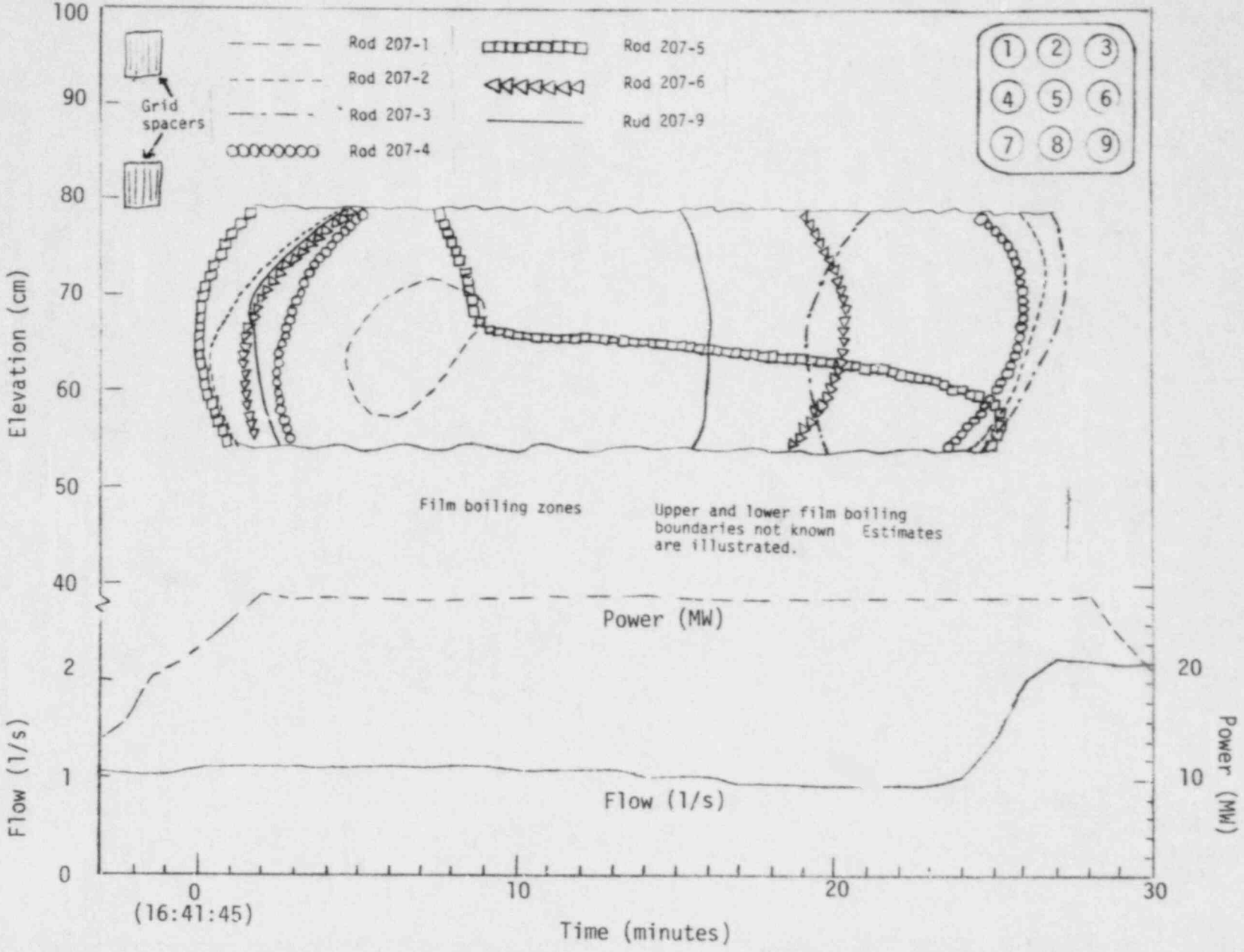

Figure 14. Test PCM-7 fuel rod film boiling histories showing estimated duration and axial extent of film boiling from on-line measurement data.

The influence of PBF power and coolant flow rate on the observed film boiling response of Rod 207-5 at the 0.58- and 0.68-m elevations is presented in Figure 15. As reactor power was increasing, film boiling was detected at the 0.68-m elevation. Approximately 40 s later, the 0.58-m elevation surpassed boiling transition. At about 460 seconds, the thermocouple at the 0.68-m elevation indicated rewet of the rod at that elevation. Cladding temperatures of 1200 to 1220 K were experienced at the 0.68-m elevation. No significant change in power or coolant flow was apparent at the time of quench at the 0.68-m elevation.

High temperature operation at the 0.58-m location continued for the majority of the transient and was not terminated until the coolant flow rate was increased. As shown on Figure 15, a peak measured cladding temperature of approximately 1300 K was attained at the 0.58-m elevation. The fact that the fuel rod power is higher at 0.58 m than 0.68 m could explain the fact that Rod 207-5 remained in film boiling longer at the 0.58-m elevation. In addition, the potential for thermocouple effects at the 0.68-m elevation is greater than at the 0.58-m elevation. Two thermocouple junctions and two thermocouple leads cross the 0.68-m elevation at four circumferential orientations, as opposed to the one thermocouple junction at the 0.58-m location. Thermocouples and lead wires are known to influence cladding temperatures and rewet conditions due to fin cooling effects.

Figure 16 illustrates the PBF reactor power and the shroud coolant flow rate at the time of film boiling operation on Rod 207-1. At the time film boiling commenced on Rod 207-1, the reactor power and coolant flow rate were essentially constant at 19.5 MW (55.2 kW/m peak rod power) and 1.1 L/s, respectively. The fuel rod continued to operate in film boiling for ~230 s, and then quenched at essentially the same conditions. This suggests that Rod 207-1 probably operated in film boiling at the minimal boundary conditions that would initiate boiling transition.

Peak measured cladding temperatures on the seven fuel rods known to have operated in film boiling ranged from 1025 to 1300 K. Rod 207-5 was the hottest at approximately 1300 K. The maximum indicated cladding

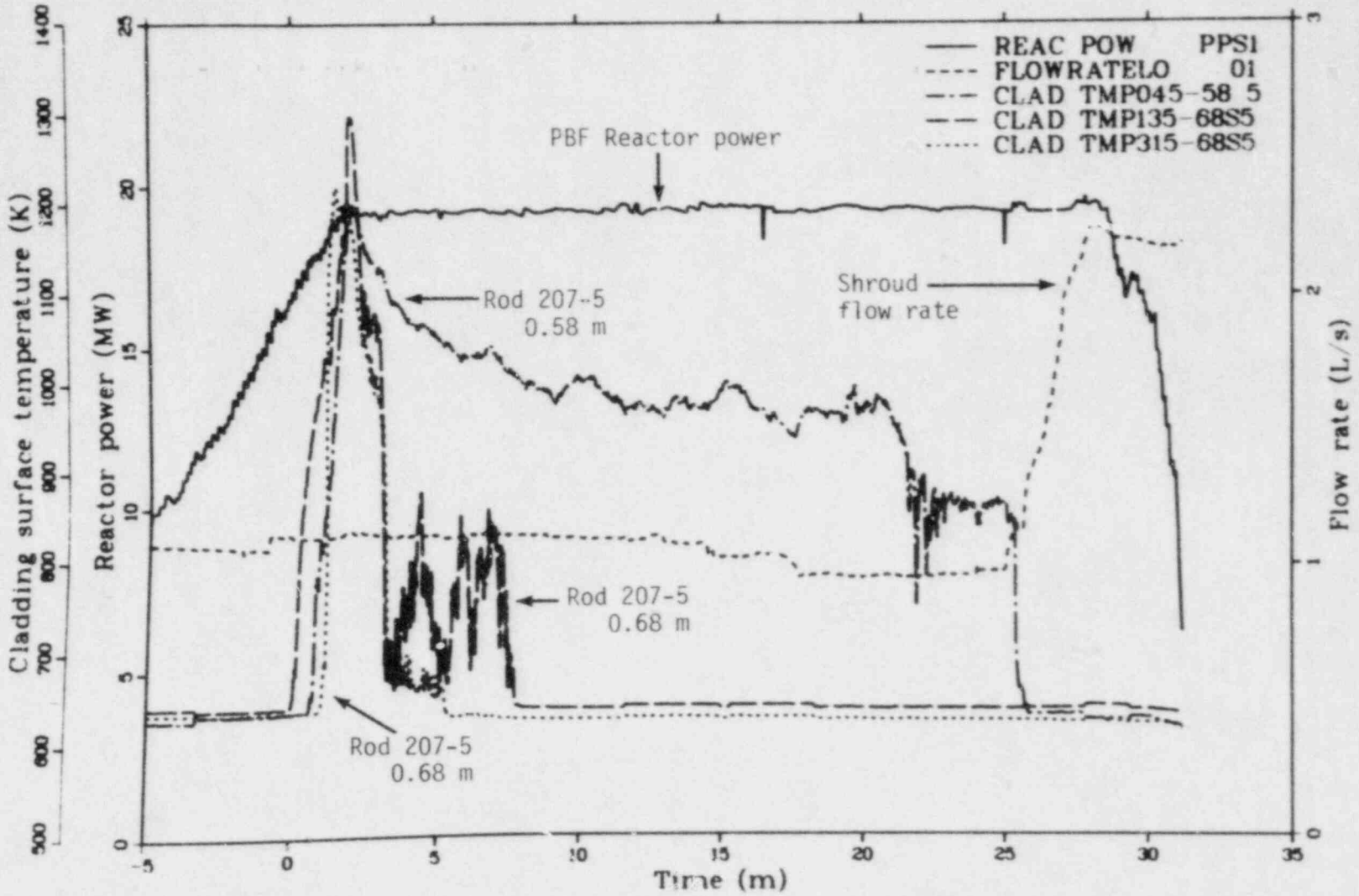

Figure 15. Reactor power, shroud flow rate, and measured cladding surface temperatures for Rod 207-5 at the 0.58- and 0.68-m elevations illustrating rewet at the 0.68-m elevation and continued film boiling operation at the 0.58-m elevation.

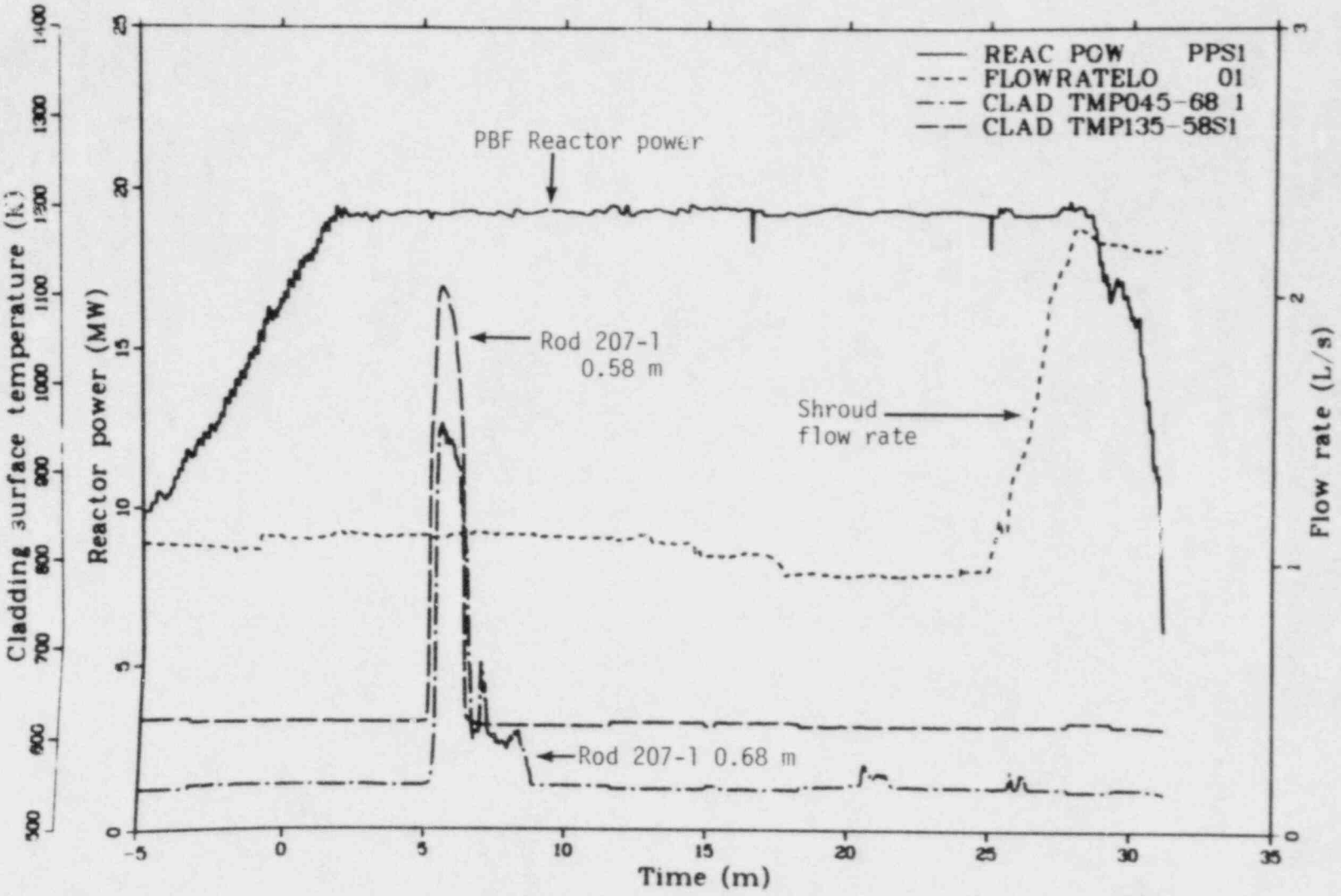

Figure 16. Reactor power, shroud flow rate and measured cladding surface temperatures for Rod 207-1 at the 0.58- and 0.68-m elevations illustrating the onset of boiling transition and rod quench.

surface temperature and measurement location are presented in Table 4. It is expected that the peak cladding temperatures determined by post irradiation examination will be considerably higher than those measured during the test by the thermocouples. It was determined in Test PCM-5[2] that a measured cladding temperature of 1110 K corresponded to an actual cladding temperature of near 1540 K. This temperature differential is due to increased heat transfer associated with thermocouple fin effects.

3.2 Film Boiling Destabilization (Quench)

Return to nucleate boiling may be viewed as a thermal-hydraulic cooling process which results in a localized surface temperature or heat flux decrease sufficient to permit direct heater surface to coolant contact (rewetting). A typical cladding surface thermocouple response during subcooled or nucleate boiling, film boiling operation, and return to nucleate boiling is shown in Figure 17. Temperatures corresponding to points C and D are commonly referred to as the quench (or film boiling destabilization) and rewet temperatures, respectively.

Within the Test PCM-7 nine-rod cluster, at least seven of the nine fuel rods experienced film boiling operation for various times during the final boiling transition test phase. Figure 18 illustrates the 0.63-m elevation thermocouple response during the boiling transition test phase for Rod 207-3. The points of onset of boiling transition (BT) and quench are indicated on the figure. The inset on Figure 18 illustrates a time enlargement of the return to nucleate boiling process, including rewet. The driving mechanism for return to nucleate boiling was the coolant flow increase.

As observed in Test PCM-7 and previous PCM experiments,[1] a cladding thermocouple trace (Figure 18, inset) exhibits several regions (seen as slope changes) prior to return to nucleate boiling, indicating several modes of heat transfer during the quenching process. This observation is

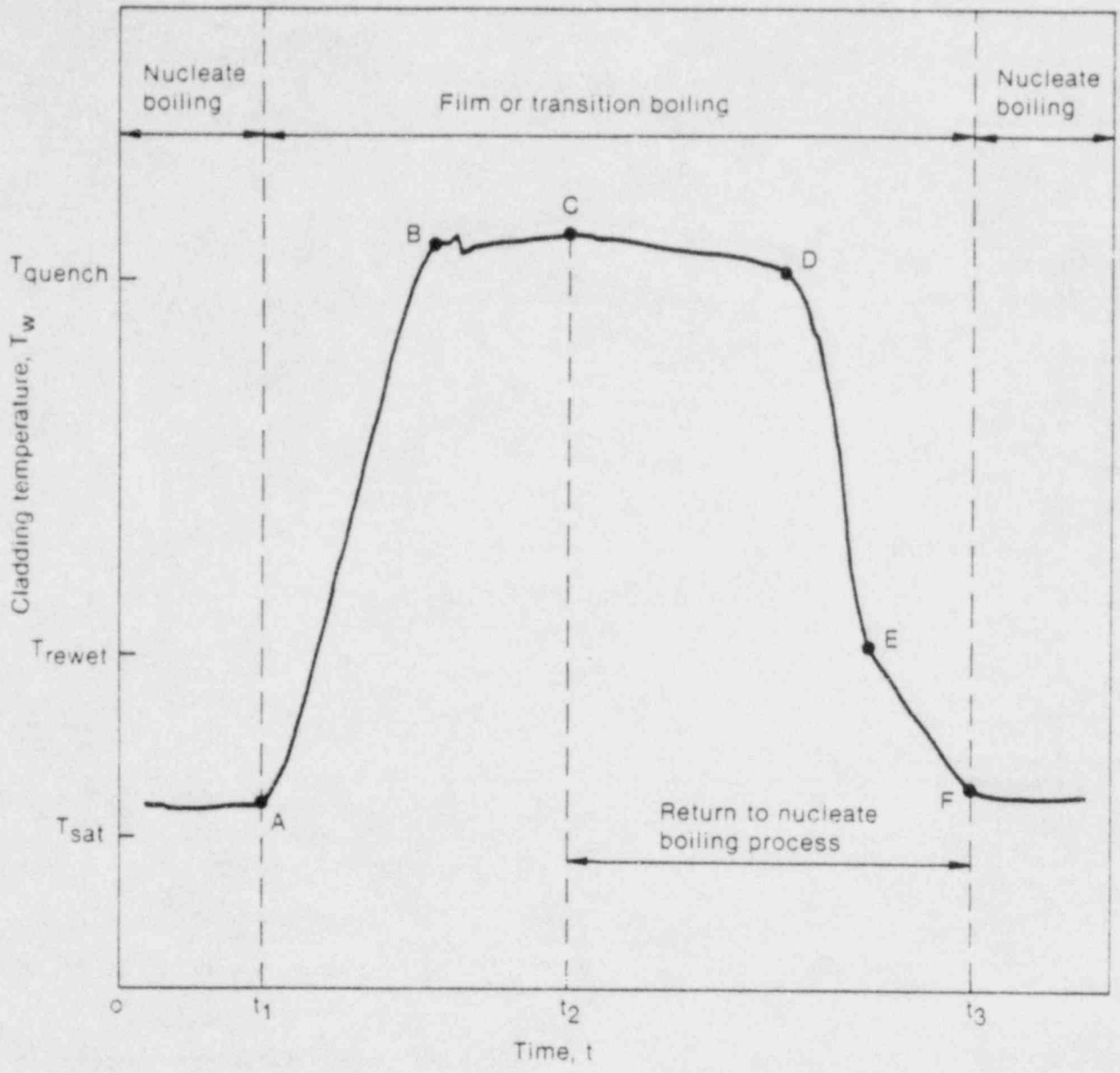

A = Departure from nucleate boiling
B.C = Stable film boiling
D = Quench
E = Rewet
F = Return to nucleate boiling

Figure 17. Typical cladding thermocouple response observed during a film boiling period.

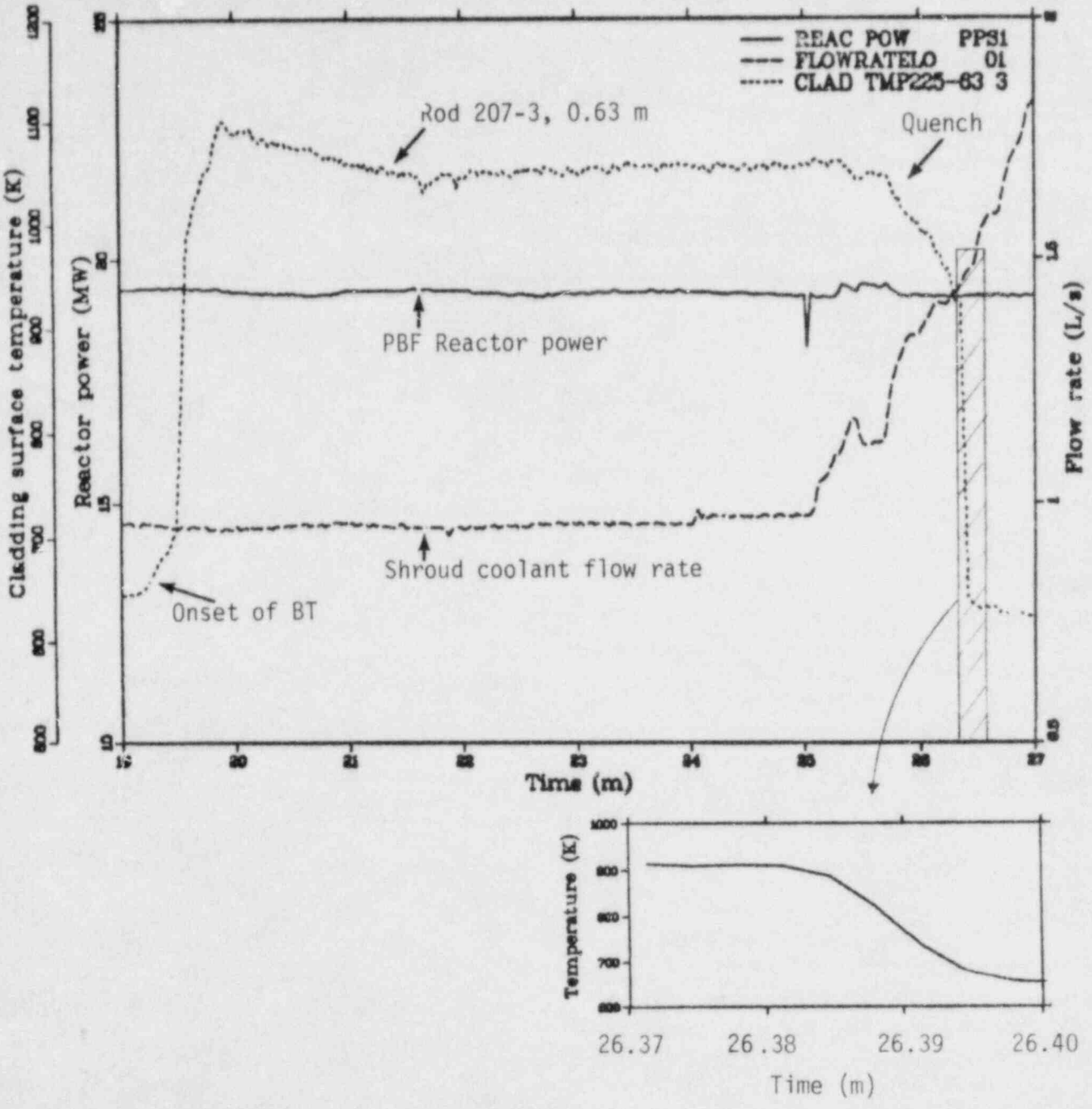

Figure 18. Reactor power, shroud coolant flow rate and cladding surface temperature for Rod 207-3 at 0.63-m elevation during a period of film boiling operation. Inset illustrates the return to nucleate boiling process.

consistent with the findings of other investigators. In 1976, Iloeje et al., proposed a three-step model for dispersed flow heat transfer during a post boiling transition period with vertical flow; the model includes:

1. Heat transfer from the wall to the bulk vapor component of the two-phase flow

2. Heat transfer from the wall to liquid droplets which are in the thermal boundary layer but do not touch the wall

3. Direct heat transfer from the wall to liquid droplets which touch the wall.

This three-step model may be used to explain the several different modes of heat transfer observed (Figure 18, inset) during the return to nucleate boiling process. The final step corresponds to a heat transfer mode which follows rewetting. Table 5 lists the thermal-hydraulic conditions at the time of film boiling destabilization for the Test PCM-7 fuel rods.

3.3 Rod-to-Rod Interactions

A primary objective of Test PCM-7 was to evaluate the potential for film boiling and fuel rod failure propagation within the cluster. Although evaluation of rod failure propagation will require extensive posttest evaluation, some observations regarding film boiling propagation in the cluster can be made from the on-line "quick look" data.

The apparent order in which the Test PCM-7 rods attained boiling transition can be seen from Figure 14 (Section 3.1). The first indication of boiling transition was on the center fuel rod (207-5) at the 0.66-m elevation. The subsequent order that film boiling was detected was; side Rod 207-2, side Rod 207-6, corner Rod 207-9, side Rod 207-4, corner Rod 207-1, and finally corner Rod 207-3. The described order in which the rods attained boiling transition in the cluster does not suggest a systematic propagation of film boiling through the cluster. Rather, the

TABLE 5. SUMMARY OF TEST PCM-7 QUENCH CONDITIONS

Fuel Rod	Fuel Rod Peak Power at Onset of Quench (kW/m)	Bundle Coolant Mass Flux at Quench ($kg/s \cdot m^2$)	Inlet Coolant Subcooling at Quench (K)
207-1	55.88	579.1	16.3
207-2	56.48	776.7	16.3
207-3	58.21	751.3	16.3
207-4	55.18	591.8	15.5
207-5	57.10	668.4	15.5
207-6	53.69	505.6	15.5
207-9	55.31	540.5	15.5

order appeared to be unrelated to the rod position in the assembly. This observation is consistent with results from the first PCM bundle test, Test PCM-5[1] and other multiple rod investigations.[4,5]

Although film boiling propagation in the cluster was not detected, the possibility of rod-to-rod interactions via hydraulic coupling cannot "a-priori" be ruled out. Figure 19 illustrates the thermocouple responses at common axial elevations for adjacent side and corner Rods 207-6 and 207-3, respectively. The quench and rewet of Rod 207-6 just prior to the onset of boiling transition on Rod 207-3 at power and coolant conditions more conducive of sustaining film boiling than quench, may be an indicator of the inherent coupling between the bundle rods. Other factors such as rod bowing, surface condition, or gap conductance may also be postulated to result in the observed response, and will require additional investigation.

Also noted on Figure 19 is the estimated time of rod failure in the bundle. The time of rod failure was deduced from the response of the fission product detection system (at 22.60 minutes) and the estimated delay time for the coolant to traverse from the flow shroud to the detector location (4.2 minutes). The resultant time of failure (18.4 minutes) is relatively close to the time frame in which Rod 207-6 was quenching and rewetting. Therefore, the initial rod failure may have been a result of thermal stresses on the highly embrittled Rod 207-6 cladding during the return to nucleate boiling process.

Shown on Figure 20 is the measured loop gamma activity during the final portion of Test PCM-7. The rapid increase in activity at about 22.6 minutes corresponds to rod failure about 4.2 minutes earlier (18.4 minutes). As the bundle fuel rods rewet during the flow increase (25 to 28 minutes), additional increases in loop gamma activity (delayed about 4 minutes) are seen. These increases are likely additional rod failure or breakup of already failed fuel rods.

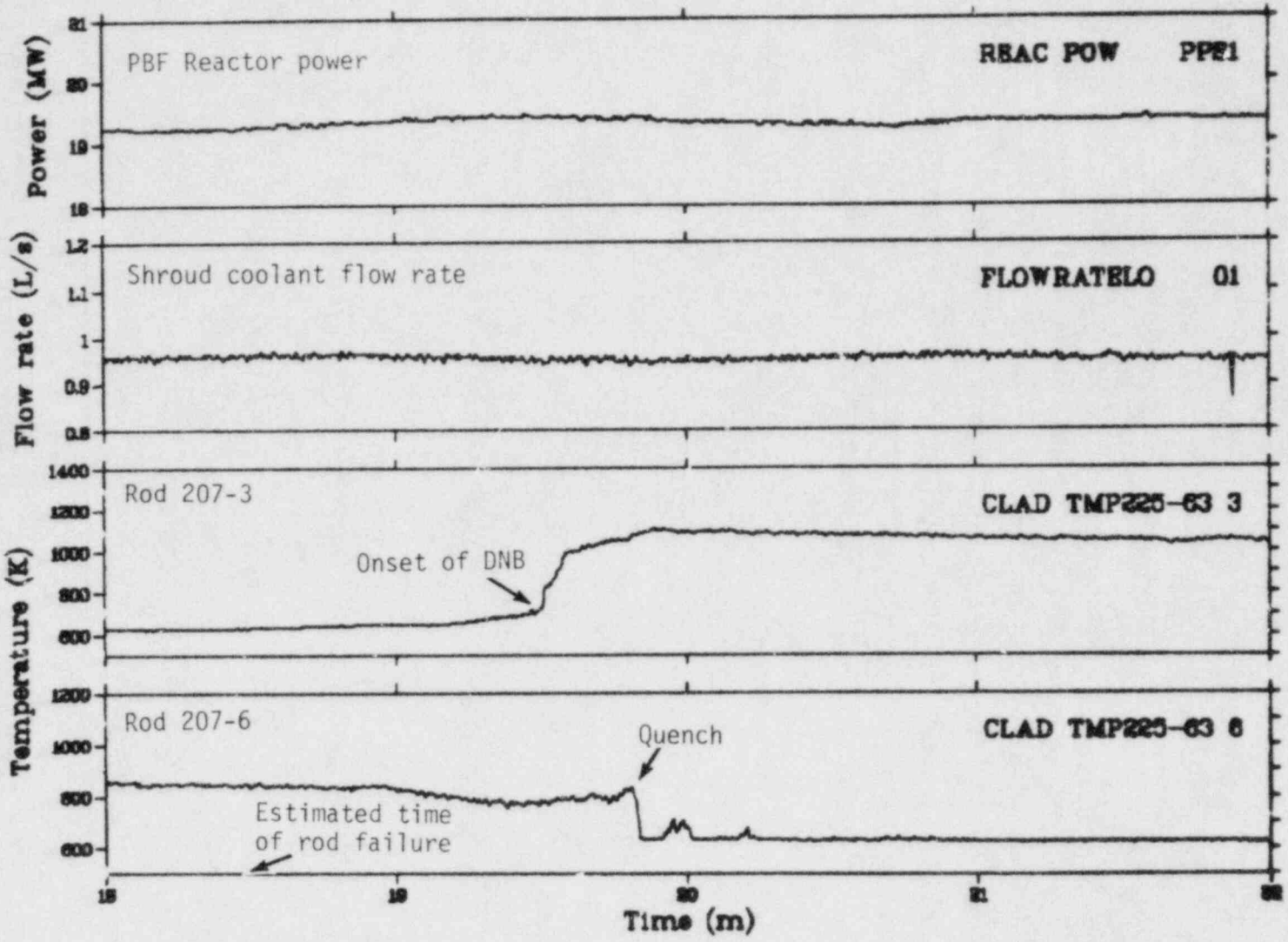

Figure 19. Reactor power, shroud coolant flow rate, and cladding surface temperature for Rods 207-3 and -6 at the 0.63-m elevation showing a possible interaction between test rods.

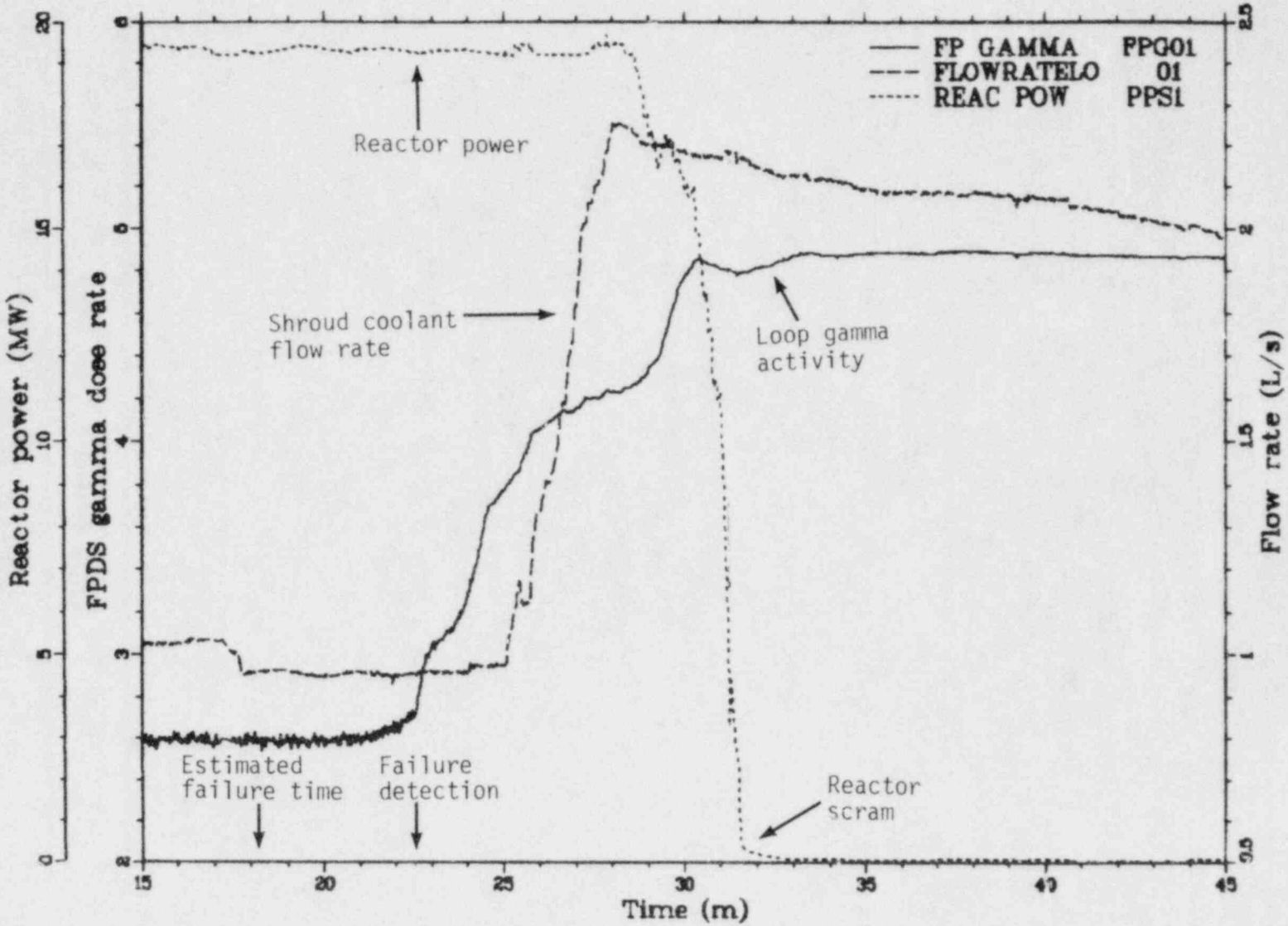

Figure 20. Loop gamma activity, reactor power and coolant flow rate during final (rewet) portion of Test PCM-7 showing rod failure and subsequent rod breakup indications.

3.4 Comparison with Previous PCM Tests

Test PCM-7 was the second experiment in the Power-Cooling-Mismatch Test Series to incorporate a nine-rod cluster geometry. Most other PCM tests utilized a single- or four-rod test configuration, with each rod thermally isolated by individual coolant flow shrouds. The net effect of individual flow shrouds is to eliminate the potential for direct rod-to-rod interaction. It is therefore of fundamental interest to assess the applicability of individually shrouded fuel rod data to cluster geometries.

It may be postulated that a hot fuel rod contained within a coolant flow shroud may be subjected to flow stratification in which cooler liquid flows adjacent to the cooler flow shroud wall, and hotter coolant flows adjacent to the hot rod. Should such stratification occur, higher cladding temperatures may result. In a multiple rod geometry, however, in which many hydraulically coupled subchannels exist, the potential for flow stratification is reduced. Comparison of results from the first PCM bundle test, Test PCM-5, with individually shrouded rod behavior data under similar power-coolant conditions did not suggest significant flow stratification in the single rod tests.[1] Since the Test PCM-7 measured surface temperatures were similar to the Test PCM-5 measured temperatures (1000 to 1300 K), the Test PCM-7 results also support this observation.

The power and coolant mass flux at the onset of boiling transition for the PCM test series fuel rods are illustrated in Figure 21. As shown, the general trend is an increase in test rod peak power with an increase in coolant mass flux. All data except that from Tests PCM-5 and PCM-7 are for isolated, individually shrouded test rods. As indicated, the central rod conditions at onset of boiling transition for the bundle tests are generally consistent with the trend of single rod test results. The peripheral rod data (side and corner bundle rods) are slightly outside the general trends. In general, a higher test rod power at a given mass flux is required for the peripheral rods to initiate boiling transition. Such behavior may indicate a slightly more effective cooling of the side and corner rods, perhaps due to coolant intermixing and cross flow, or rod bowing and the near presence of the cooler shroud wall.

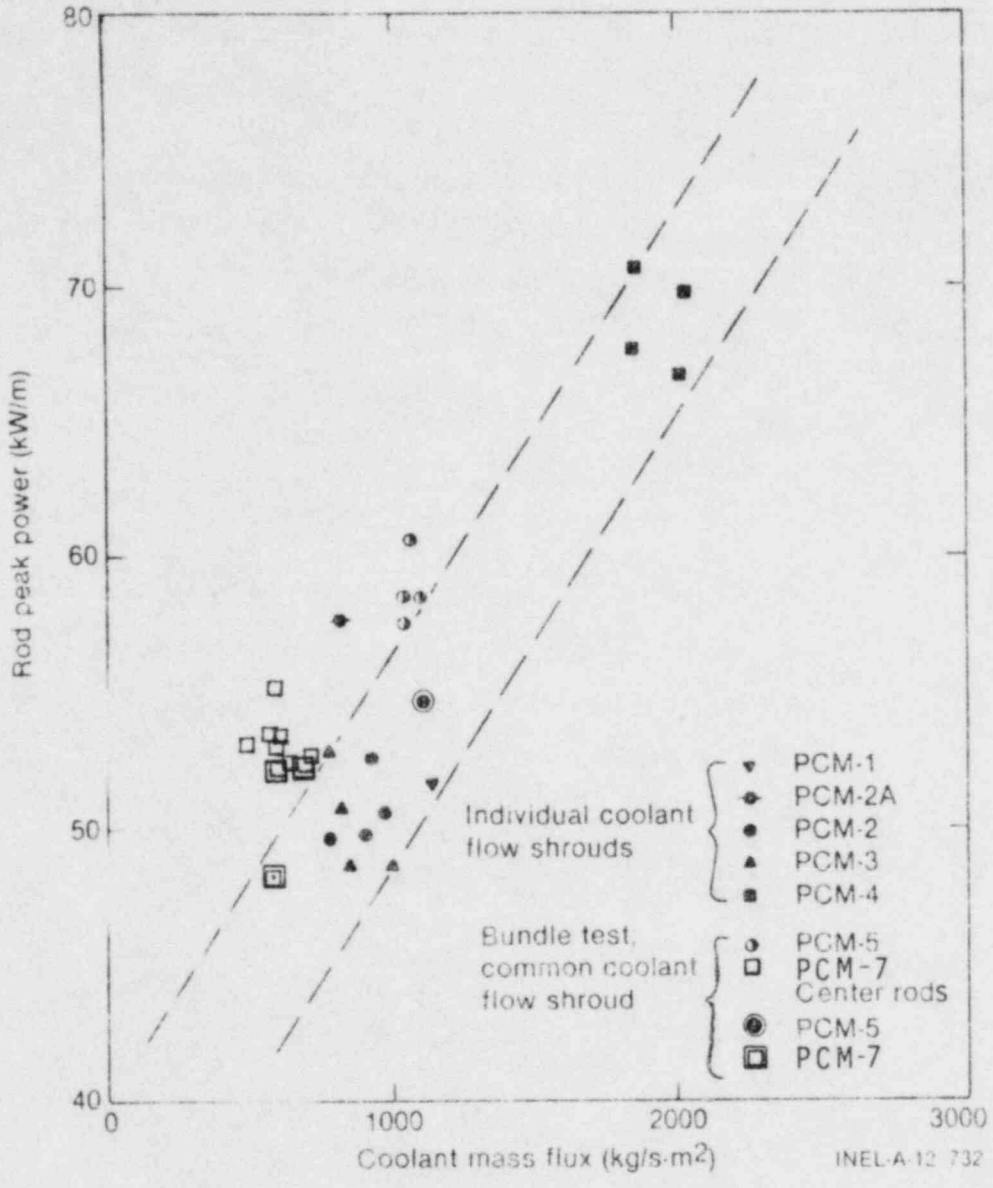

Figure 21 Comparison of the conditions at first indication of film boiling for PCM test series.

The conditions at onset of boiling transition for the central bundle fuel rods corresponds well with that expected for an individually shrouded test rod. The boiling transition data base obtained for individually shrouded rods is, therfore, apparently applicable for determining the conditions at onset of boiling transition for a fuel rod located within the inner regions of a fuel bundle.

Figure 22 illustrates the PCM Test Series data for both the onset of boiling transition and quench. The abscissa of Figure 22 represents a best fit regression of the PBF boiling transition and quench data[6] from both the Power-Cooling-Mismatch (PCM) and Irradiation Effects (IE) test series. The fit is of the form

$$P_p = 8.24\ G^{0.25}\ \Delta T_{sc}^{0.057} \qquad (1)$$

Where: P_p = Peak rod power (chopped cosine axial power shape with 1.36 peak to average) in kW/m

G = Coolant mass flux in $kg/s \cdot m^2$

ΔT_{sc} = Inlet coolant subcooling in K.

The estimated 97% confidence level of the correlation (Equation 1) is shown as the dashed lines of Figure 22, and is approximately $\pm$ 20%. As illustrated, the Test PCM-7 conditions at onset of boiling transition and querch agree well with the derived PBF empirical correlation. Of notable importance from Figure 22 is the indistinguishable difference between the conditions at the onset of film boiling (open symbols) and the conditions at the onset of film boiling destabilization or quench (solid symbols). This observation suggests that the onset of boiling transition and the return to nucleate boiling processes proceed on similar paths with little or no hysteresis. This implies that the classical "transition boiling" heat transfer regime is difficult to attain under the Test PCM-7 conditions and is traversed very rapidly in the quenching process.

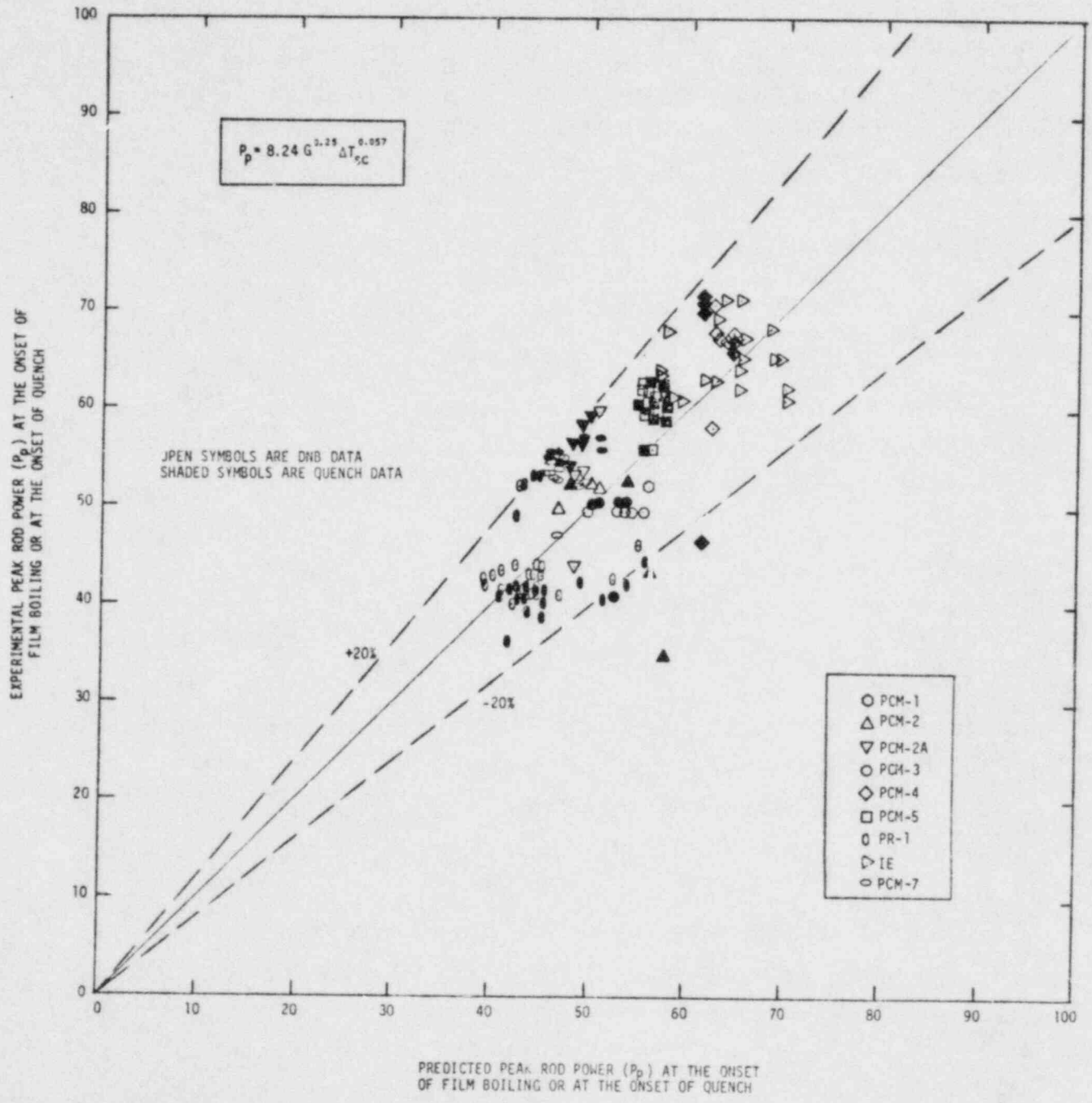

Figure 22. Comparison of experimental peak rod power at onset of film boiling and quench with PBF correlation predicted power for PCM test series.

4. RESULTS AND OBSERVATIONS

The primary objectives of Test PCM-7 were to evaluate the potential for film boiling and rod failure propagation in a small cluster geometry. Observations can be made from the preliminary data contained in this report regarding the potential for film boiling propagation. Extensive posttest visual and metallurgical examination of the cluster will be required to formulate an evaluation of rod failure propagation. In addition to the primary objectives, Test PCM-7 provided data to enlarge the existing base of boiling transition and quench information under power-cooling-mismatch conditions.

The apparent order of boiling transition occurrence in the cluster does not suggest propagation of film boiling from rod-to-rod. The first indication of boiling transition was on the center rod (207-5), followed by two side rods (207-2 and 207-6), a corner rod (207-9), a side rod (207-4), a corner rod (207-1), and finally, at a later time, a corner rod (207-3). The described order implies that the onset of boiling transition was unrelated to the rod position in the cluster, rather than a systematic propagation through the assembly.

Inherent rod-to-rod hydraulic coupling in the cluster may have been observed in the quench and rewet of Rod 207-6 near the time of onset of boiling transition on Rod 207-3, when conditions apparently favored sustaining film boiling operation. Other factors such as rod bowing, coolant intermixing, etc., may have contributed to the observed response.

The conditions at onset of film boiling and quench for Test PCM-7 were consistent with previous PCM results. As observed from the first PCM nine-rod Test (PCM-5), the peripheral rods required slightly higher power levels to initiate boiling transition than the central rod, but all Test PCM-7 boiling transition and quench conditions were within the uncertainties of an empirical correlation derived from previous PCM results in the PBF. The thermal-hydraulic conditions to initiate film boiling were

indistinguishable from the conditions required to quench the fuel rods. This observation implies that the transition from nucleate boiling to film boiling and from film boiling to nucleate boiling traverse similar paths with little or no hysteresis.

The measured cladding temperatures during Test PCM-7 (1000 to 1300 K maximum) imply temperatures in the β-zircaloy (T > 1245 K) regime since the cladding thermocouples act as cooling fins and measure temperatures significantly lower (200 to 400 K) than actual. The long time (>18 min.) at high cladding temperatures prior to detected rod failure suggest that failure was either due to high temperature nil-ductility or the thermal shock induced embrittlement failure of Rod 207-6. Additional breakup of either the previously failed rod or other highly embrittled rods was likely during the rewet sequence.

5. REFERENCES

1. F. S. Gunnerson and D. T. Sparks, Behavior of a Nine-Rod Fuel Assembly During Power-Cooling-Mismatch Conditions-Results of Test PCM-5, NUREG/CR-1103, EGG-2002 November 1979.

2. D. K. Kerwin, Test PCM-5 Fuel Rod Materials Behavior, NUREG/CR-1430, EGG-2033, May 1980.

3. O. C. Iloeje, W. M. Rohsenow and P. Griffith, "Three-Step Model of Dispersed Flow Heat Transfer (Post-CHF Vertical Flow)," ASME 75-WA/HT-1 1975.

4. J. Weisman, et al., "Experimental Determination of the Departure from Nucleate Boiling in Large Rod Bundles at High Pressures," AIChE Preprint 29, Proceedings of the Ninth National Heat Transfer Conference, Seattle, 1967.

5. L. S. Tong, "Critical Heat Fluxes in Rod Bundles," Two-Phase Flow and Heat Transfer in Rod Bundles, V. E. Schrock (ed.), ASME Publication, 1969.

6. F. S. Gunnerson and P. S. Dunphy, A Study of Film Boiling, Quench and Rewet Phenomenon During High Pressure Power-Cooling-Mismatch Testing, To Be Published September 1980.

APPENDIX A

PRELIMINARY DATA FOR FINAL BOILING TRANSITION TEST PHASE OF TEST PCM-7

APPENDIX A

This Appendix presents the preliminary "quick look" data utilized for the preparation of this report. Included is only data from the final portion of the boiling transition test phase. These data are unqualified as to relative (& absolute) uncertainties, and have not been corrected for instrument offsets or electronic drift. Instrument identifiers shown on the plots are correlated to specific instruments in Table A-1. Some instrumentation had failed prior to or during testing but are included in this appendix.

TABLE A-1. TEST PCM-7 INSTRUMENT IDENTIFICATION

Instrument Group	Measurement	Instrument	Location[a]	PBF/DARS Identifier
Fuel Rod 207-1	Fuel Rod Elongation	LVDT	Upper End of Rod	CLAD DSP 01
	Fuel Rod Pressure	Kaman 17 MPa PXD	Fuel Rod Plenum	ROD PRES 01
	Fuel Centerline Temp.	W 5% Re/W 26% Re TC	Fuel C_L 0.68 m	FUEL TMP 000-68 1
	Cladding Surface Temp.	Type S TC	045° - 0.68 m	CLAD TMP 045-68 1
	Cladding Surface Temp.	W 5% Re/W 26% Re TC	135° - 0.58 m	CLAD TMP 135-5851
	Cladding Surface Temp.	Type S TC	225° - 0.68 m	CLAD TMP 225-68 1
Fuel Rod 207-2	Cladding Surface Temp.	Type S TC	045° - 0.68 m	CLAD TMP 045-63 3
	Cladding Surface Temp.	Type S TC	225° - 0.68 m	CLAD TMP 225-63 2
Fuel Rod 207-3	Cladding Surface Temp.	Type S TC	045° - 0.63 m	CLAD TMP 045-63 3
	Cladding Surface Temp.	Type S TC	225° - 0.63 m	CLAD TMP 225-63 3
Fuel Rod 207-4	Cladding Surface Temp.	Type S TC	135° - 0.63 m	CLAD TMP 135-63 4
	Cladding Surface Temp.	Type S TC	315° - 0.63 m	CLAD TMP 315-63 4
Fuel Rod 207-5	Fuel Rod Elongation	LVDT	Upper End of Rod	CLAD DSP 05
	Fuel Rod Pressure	KAMAN 17 MPa PXD	Fuel Rod Plenum	ROD PRES 05
	Plenum Temperature	W5% RE/W 26% Re	Fuel Rod Plenum	PLNM TMP 05
	Fuel Centerline Temp.	W 5% Re/W 26% Re TC	Fuel C_L 0.68 m	FUEL TMP 000-68 5
	Cladding Surface Temp.	W5%Re/W 26% Re TC	045° - 0.58 m	CLAD TMP 045-58 5
	Cladding Surface Temp.	Type S TC	135° - 0.68 m	CLAD TMP 135-6855
	Cladding Surface Temp.	W 5% Re/W 26% Re TC	225° - 0.63 m	CLAD TMP 225-63 5
	Cladding Surface Temp.	Type S TC	315° - 0.68 m	CLAD TMP 315-6855
Fuel Rod 207-6	Fuel Rod Elongation	LVDT	Upper End of Rod	CLAD DSP 06
	Fuel Rod Pressure	KAMAN 17 MPa PXD	Fuel Rod Plenum	ROD PRES 06
	Fuel Centerline Temp.	W5% Re/W 26% Re	Fuel C_L 0.68 m	FUEL TMP 000-68 6
	Cladding Surface Temp.	Type S TC	045° - 0.58 m	CLAD TMP 045-58 6
	Cladding Surface Temp.	Type S TC	135° - 0.58 m	CLAD TMP 135-58 6
	Cladding Surface Temp.	Type S TC	225° - 0.63 m	CLAD TMP 225-63 6
	Cladding Surface Temp.	Type S TC	315° - 0.68m	CLAD TMP 315-68 6
Fuel Rod 207-7	Fuel Rod Elongation	LVDT	Upper End of Rod	CLAD DSP 07
Fuel Rod 207-8	Fuel Rod Elongation	LVDT	Upper End of Rod	CLAD DSP 08
Fuel Rod 207-9	Cladding Surface Temp.	Type S TC	135° - 0.68 m	CLAD TMP 135-68 4
	Cladding Surface Temp.	Type S TC	315° - 0.68 m	CLAD TMP 315-68 4

TABLE A-1. (continued)

Instrument Group	Measurement	Instrument	Location[a]	PBF/DAKS Identifier
Test Train	Coolant Pressure	EG&G 17 MPa PXD	Lower Test Assembly	SYS PRES LO-17 01
	Coolant Pressure	EG&G 69 MPa PXD	Upper Test Assembly	SYS PRES HI-69 02
	Coolant Inlet Temperature	Type K TC	Flow Shroud Inlet	INLET TMP 0001
	Coolant Inlet Temperature	Type K TC	Flow Shroud Inlet	INLET TMP 0002
	Coolant Outlet Temperature	Type K TC	Flow Shroud Outlet	OUT TMP 0001
	Coolant Outlet Temperature	Type K TC	Flow Shroud Outlet	OUT TMP 0002
	Shroud Pressure Drop	ΔP PXD	Shroud Inlet and Outlet	SHRD DEL PRS
	Shroud Coolant Temp. Rise	Type T ΔT TC	Top & Bottom Fuel Shroud	DEL TMP SHR 0001
	Shroud Coolant Temp. Rise	Type T ΔT TC	Top & Bottom Fuel Shroud	DEL TMP SHR 0002
	Shroud Coolant Temp. Rise	Type T ΔT TC	Top & Bottom Fuel Shroud	DEL TMP SHR 0003
	Shroud Coolant Temp. Rise	Type T ΔT TC	Top & Bottom Fuel Shroud	DEL TMP SHR 0004
	Recombined Coolant Temp. Rise	Type T ΔT TC	Top & Bottom of Assembly	DEL TMP ASM 0005
	Recombined Coolant Temp. Rise	Type T ΔT TC	Top & Bottom of Assembly	DEL TMP ASM 0006
	Recombined Coolant Temp. Rise	Type T ΔT TC	Top & Bottom of Assembly	DEL TMP ASM 0007
	Recombined Coolant Temp. Rise	Type T ΔT TC	Top & Bottom of Assembly	DEL TMP ASM 0008
	Coolant Flow, IPT	Flow Turbine	Inlet Spool Piece	IC FLOW IN IC-01
	Coolant Flow, Assembly	Flow Turbine	Upper Test Train	ASSEM FLOW IPT-02
	Coolant Flow, Shroud	Flow Turbine	Lower Shroud Extention	FLOWRATE LO 01
	Coolant Flow, Shroud	Flow Turbine	Lower Shroud Extention	FLOWRATE UP 02
	Neutron Flux No. 1[b]	SPND	Shroud, 90° - 0.152 m	NEUT FLX 090-01
	Neutron Flux No. 2	SPND	Shroud, 90° - 0.304 m	NEUT FLX 090-02
	Neutron Flux No. 3	SPND	Shroud, 90° - 0.457 m	NEUT FLX 090-03
	Neutron Flux No. 4	SPND	Shroud, 90° - 0.610 m	NEUT FLX 090-04
	Neutron Flux No. 5	SPND	Shroud, 90° - 0.762 m	NEUT FLX 090-05
	Neutron Flux No. 6	SPND	Shroud, 270° - 0.152 m	NEUT FLX 270-06
	Neutron Flux No. 7	SPND	Shroud, 270° - 0.304 m	NEUT FLX 270-07
	Neutron Flux No. 8	SPND	Shroud, 270° - 0.457 m	NEUT FLX 270-08
	Neutron Flux No. 9	SPND	Shroud, 270° - 0.610 m	NEUT FLX 270-09
	Neutron Flux No. 10	SPND	Shroud, 270° - 0.762 m	NEUT FLX 270-10
Fission Product Detection System	Gross Gamma Rate	Gamma Detector	FPDS	FPGAMMA FPG01
	Gross Gamma Rate	Gamma Detector	FPDS	FPGAMMA FPG02
	Gross Gamma Rate	Gamma Detector	FPDS	FPGAMMA FPG03
	Gross Neutron Rate	Neutron Detector	FPDS	FPNEUT FPN04
	FPDS Sample Temp.	Type K TC	FPDS	FPTEMP FPT01
	FPDS Flow Rate	Turbine Flowmeter	FPDS	FPFLOW FPF01
	FPDS Flow Rate	Turbine Flowmeter	FPDS	FPFLOW FPF02
Plant	IPT Delt Pressure	ΔP PXD	Plant	IPT DELP PT01
	System Pressure	PXD	Plant	SYS PRES PT02
	Loop Flow	Venturi	Plant	LOOP FLOW PT03
	Coolant Temperature	RTD	Inlet Spool Piece	IC IMP INLET IC03
	Core Power	Ion Chamber	Plant	REAC POW PPS1
	Core Power	Ion Chamber	Plant	REAC POW PPS2
	Core Power	Ion Chamber	Plant	REAC POW NMS 02 PT
	Core Power	Ion Chamber	Plant	REAC POW NMS 03 PT
	Core Power	Ion Chamber	Plant	REAC POW NMS 04 PT

a. All elevations measured from bottom of fuel stack.
b. SPND's will require channels for gamma compensation and polarity.

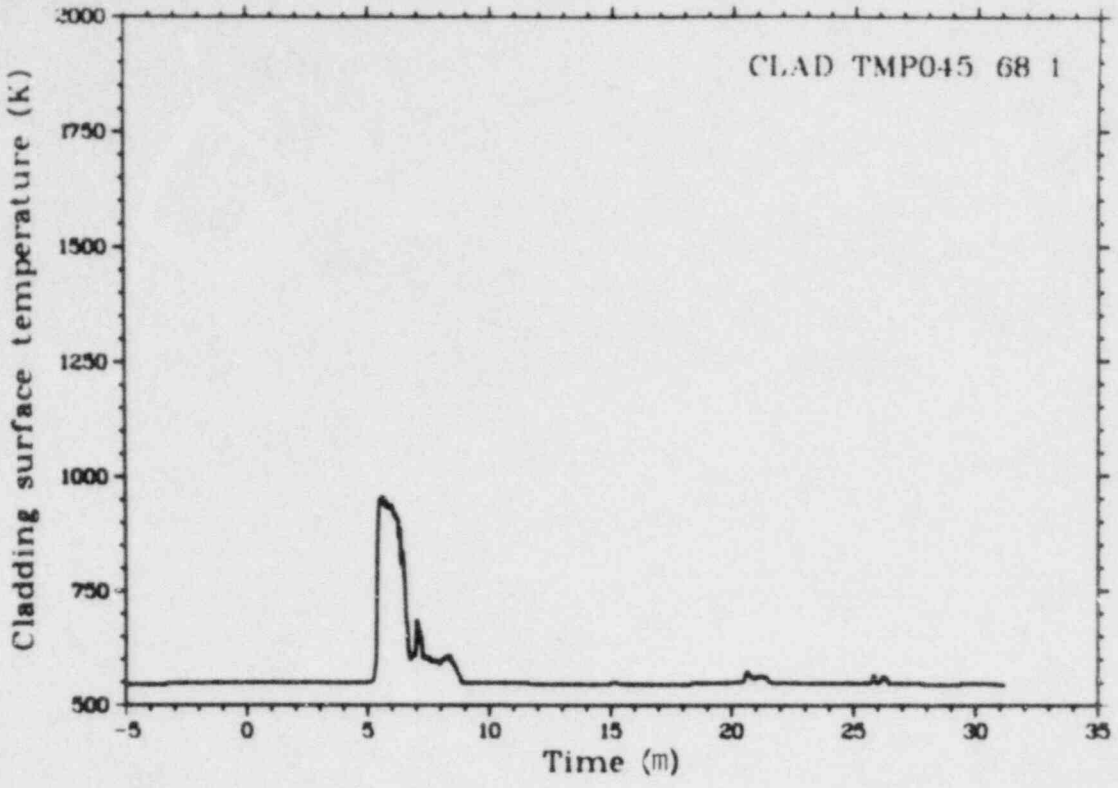
CLAD TMP045 68 1
Cladding surface temperature (K)
2000
1750
1500
1250
1000
750
500
-5
0
5
10
15
20
25
30
35
Time (m)

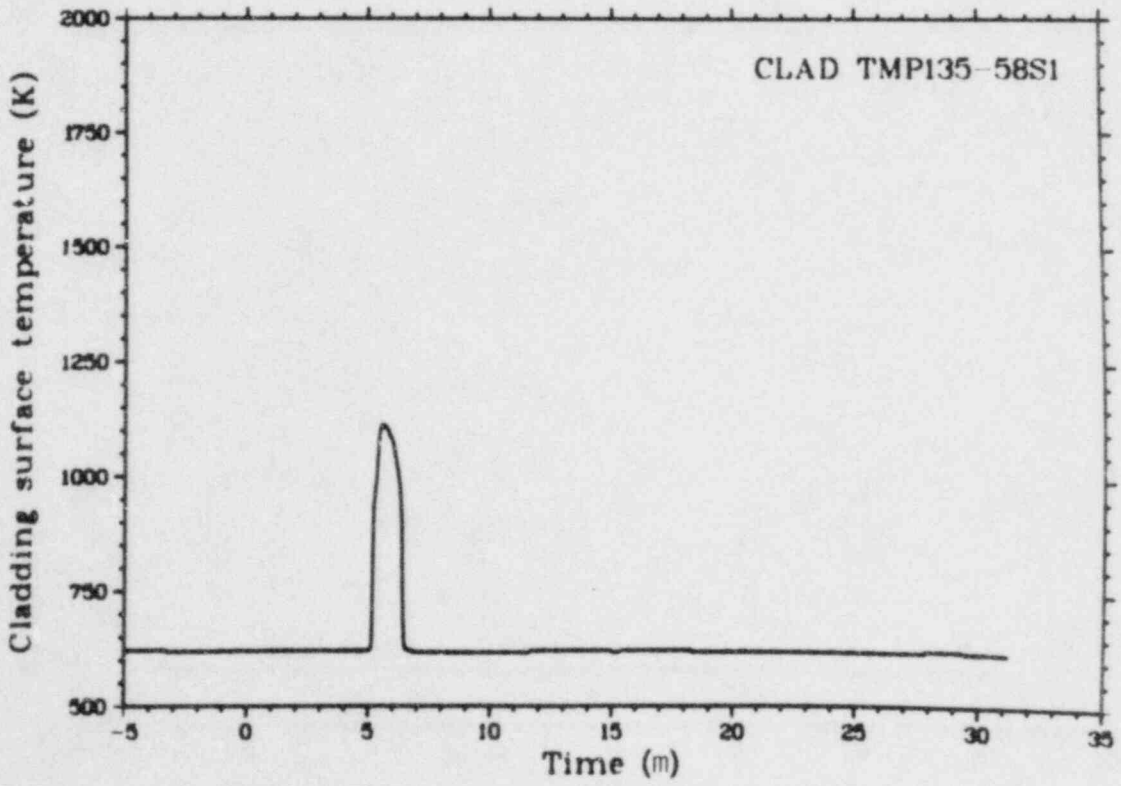
CLAD TMP135-58S1
Cladding surface temperature (K)
2000
1750
1500
1250
1000
750
500
-5
0
5
10
15
20
25
30
35
Time (m)

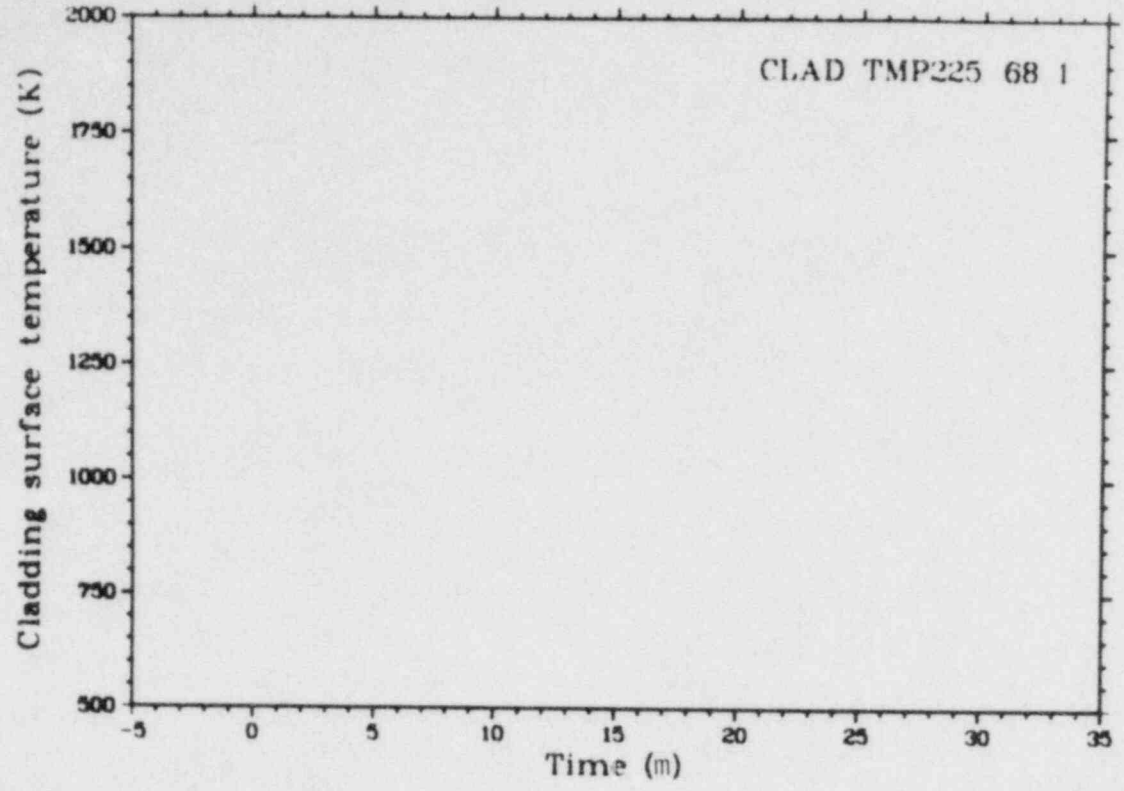
CLAD TMP225 68 1
Cladding surface temperature (K)
2000
1750
1500
1250
1000
750
500
-5
0
5
10
15
20
25
30
35
Time (m)

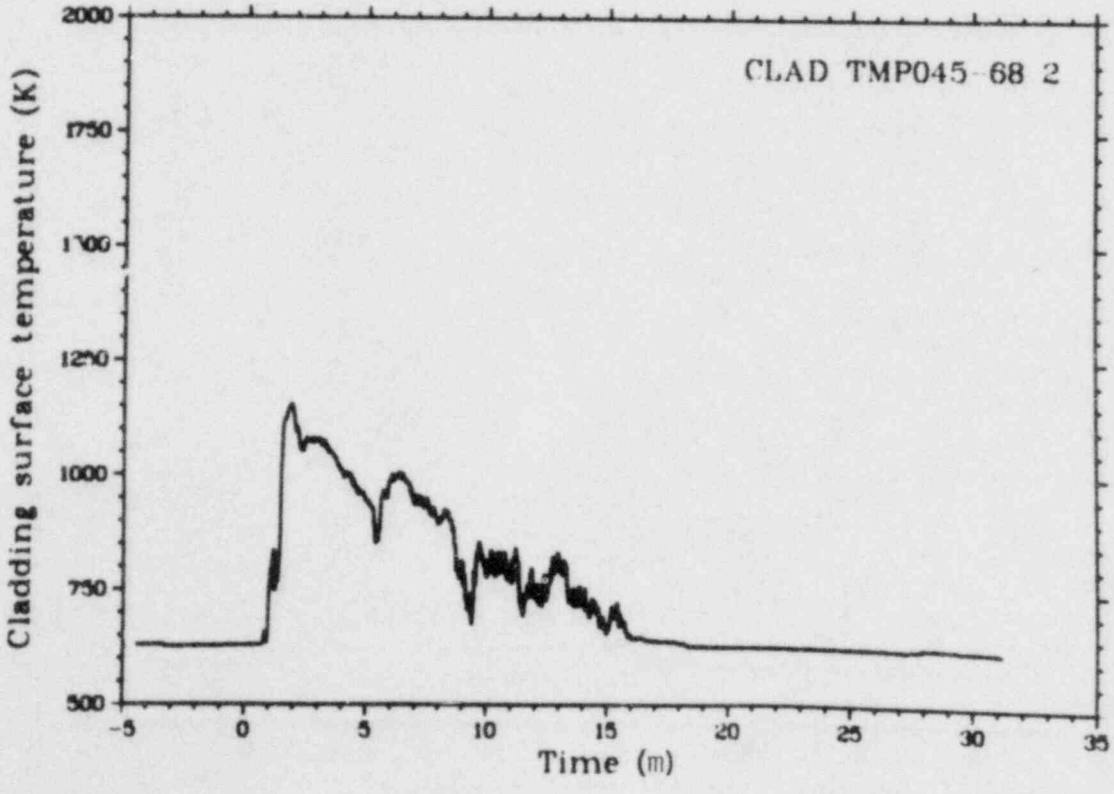
CLAD TMP045 68 2
Cladding surface temperature (K)
2000
1750
1500
1250
1000
750
500
-5
0
5
10
15
20
25
30
35
Time (m)

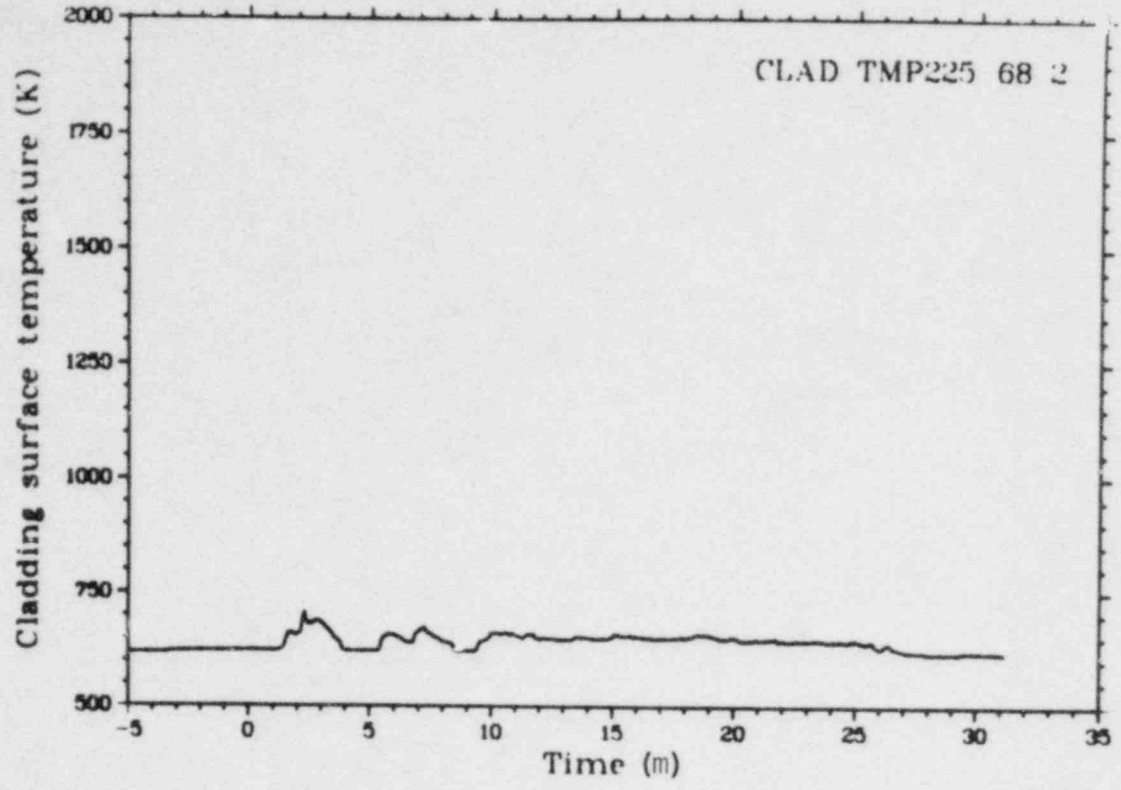
CLAD TMP225 68 2
Cladding surface temperature (K)
2000
1750
1500
1250
1000
750
500
-5
0
5
10
15
20
25
30
35
Time (m)

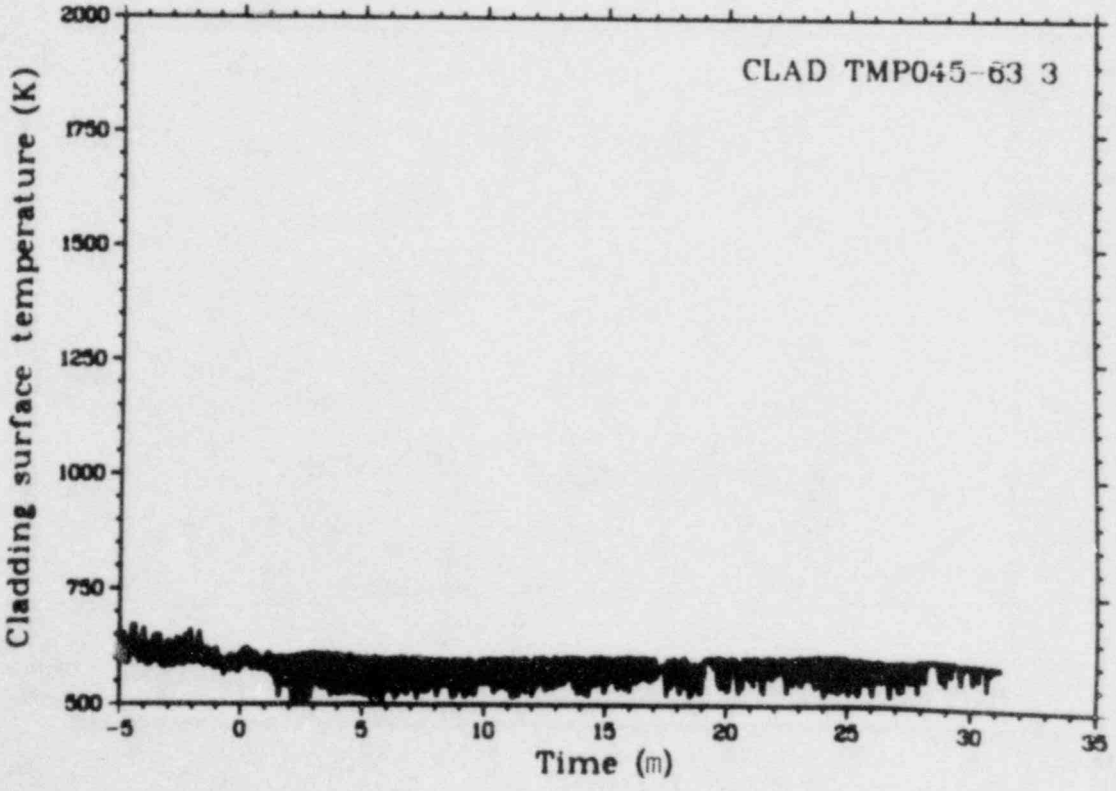
CLAD TMP045-63 3
Cladding surface temperature (K)
2000
1750
1500
1250
1000
750
500
-5
0
5
10
15
20
25
30
35
Time (m)

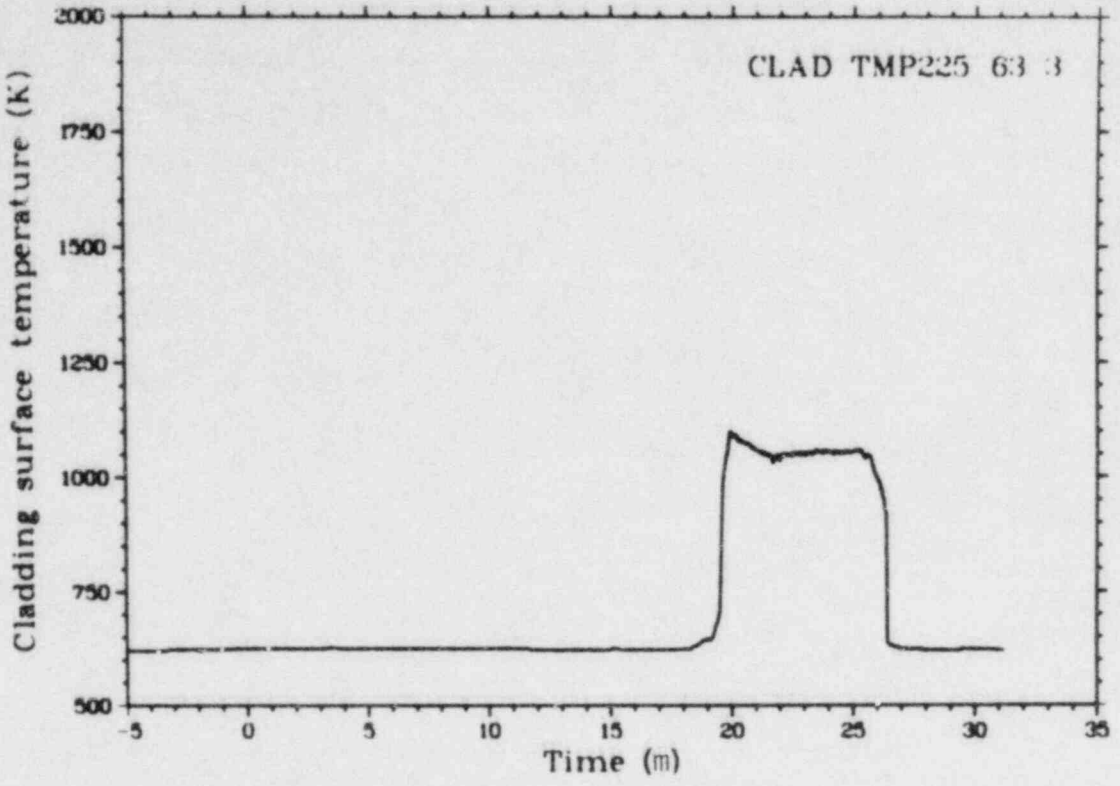
CLAD TMP225 63 3
Cladding surface temperature (K)
2000
1750
1500
1250
1000
750
500
-5
0
5
10
15
20
25
30
35
Time (m)

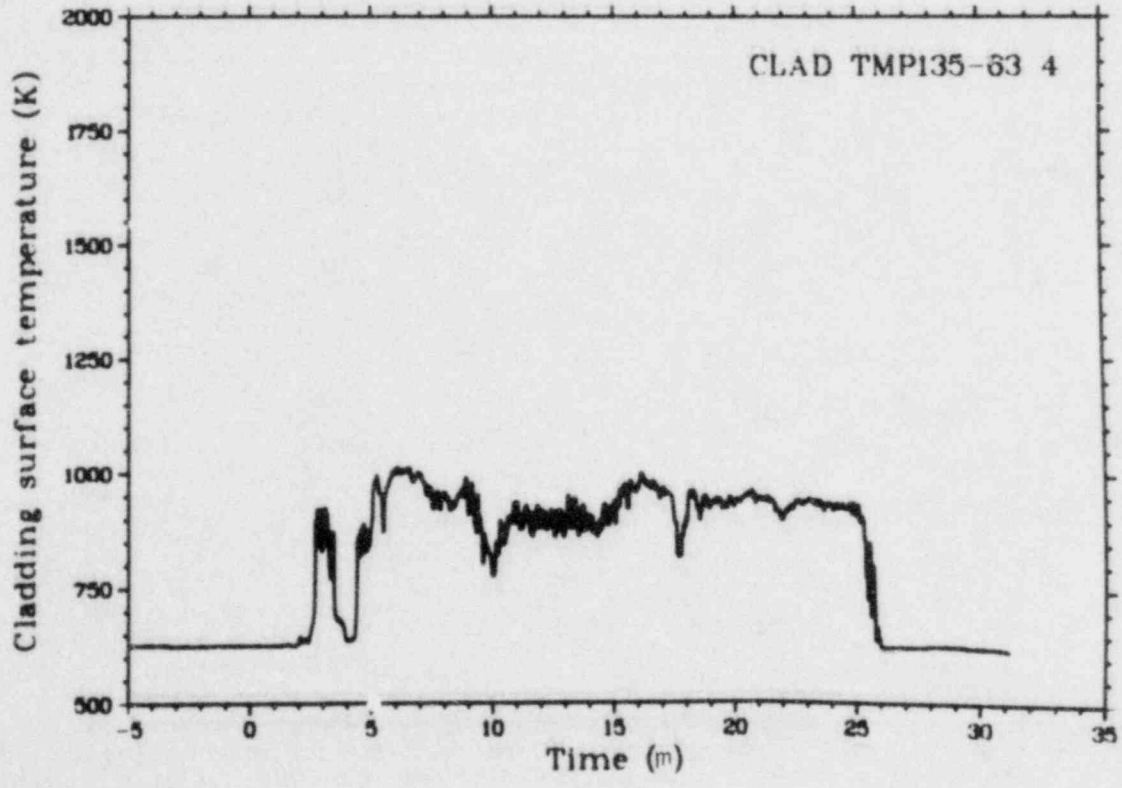
CLAD TMP135-63 4
Cladding surface temperature (K)
2000
1750
1500
1250
1000
750
500
-5
0
5
10
15
20
25
30
35
Time (m)

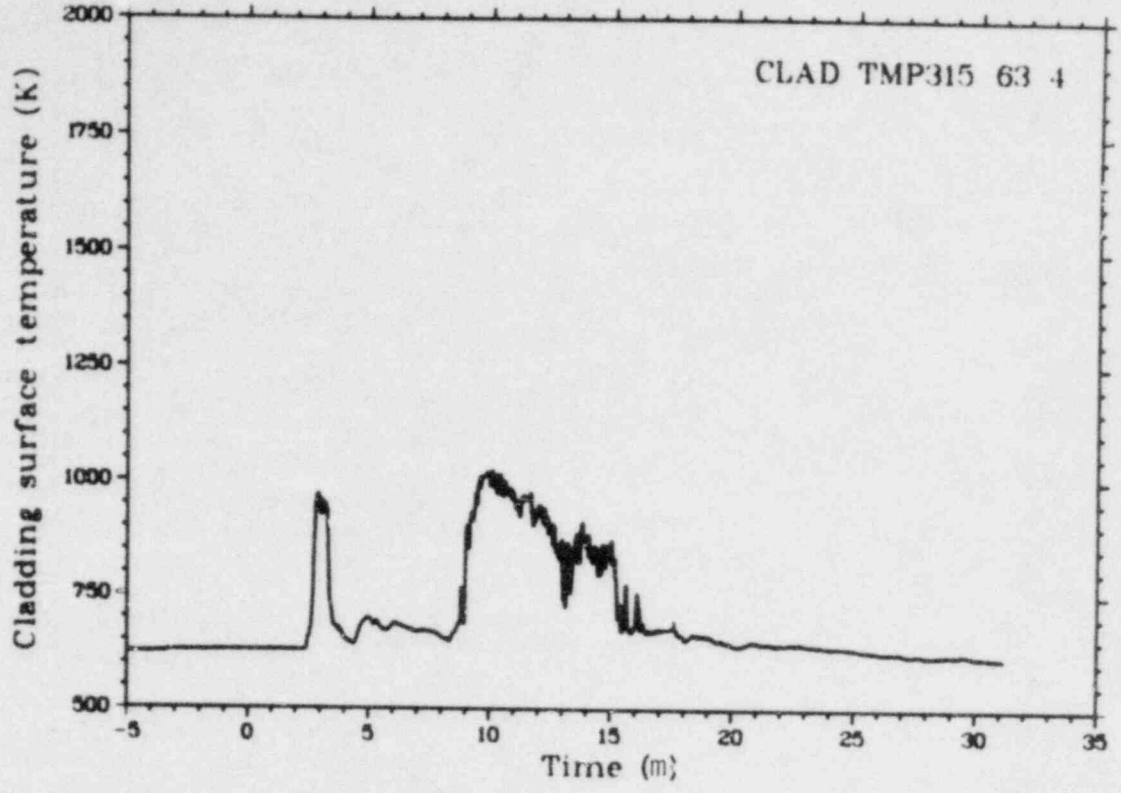
CLAD TMP315 63 4
Cladding surface temperature (K)
2000
1750
1500
1250
1000
750
500
-5
0
5
10
15
20
25
30
35
Time (m)

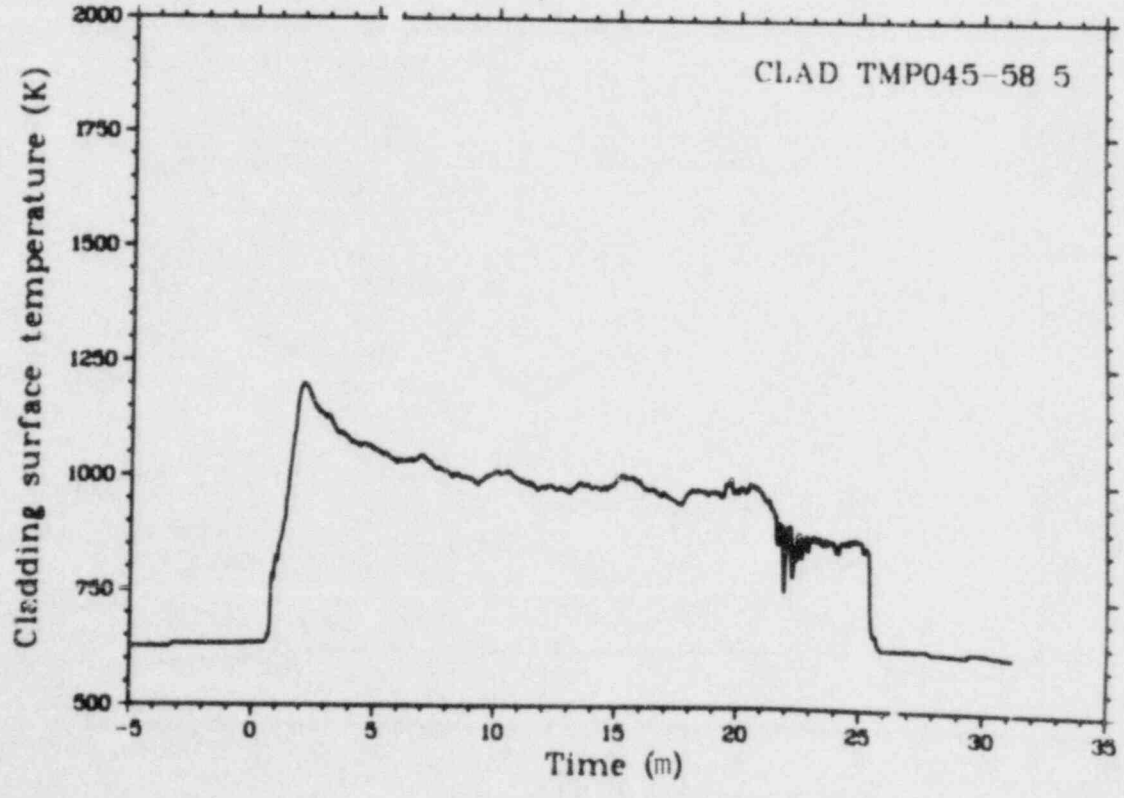
CLAD TMP045-58 5
Cladding surface temperature (K)
2000
1750
1500
1250
1000
750
500
-5
0
5
10
15
20
25
30
35
Time (m)

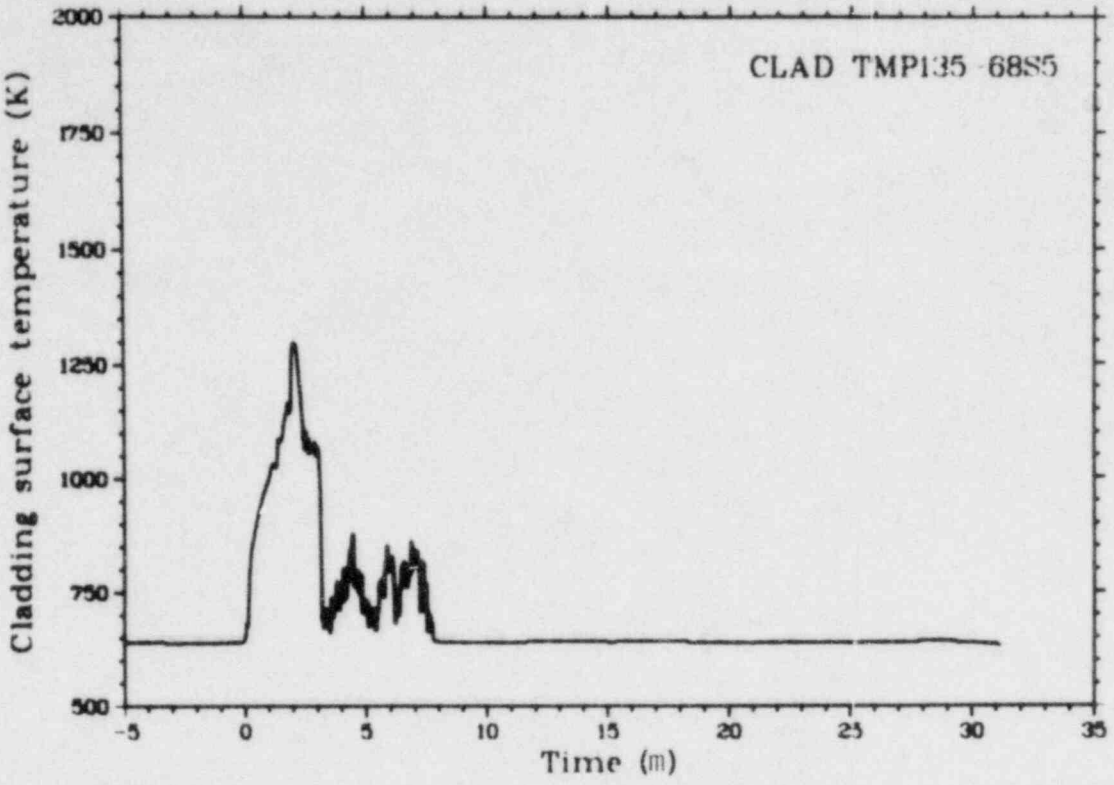
CLAD TMP135-6885
Cladding surface temperature (K)
2000
1750
1500
1250
1000
750
500
-5
0
5
10
15
20
25
30
35
Time (m)

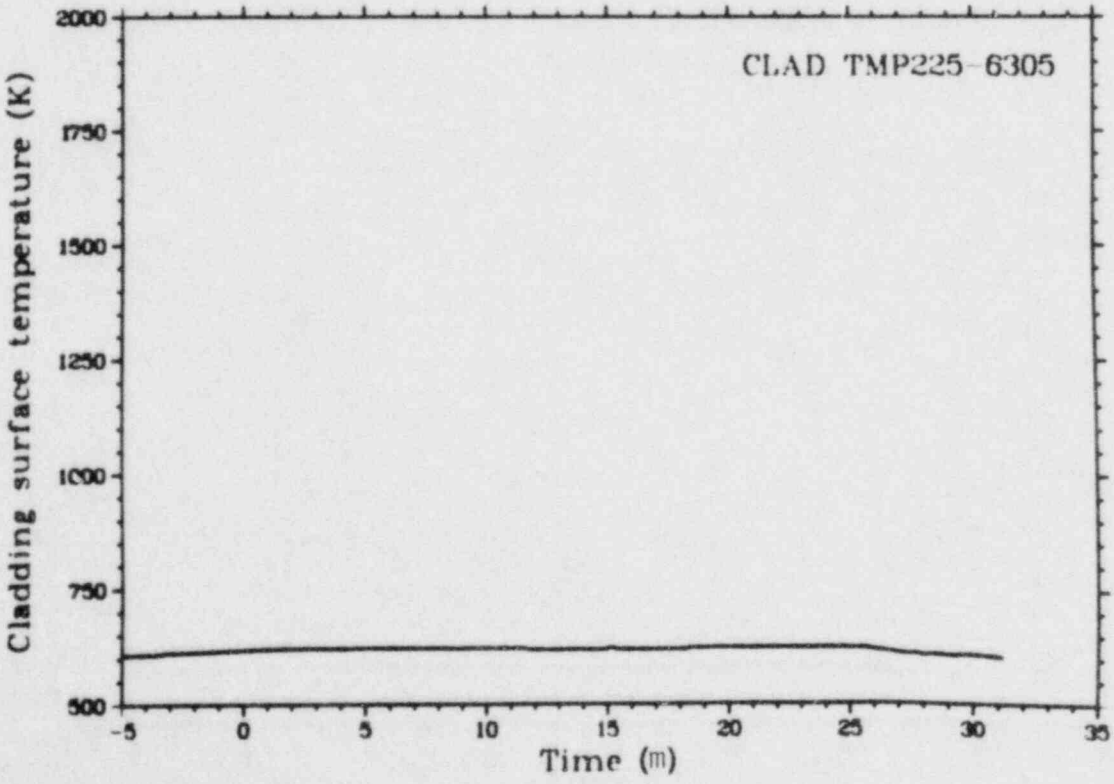
CLAD TMP225-6305
Cladding surface temperature (K)
2000
1750
1500
1250
1000
750
500
-5
0
5
10
15
20
25
30
35
Time (m)

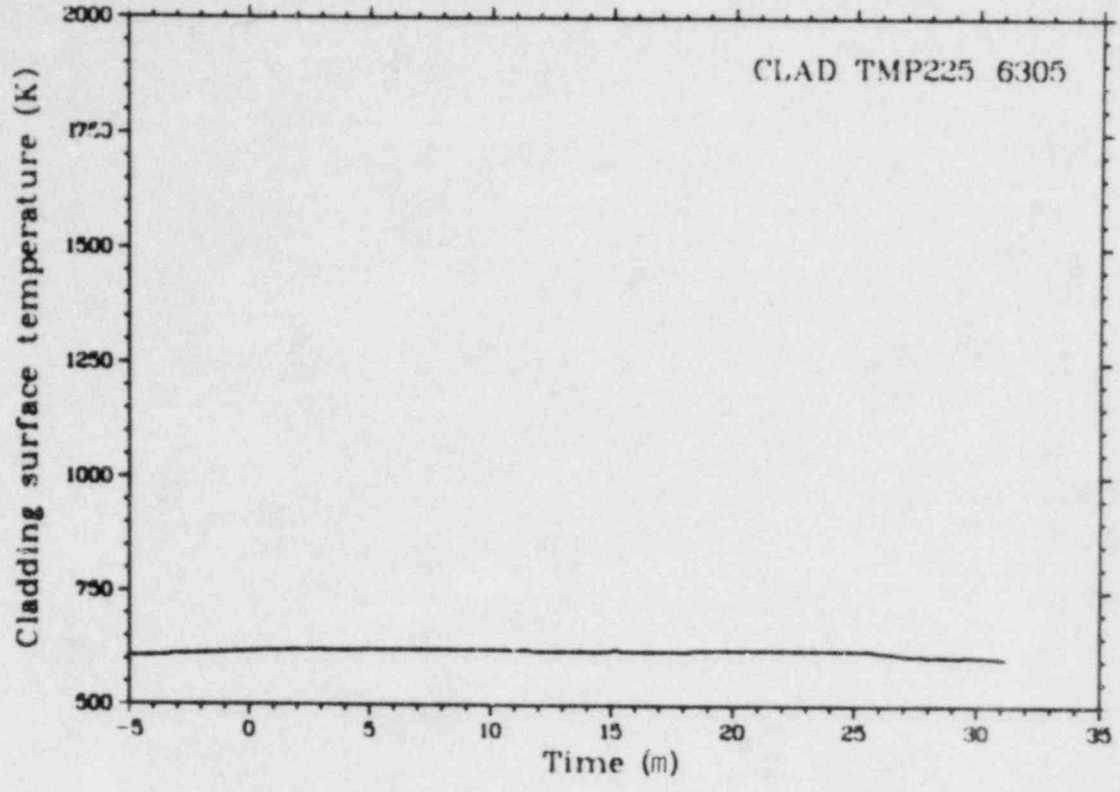
CLAD TMP225 6305
Cladding surface temperature (K)
2000
1750
1500
1250
1000
750
500
-5
0
5
10
15
20
25
30
35
Time (m)

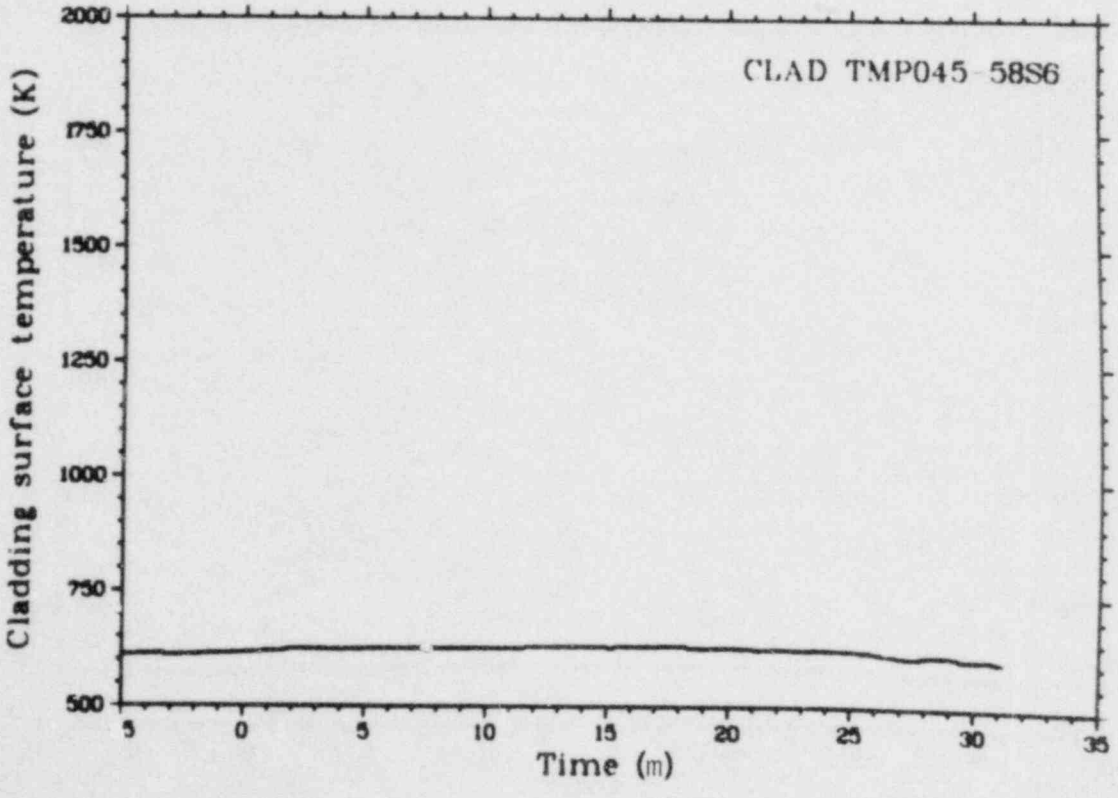
CLAD TMP045 58S6
Cladding surface temperature (K)
2000
1750
1500
1250
1000
750
500
5
0
5
10
15
20
25
30
35
Time (m)

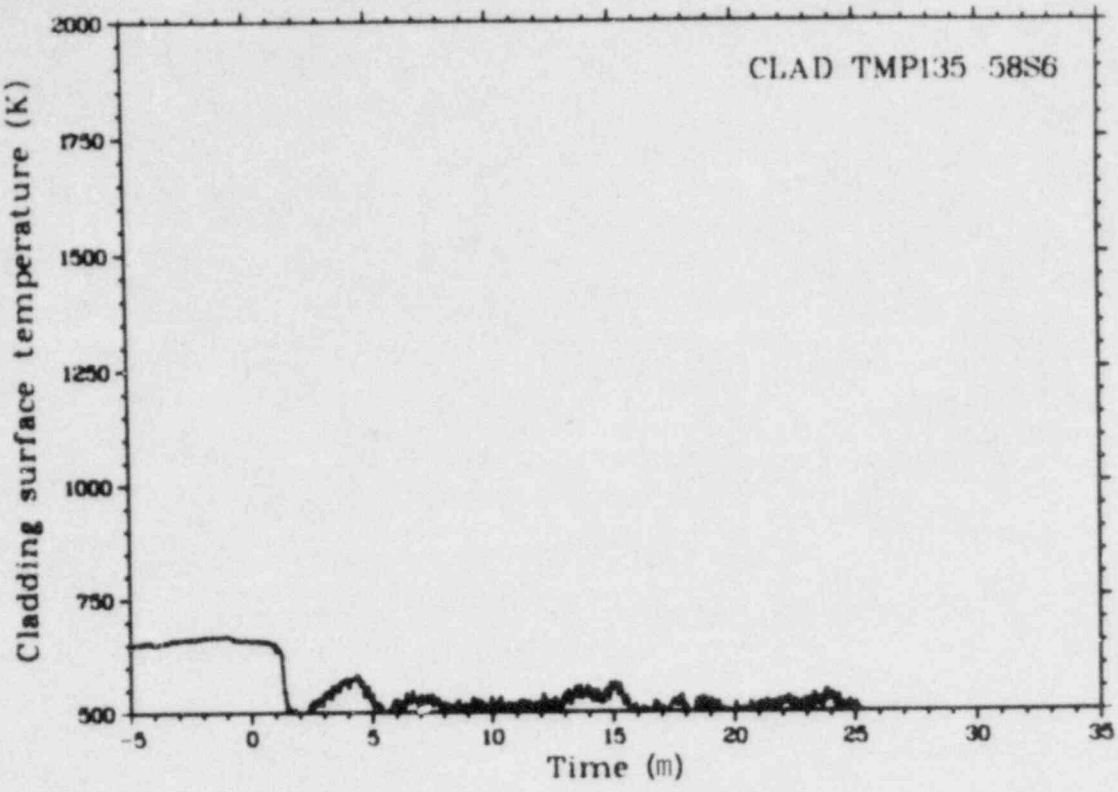
CLAD TMP135 58S6
Cladding surface temperature (K)
2000
1750
1500
1250
1000
750
500
-5
0
5
10
15
20
25
30
35
Time (m)

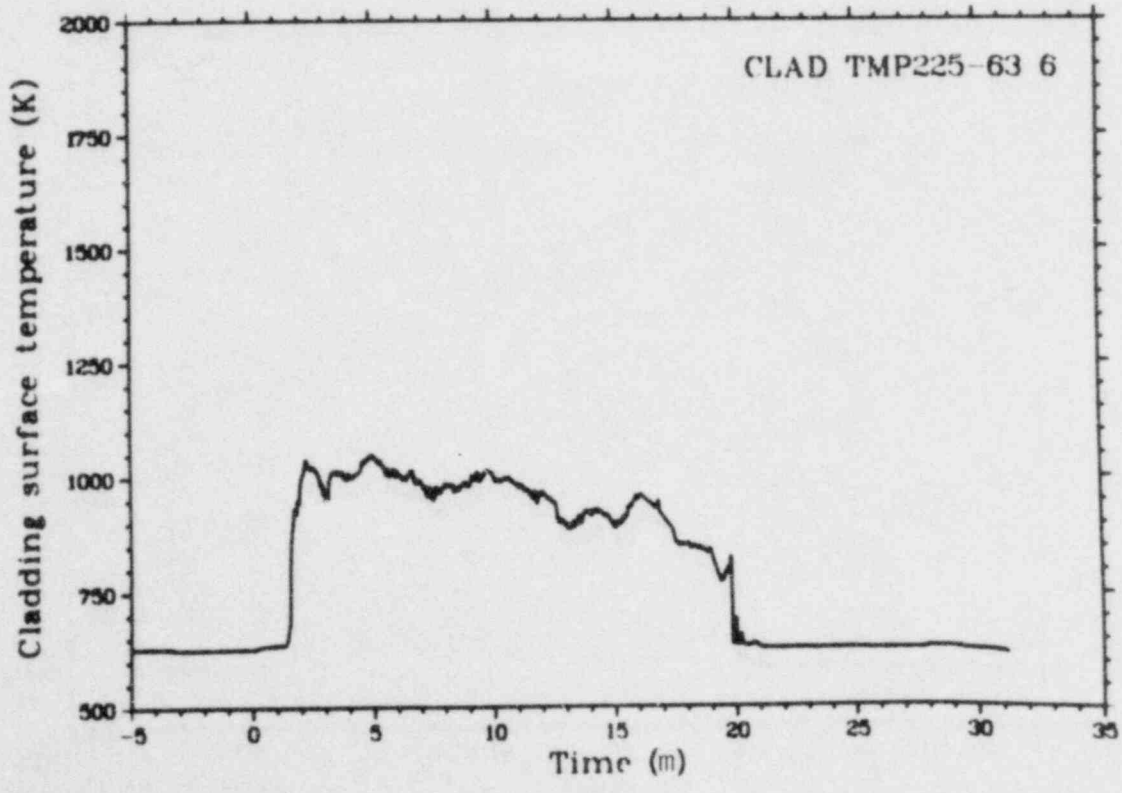
CLAD TMP225-63 6
Cladding surface temperature (K)
2000
1750
1500
1250
1000
750
500
-5
0
5
10
15
20
25
30
35
Time (m)

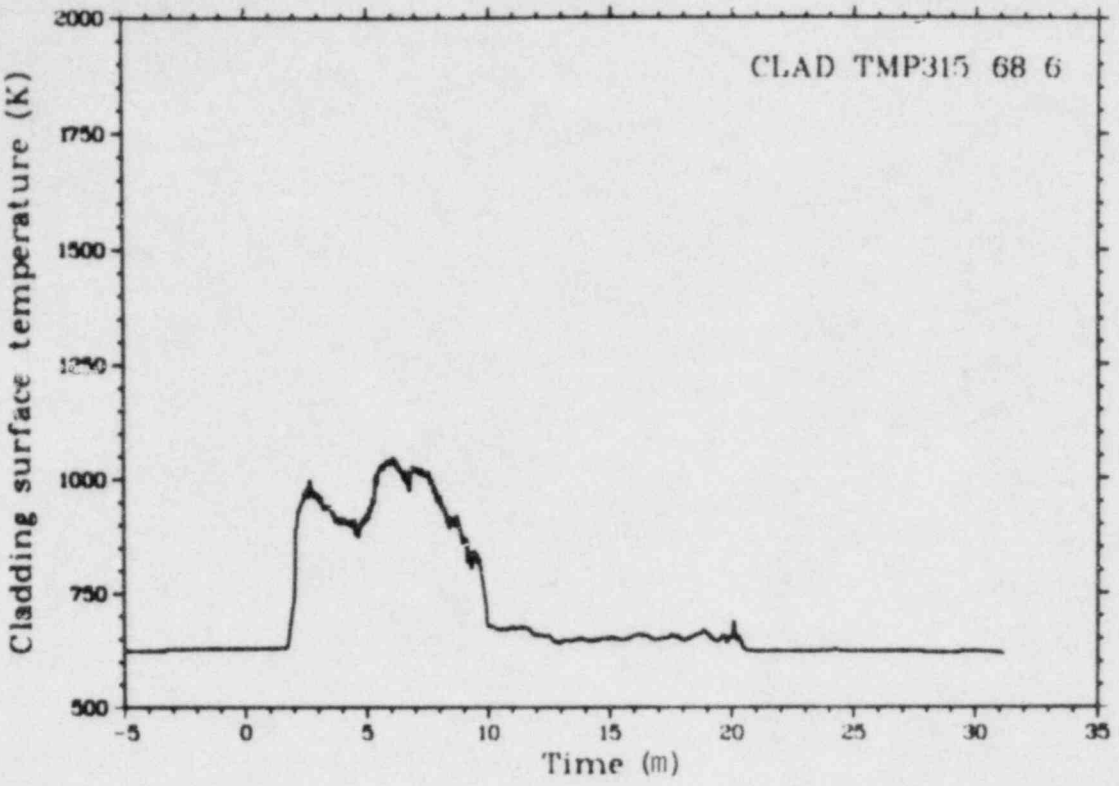
CLAD TMP315 68 6
Cladding surface temperature (K)
2000
1750
1500
1250
1000
750
500
-5
0
5
10
15
20
25
30
35
Time (m)

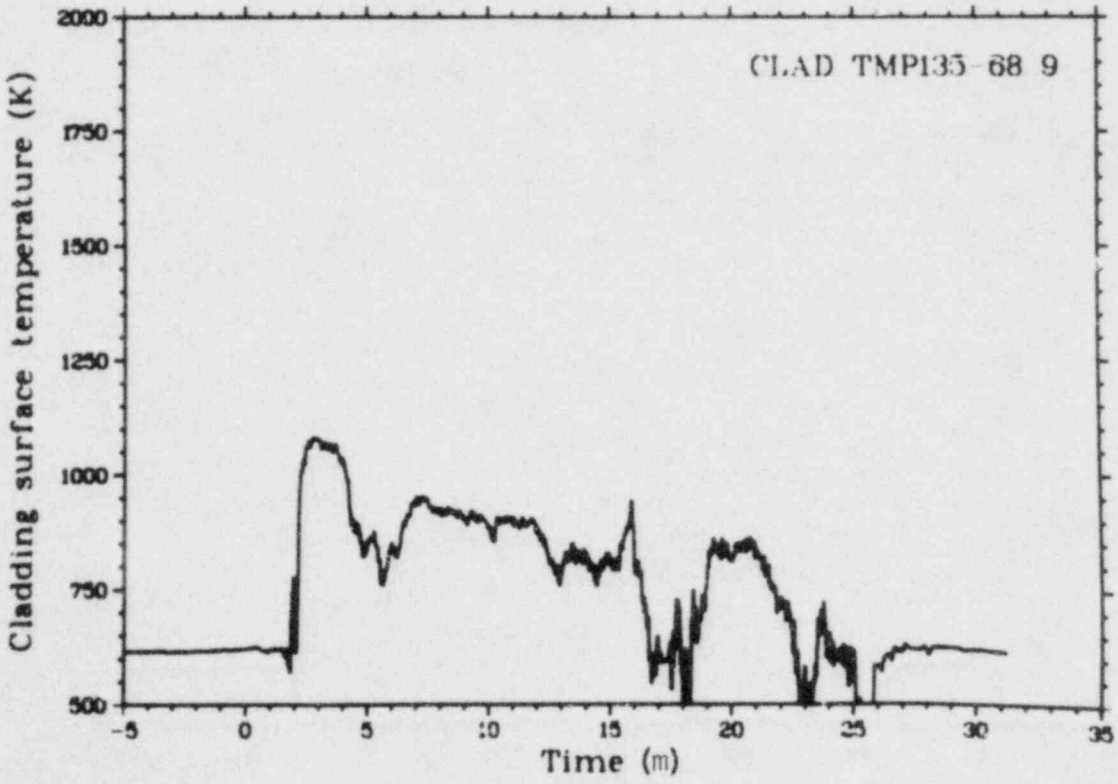
CLAD TMP135 68 9
Cladding surface temperature (K)
2000
1750
1500
1250
1000
750
500
-5
0
5
10
15
20
25
30
35
Time (m)

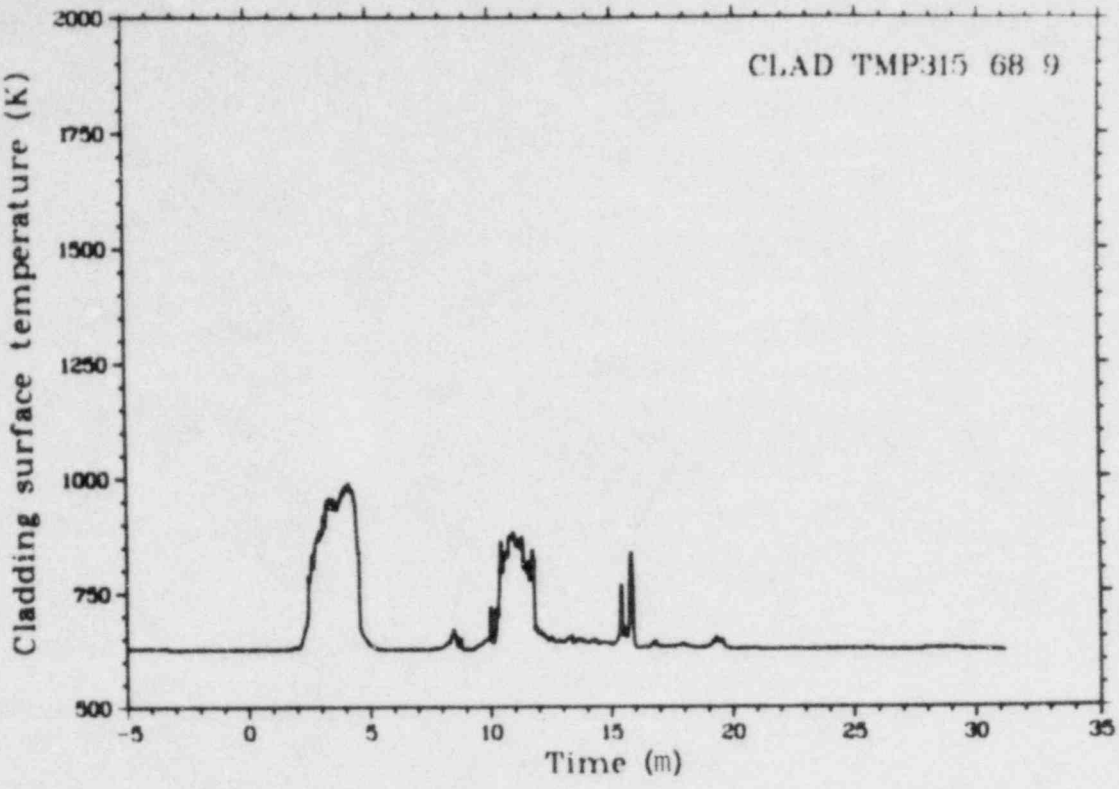
CLAD TMP315 68 9
Cladding surface temperature (K)
2000
1750
1500
1250
1000
750
500
-5
0
5
10
15
20
25
30
35
Time (m)

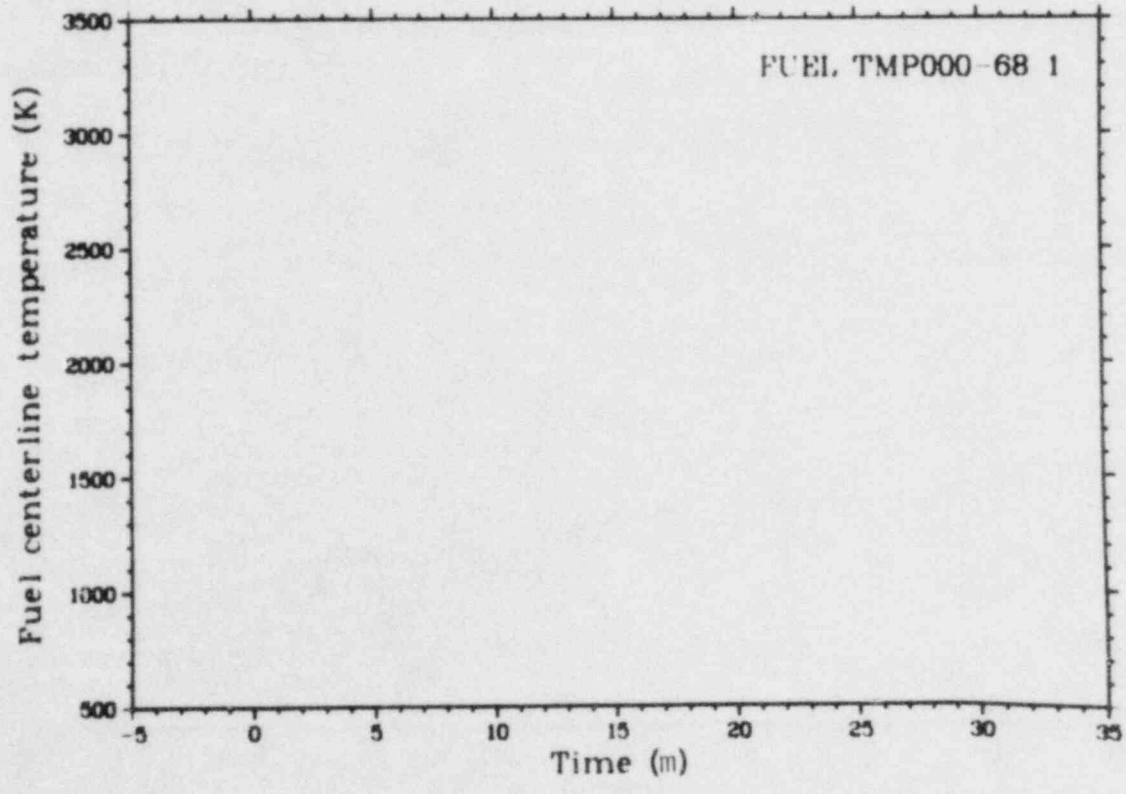
FUEL TMP000 68 1
Fuel centerline temperature (K)
3500
3000
2500
2000
1500
1000
500
-5
0
5
10
15
20
25
30
35
Time (m)

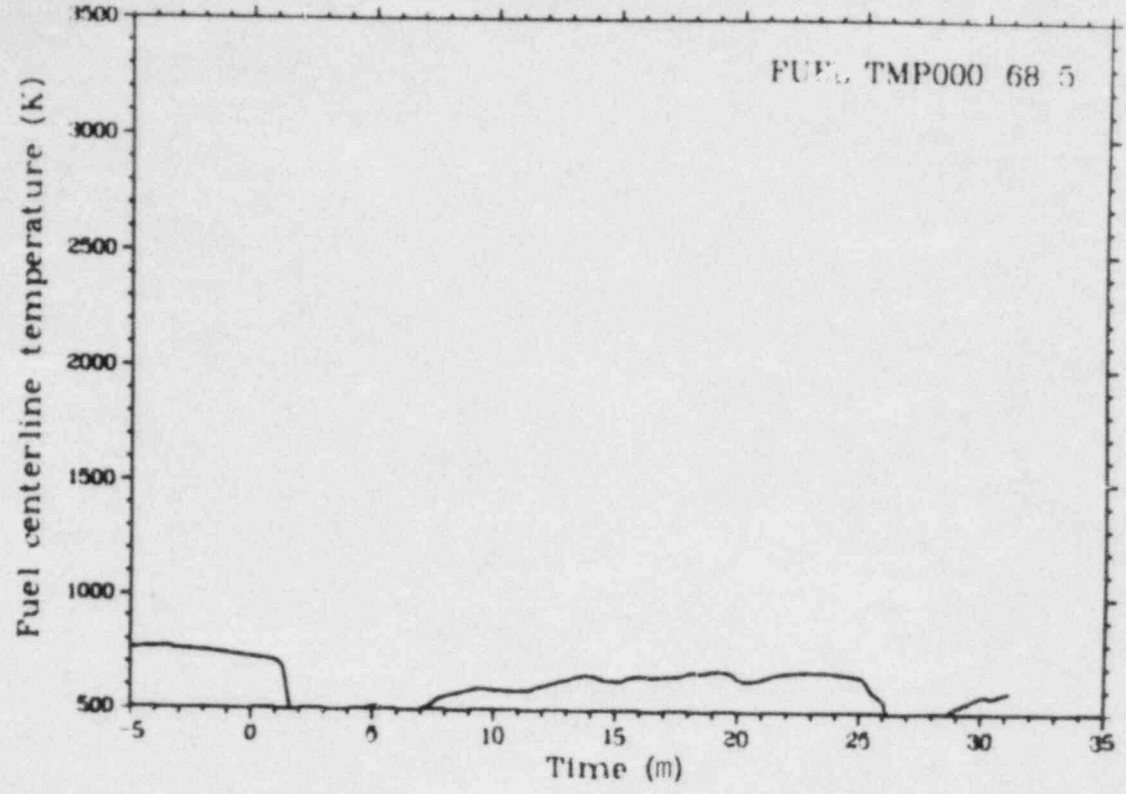
FUEL TMP000 68 5
Fuel centerline temperature (K)
3500
3000
2500
2000
1500
1000
500
-5
0
5
10
15
20
25
30
35
Time (m)

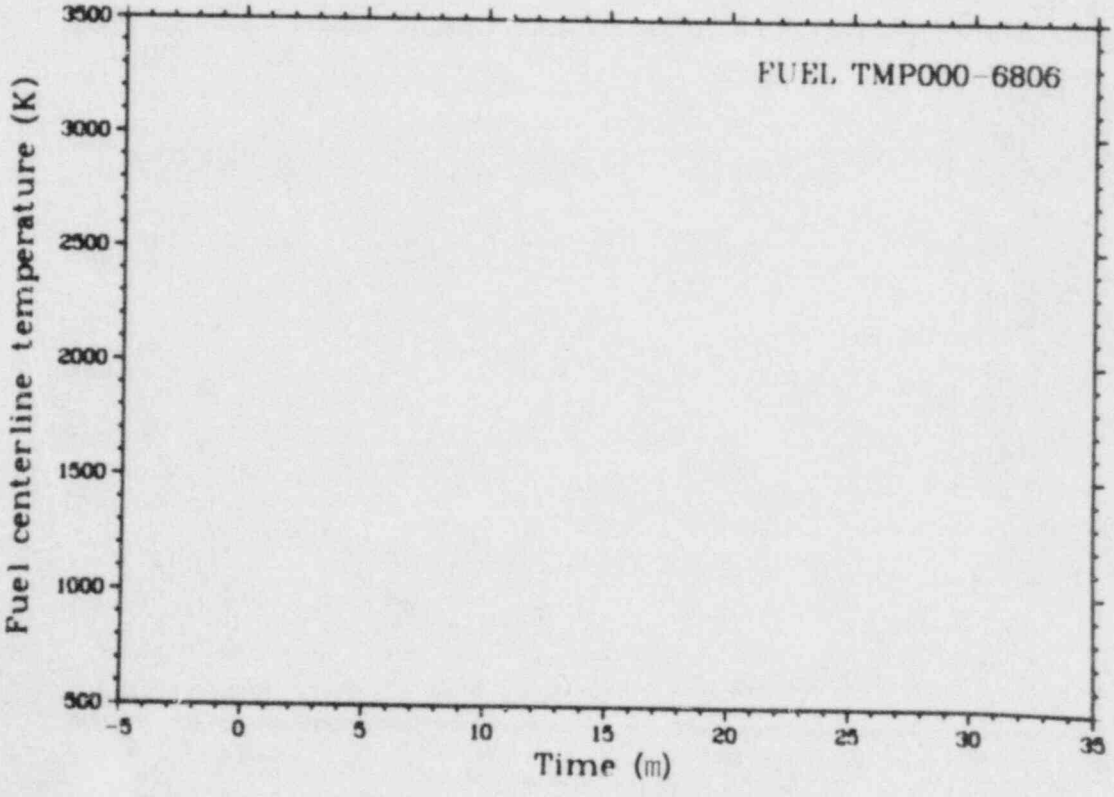
FUEL TMP000-6806
Fuel centerline temperature (K)
3500
3000
2500
2000
1500
1000
500
-5
0
5
10
15
20
25
30
35
Time (m)

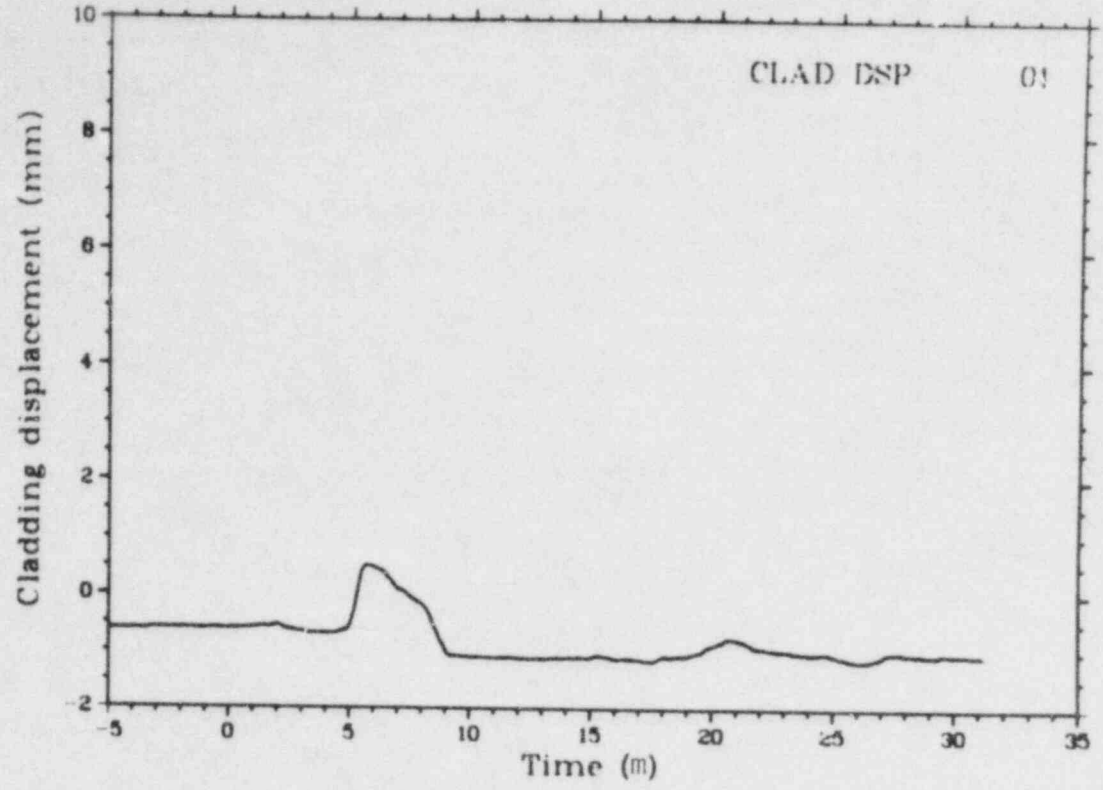
CLAD DSP 01
Cladding displacement (mm)
10
8
6
4
2
0
-2
-5
0
5
10
15
20
25
30
35
Time (m)

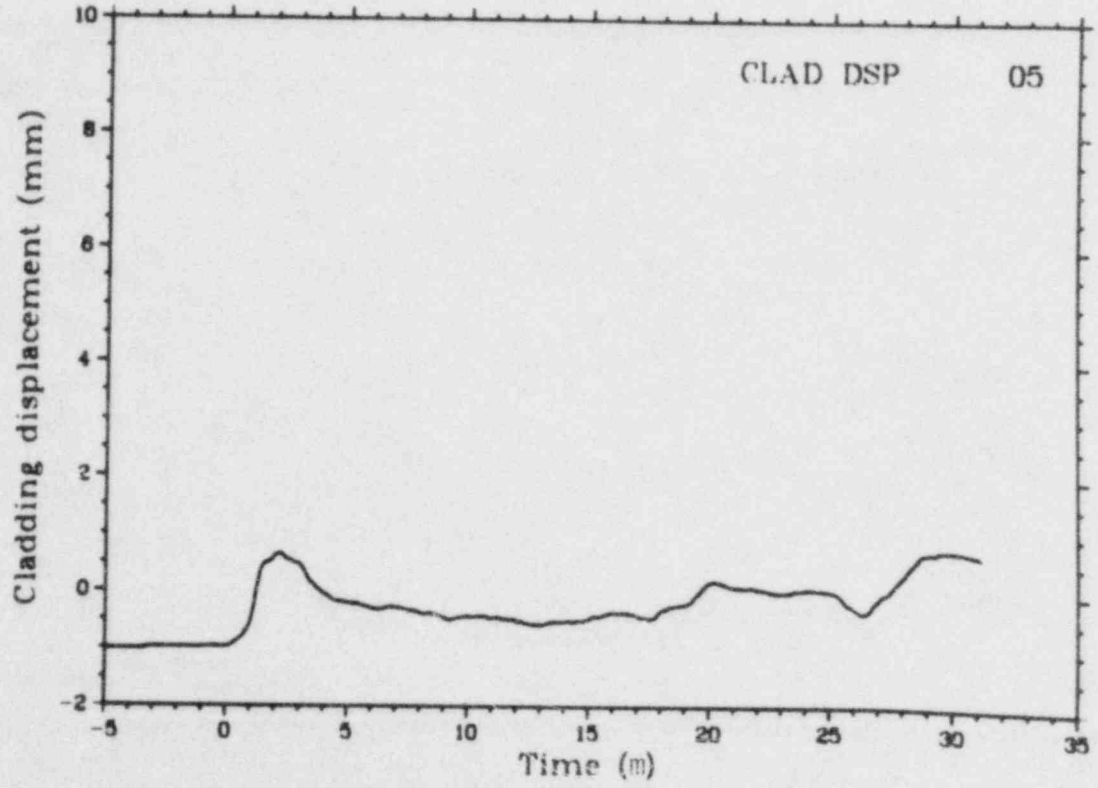
CLAD DSP 05
Cladding displacement (mm)
10
8
6
4
2
0
-2
-5
0
5
10
15
20
25
30
35
Time (m)

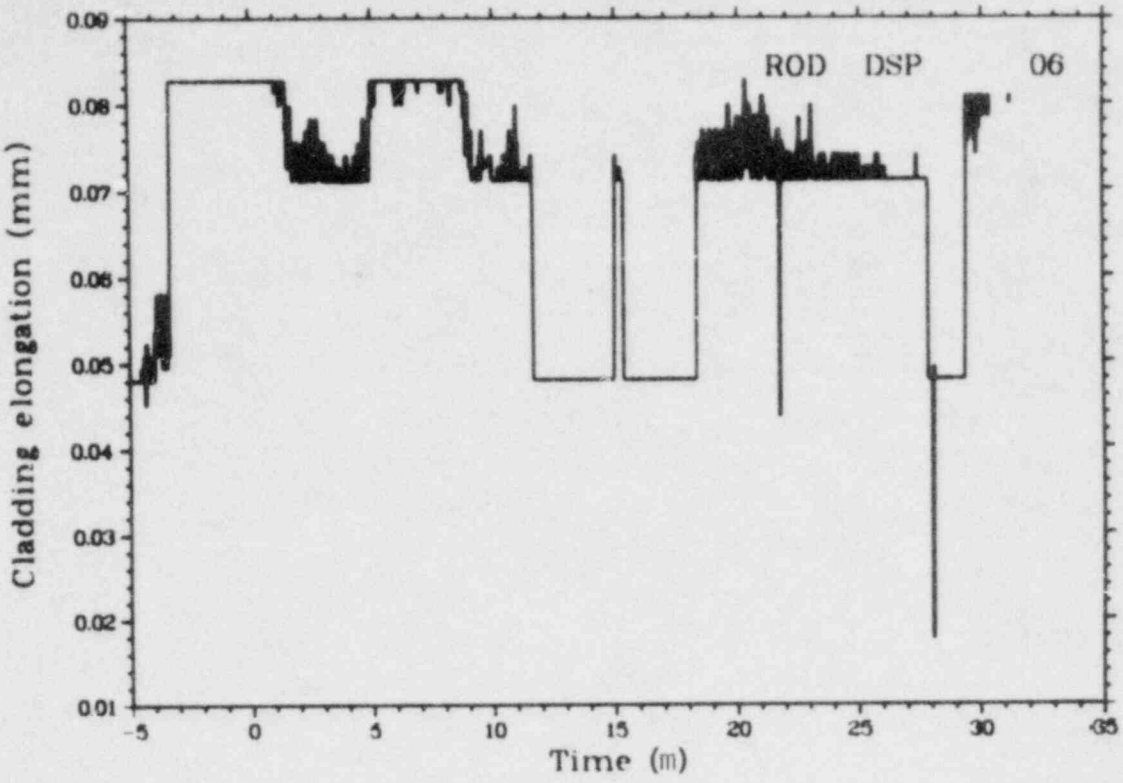
ROD DSP 06
Cladding elongation (mm)
0.09
0.08
0.07
0.06
0.05
0.04
0.03
0.02
0.01
-5
0
5
10
15
20
25
30
35
Time (m)

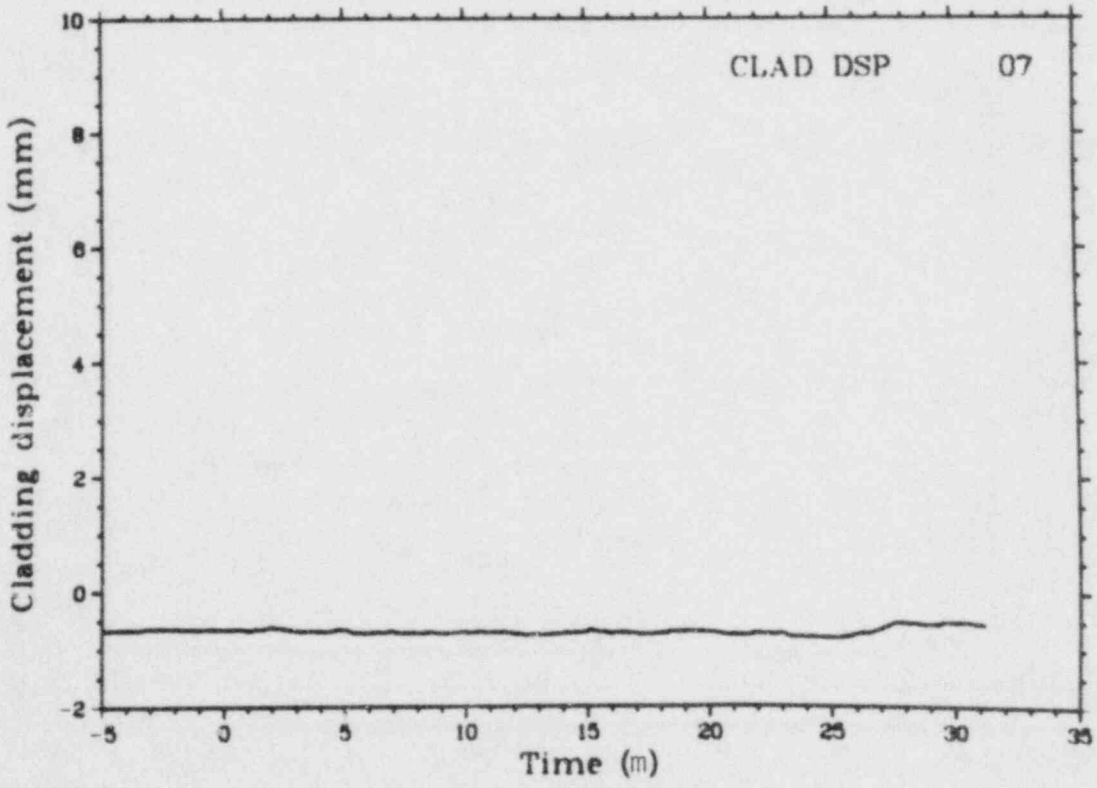
CLAD DSP 07
Cladding displacement (mm)
10
8
6
4
2
0
-2
-5
0
5
10
15
20
25
30
35
Time (m)

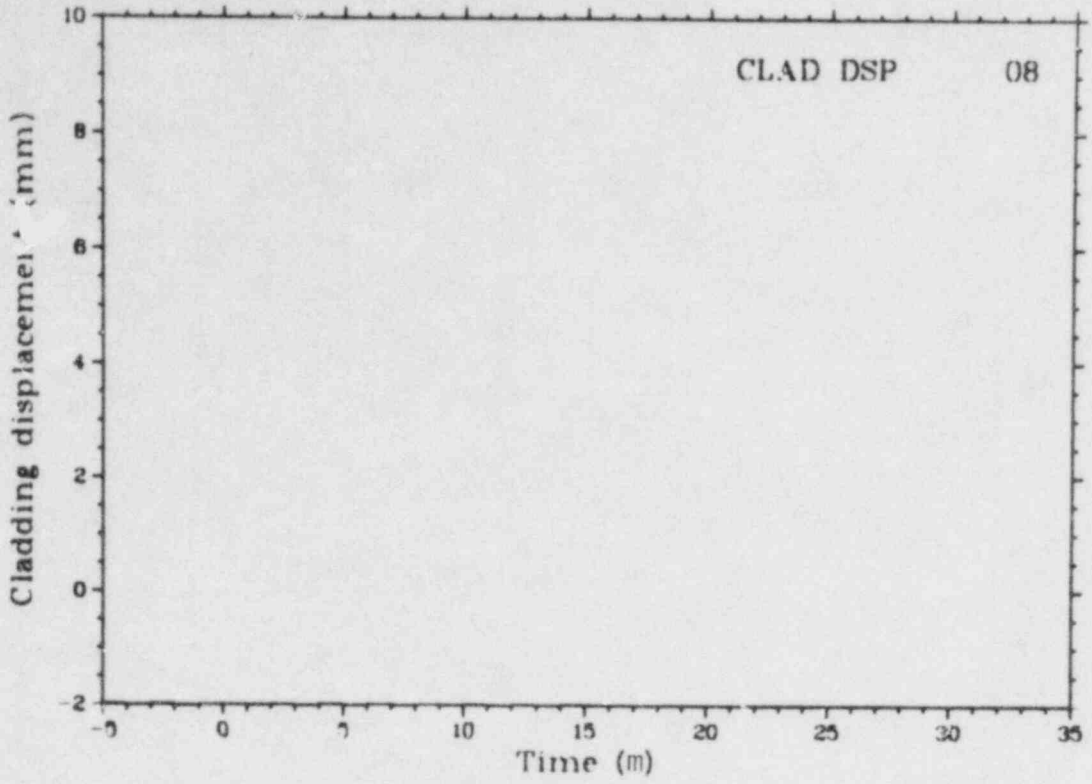
CLAD DSP 08
Cladding displacement (mm)
10
8
6
4
2
0
-2
-5
0
5
10
15
20
25
30
35
Time (m)

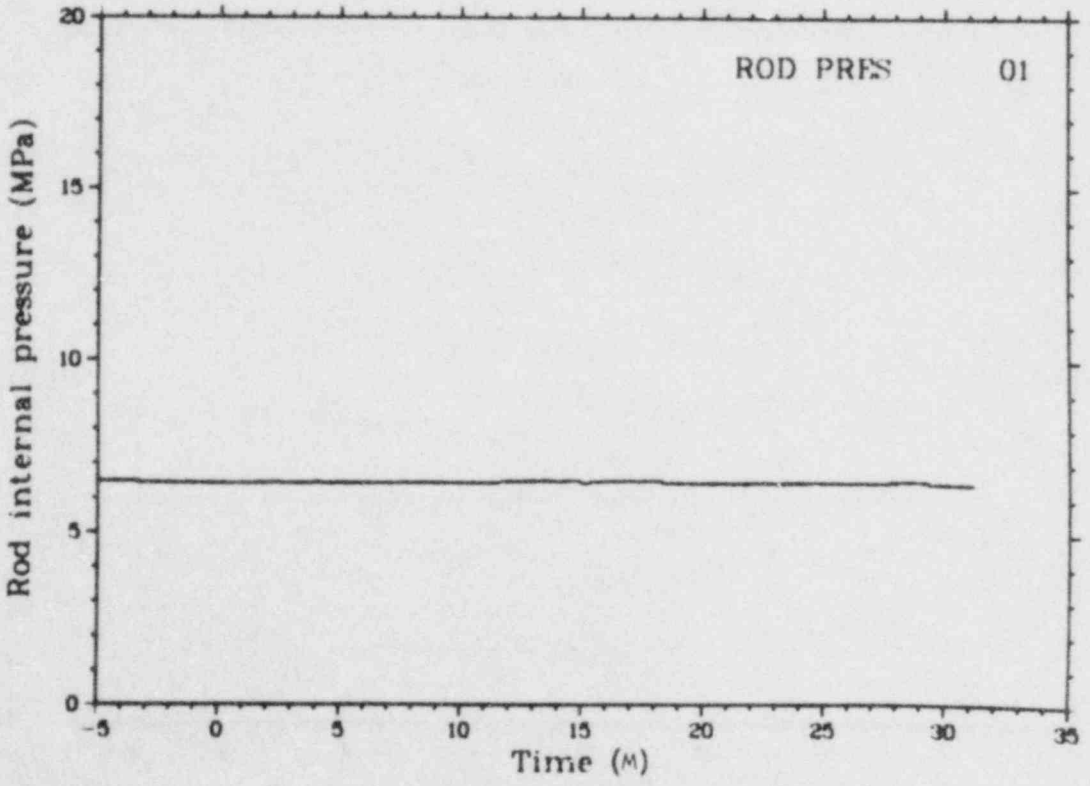
ROD PRES 01
Rod internal pressure (MPa)
20
15
10
5
0
-5
0
5
10
15
20
25
30
35
Time (M)

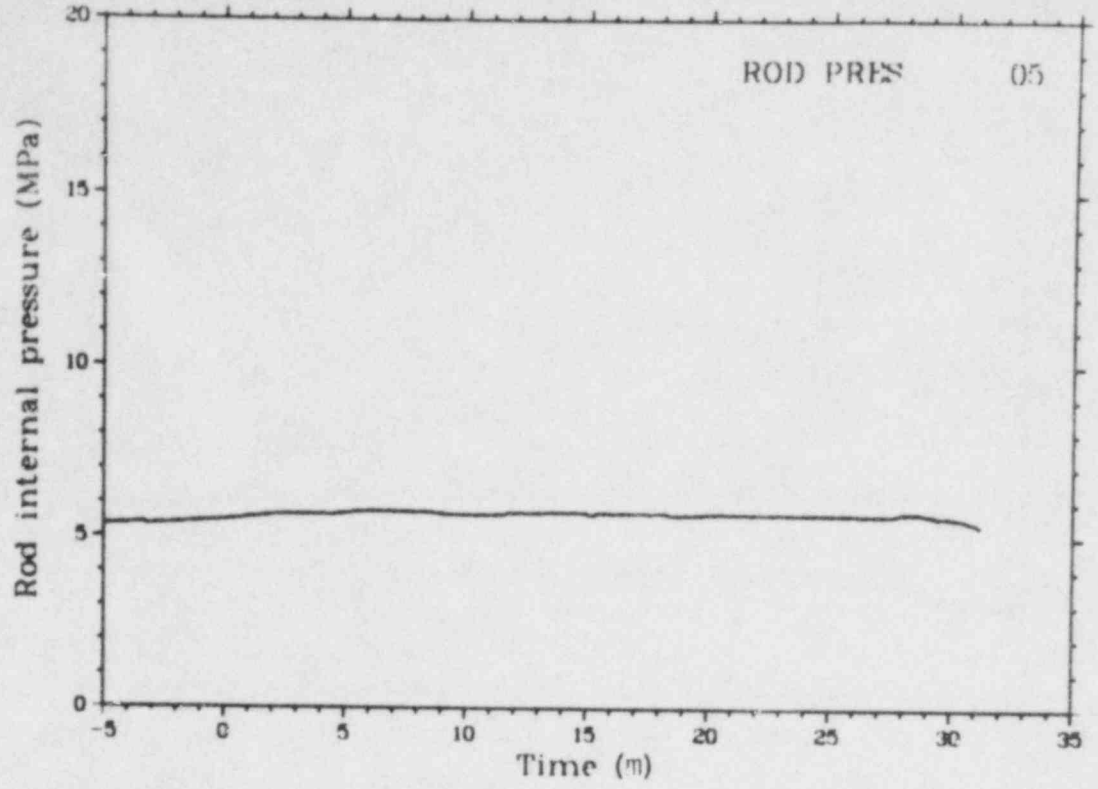
ROD PRES 05
Rod internal pressure (MPa)
0
5
10
15
20
-5
0
5
10
15
20
25
30
35
Time (m)

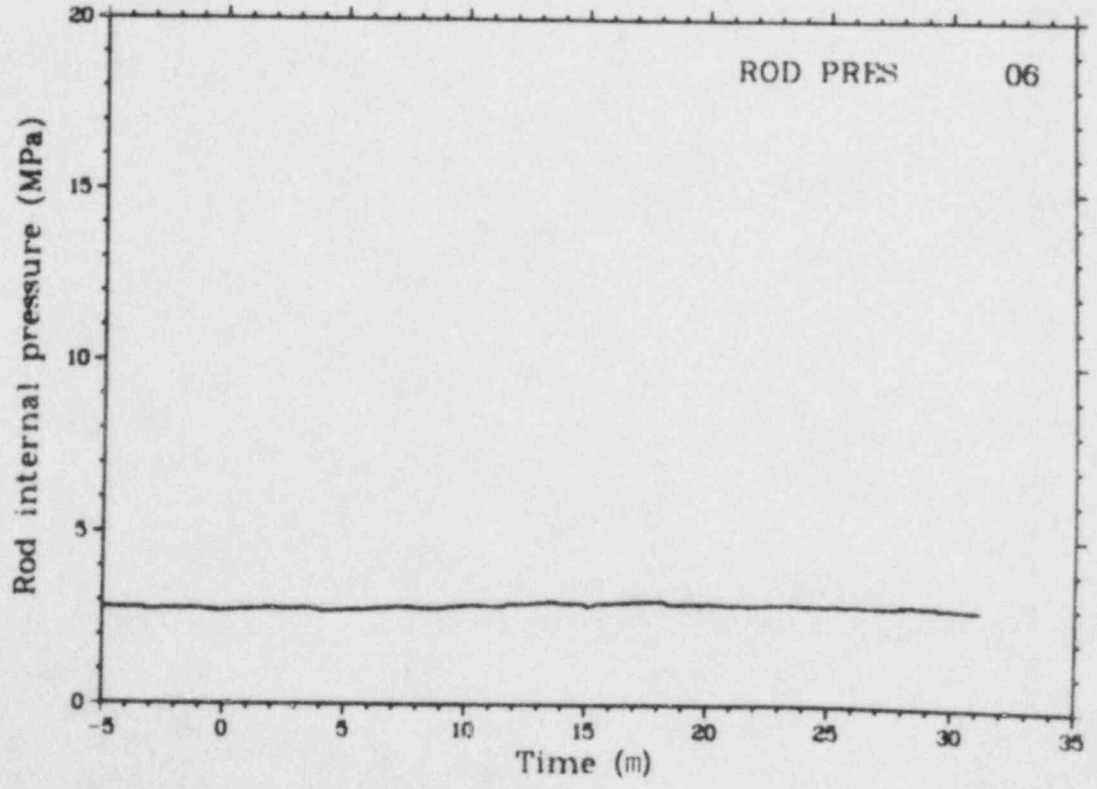
ROD PRES 06
Rod internal pressure (MPa)
0
5
10
15
20
-5
0
5
10
15
20
25
30
35
Time (m)

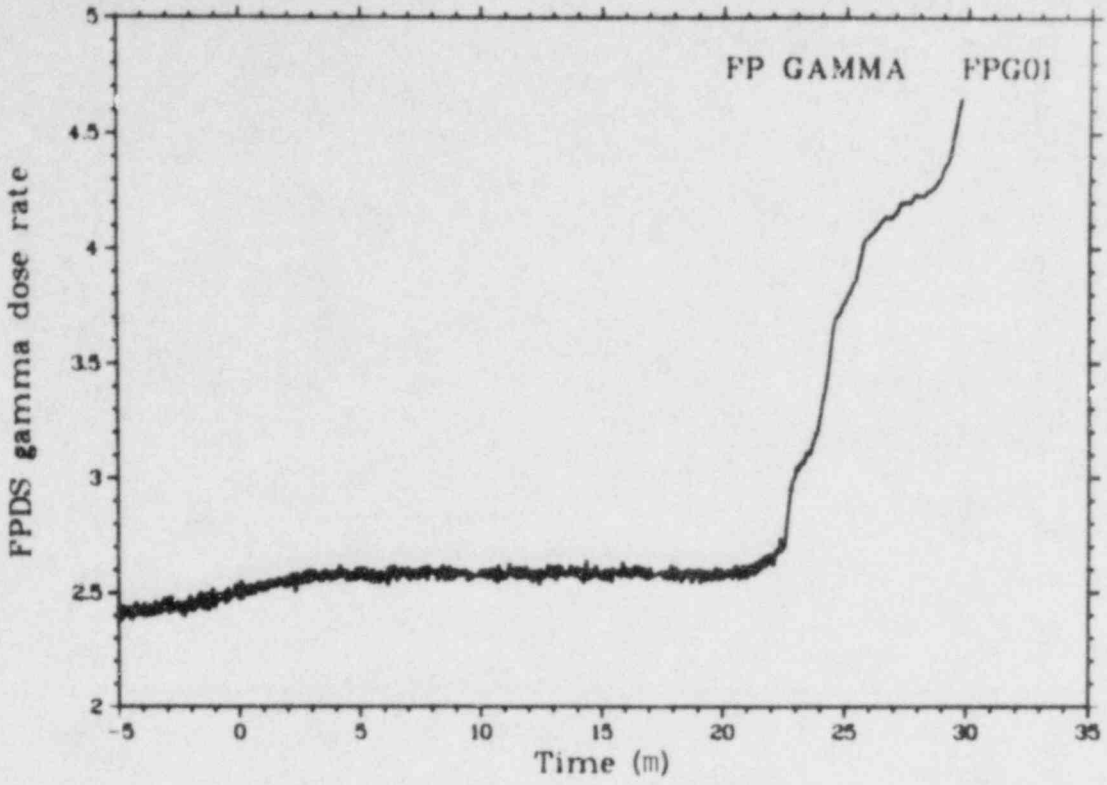
FP GAMMA FPG01
FPDS gamma dose rate
Time (m)

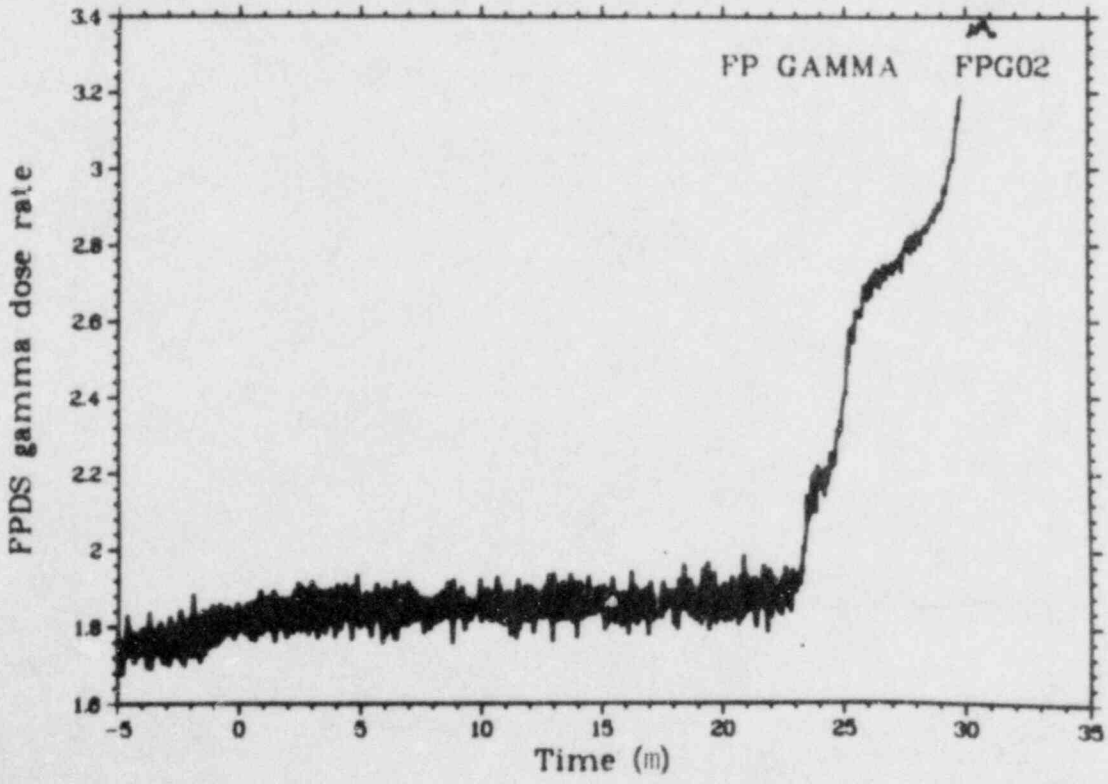
FP GAMMA FPG02
FPDS gamma dose rate
Time (m)

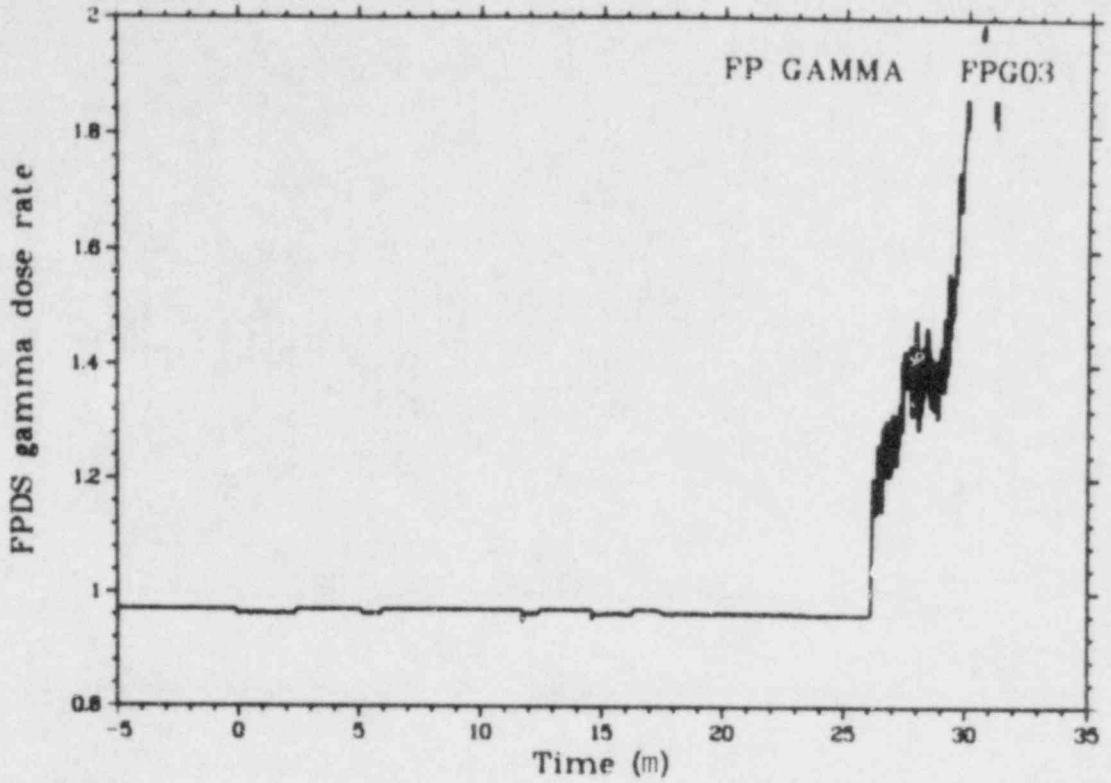
FP GAMMA FPG03
FPDS gamma dose rate
2
1.8
1.6
1.4
1.2
1
0.8
-5
0
5
10
15
20
25
30
35
Time (m)

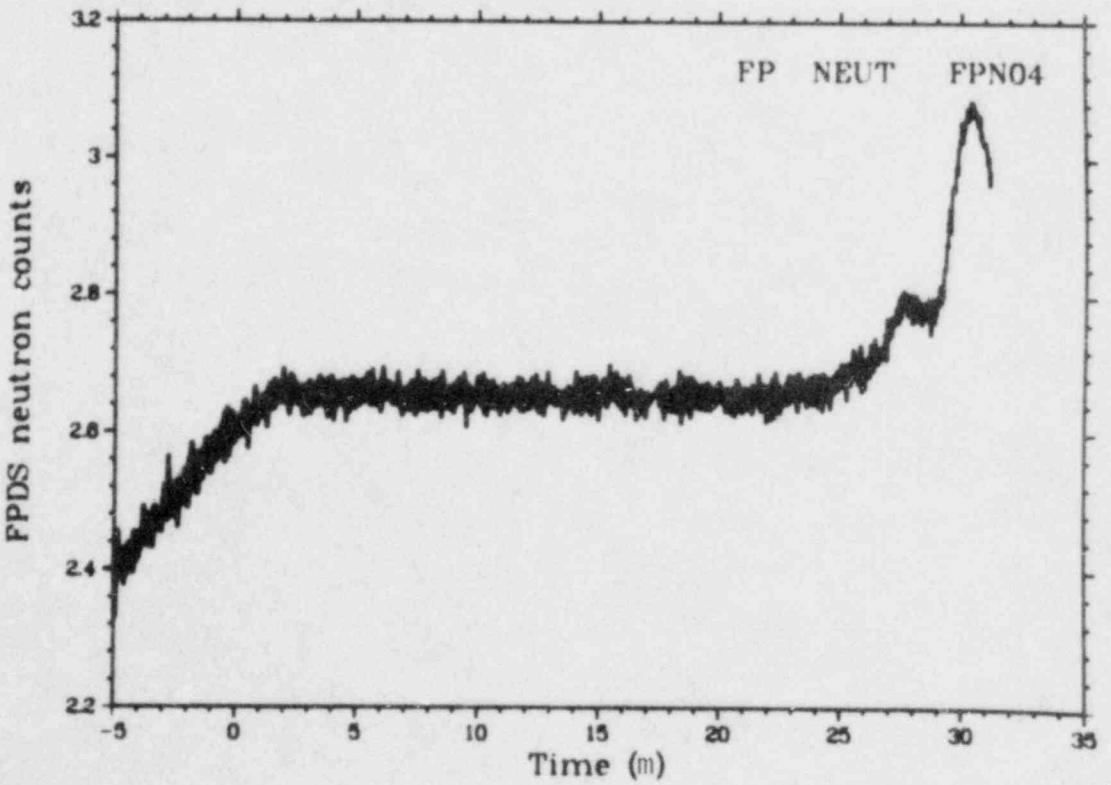
FP NEUT FPN04
FPDS neutron counts
3.2
3
2.8
2.6
2.4
2.2
-5
0
5
10
15
20
25
30
35
Time (m)

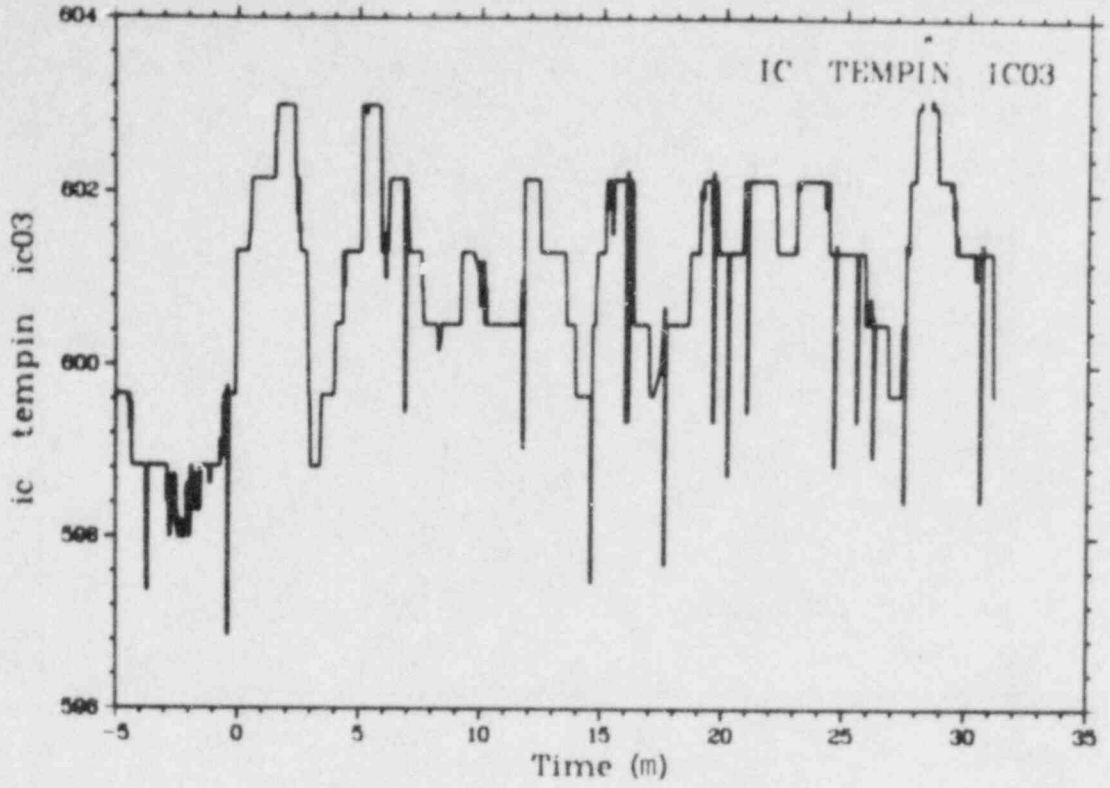
IC TEMPIN IC03
ic tempin ic03
604
602
600
598
596
-5
0
5
10
15
20
25
30
35
Time (m)

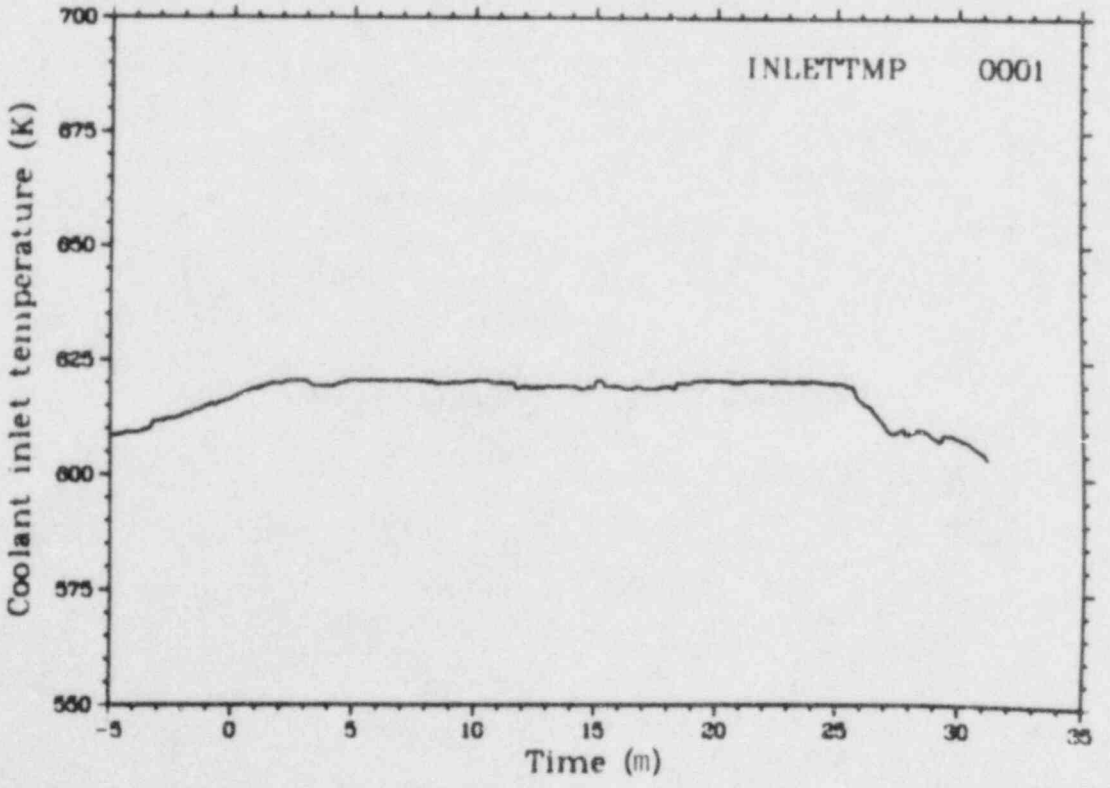
INLETTMP 0001
Coolant inlet temperature (K)
700
675
650
625
600
575
550
-5
0
5
10
15
20
25
30
35
Time (m)

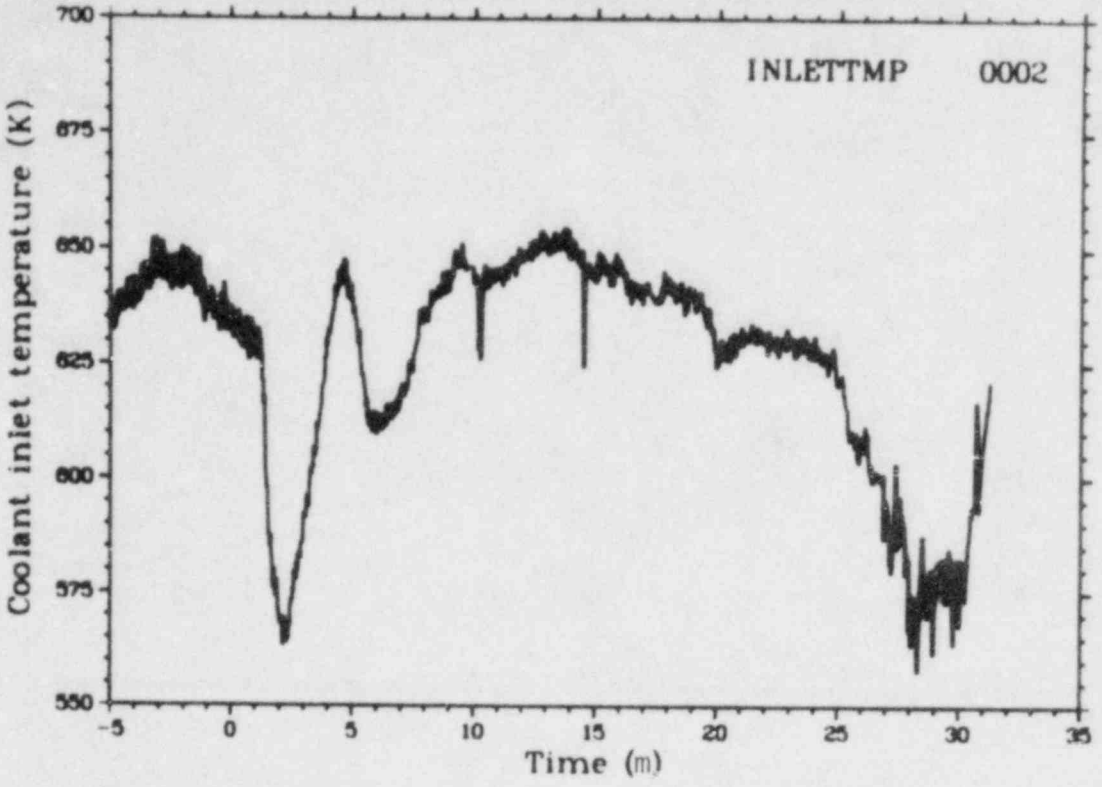
INLETTMP 0002
Coolant inlet temperature (K)
700
675
650
625
600
575
550
-5
0
5
10
15
20
25
30
35
Time (m)

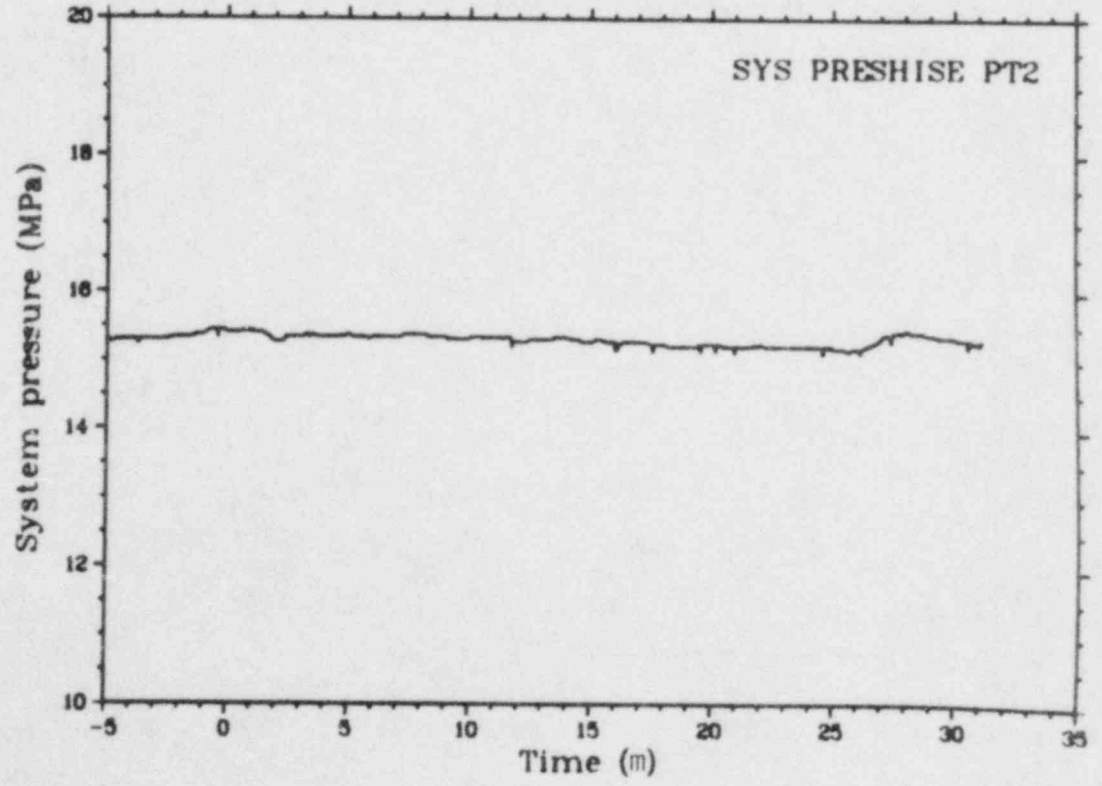
SYS PRESHISE PT2
System pressure (MPa)
20
18
16
14
12
10
-5
0
5
10
15
20
25
30
35
Time (m)

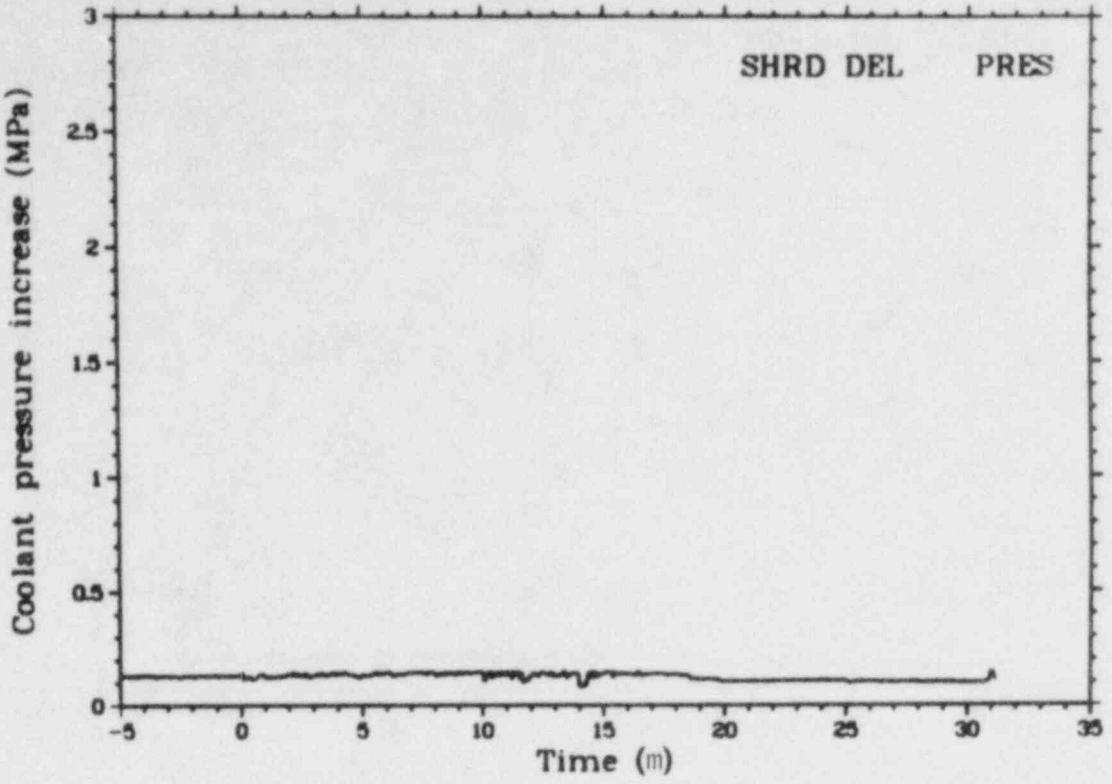
SHRD DEL PRES
Coolant pressure increase (MPa)
Time (m)

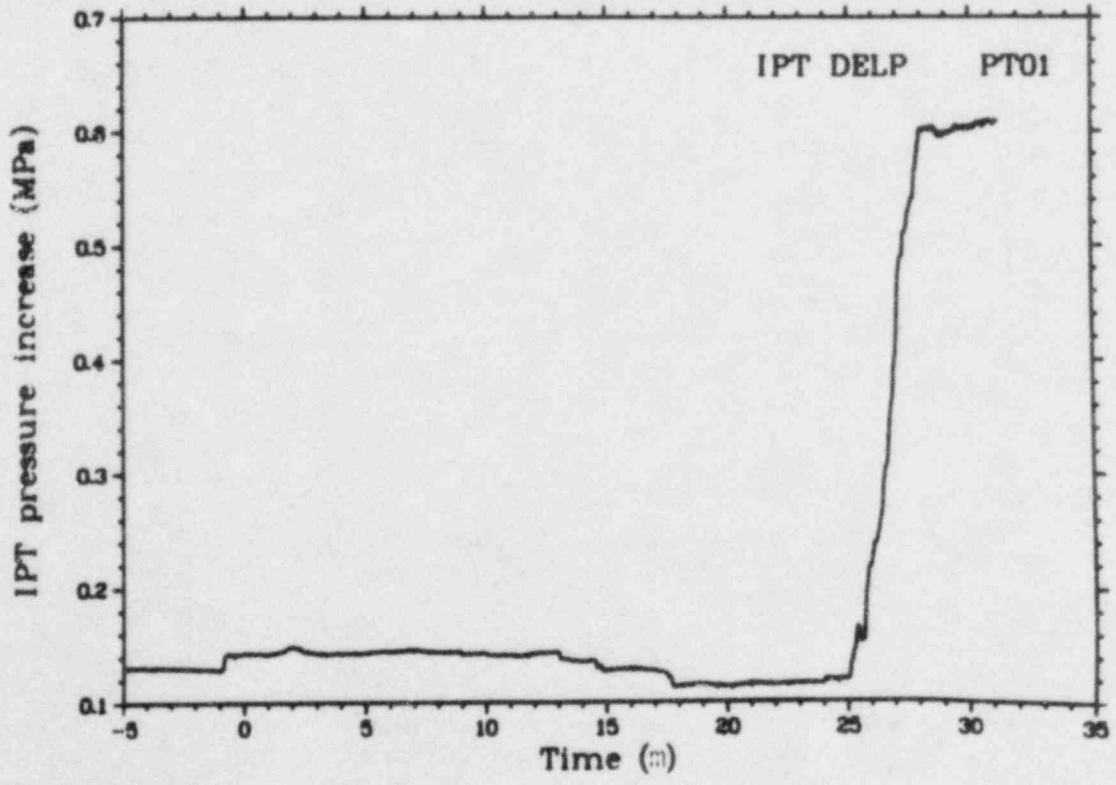
IPT DELP PT01
IPT pressure increase (MPa)
Time (m)

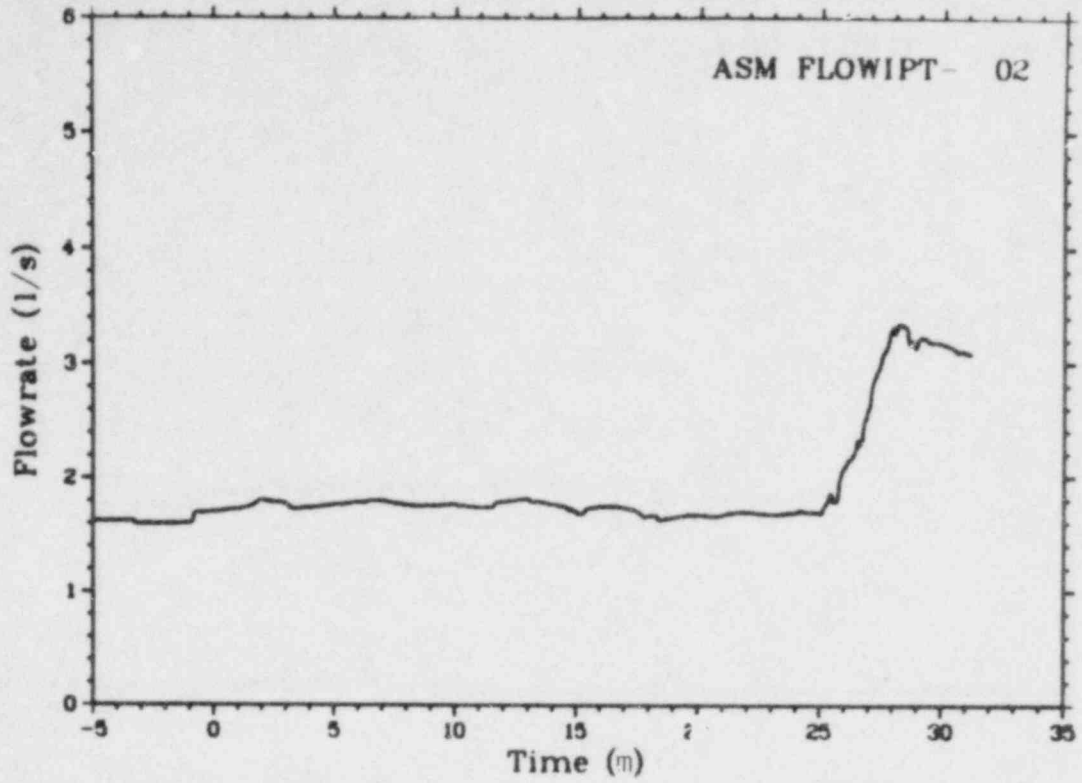
ASM FLOWIPT- 02
Flowrate (l/s)
Time (m)

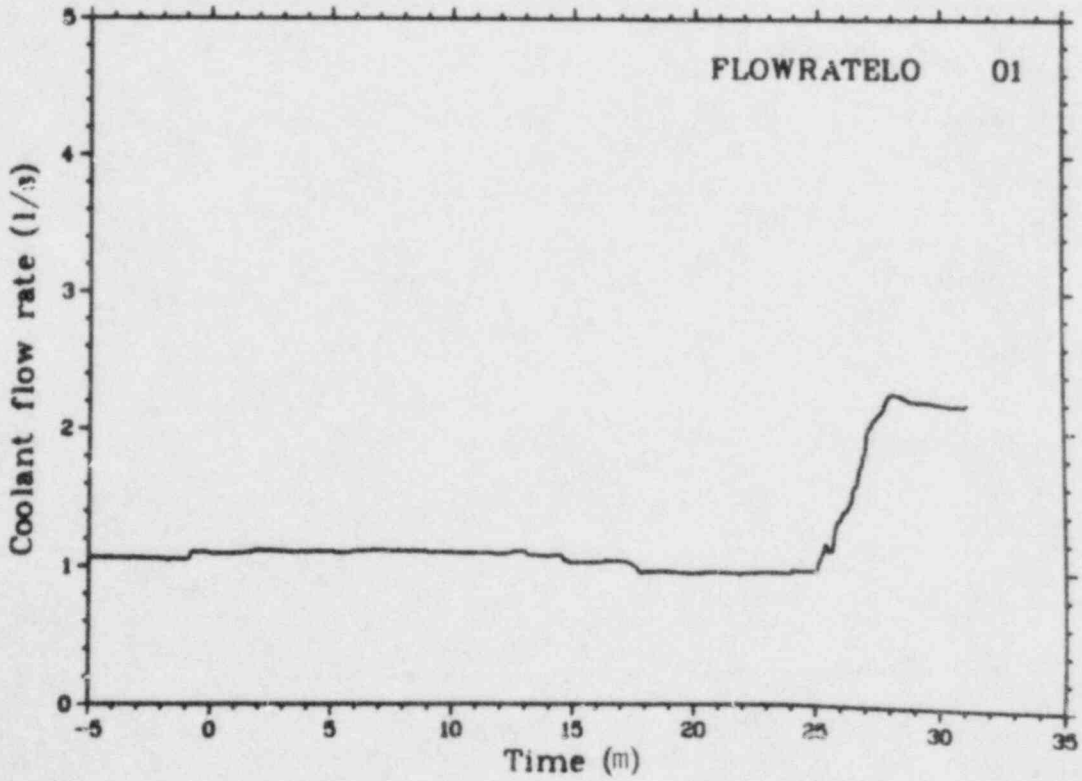
FLOWRATELO 01
Coolant flow rate (l/s)
Time (m)

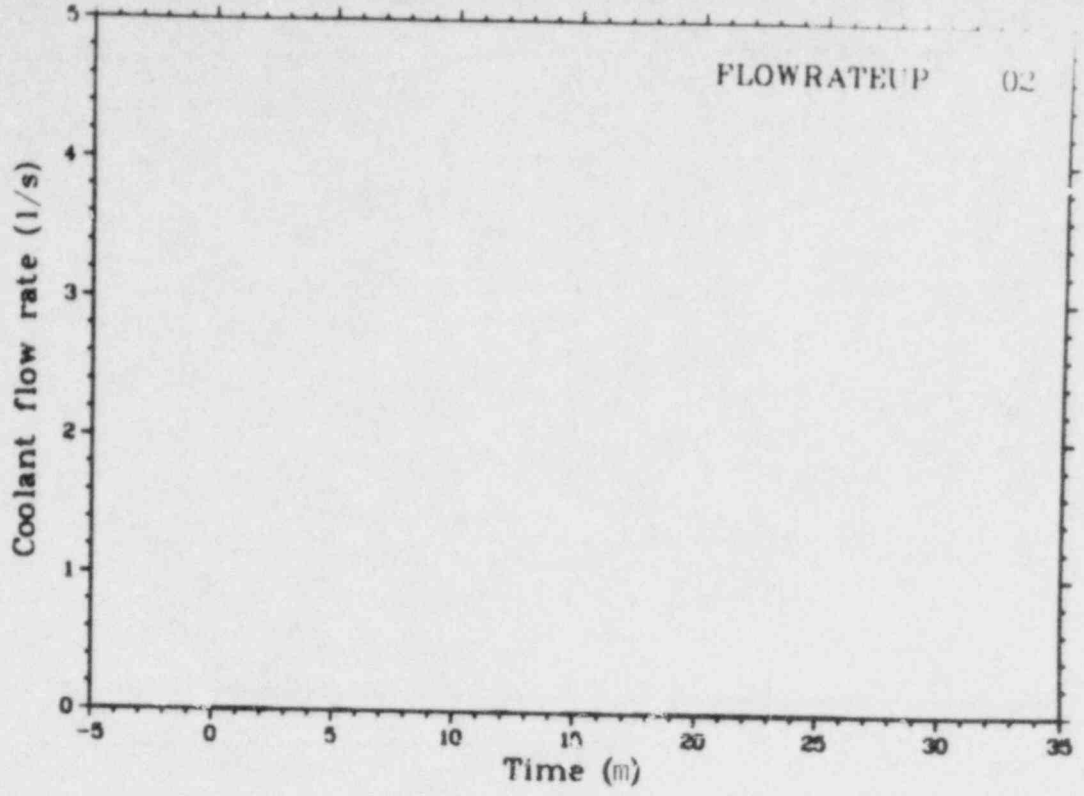
FLOWRATEUP 02
Coolant flow rate (l/s)
0
1
2
3
4
5
-5
0
5
10
15
20
25
30
35
Time (m)

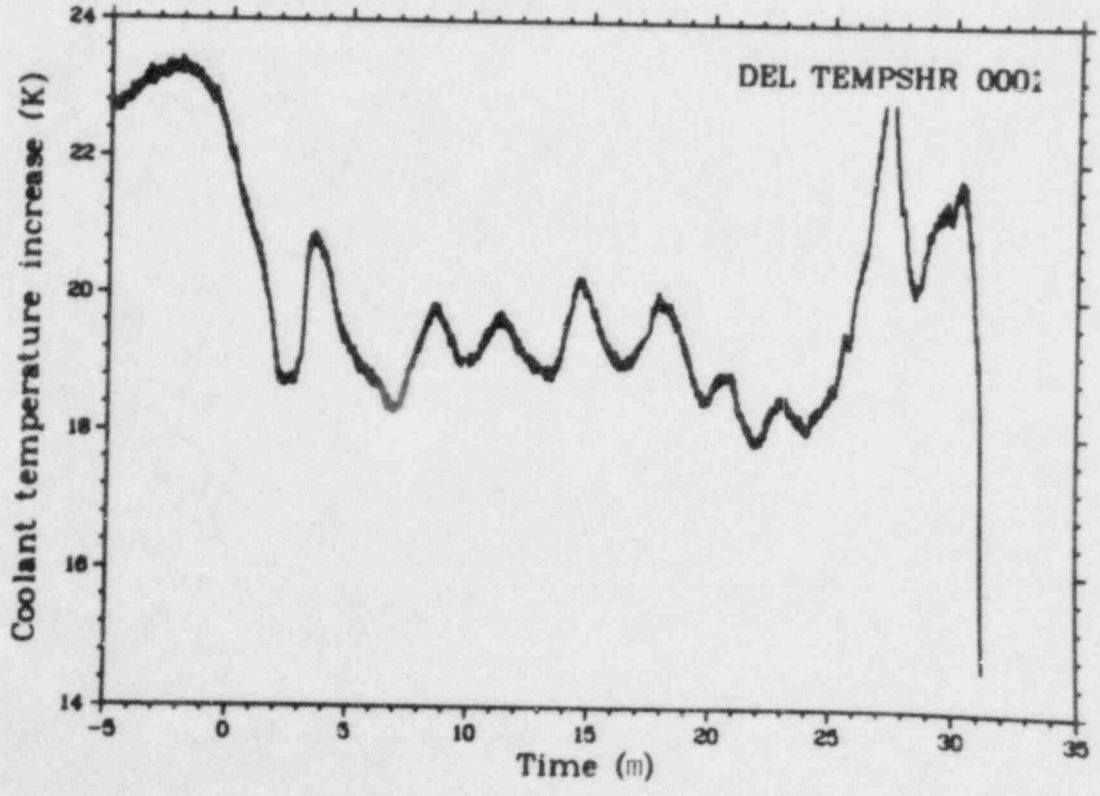
DEL TEMPSHR 000:
Coolant temperature increase (K)
14
16
18
20
22
24
-5
0
5
10
15
20
25
30
35
Time (m)

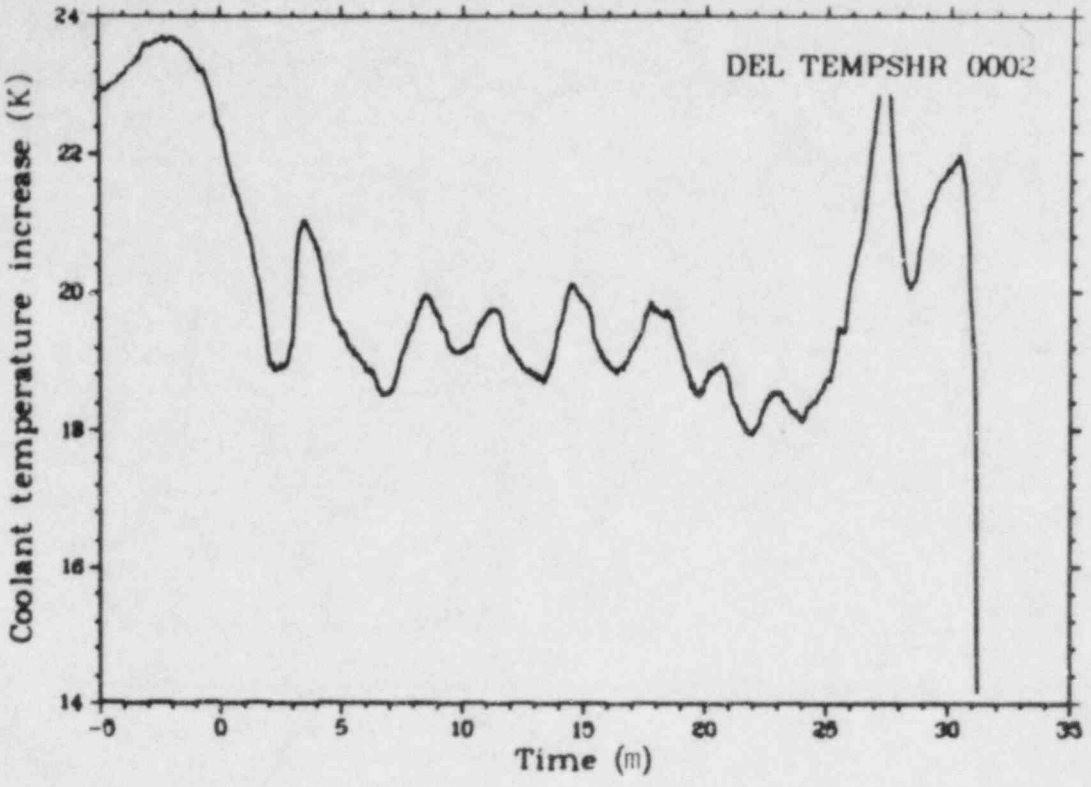
DEL TEMPSHR 0002
Coolant temperature increase (K)
24
22
20
18
16
14
-5
0
5
10
15
20
25
30
35
Time (m)

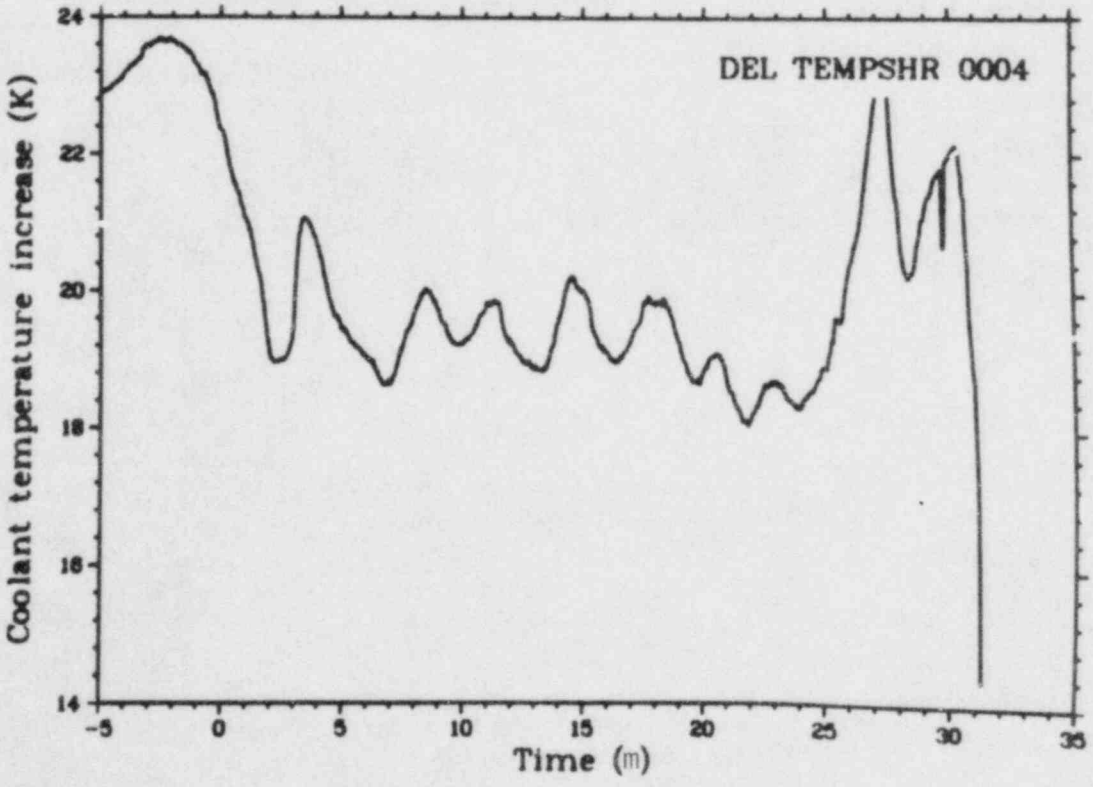
DEL TEMPSHR 0004
Coolant temperature increase (K)
24
22
20
18
16
14
-5
0
5
10
15
20
25
30
35
Time (m)

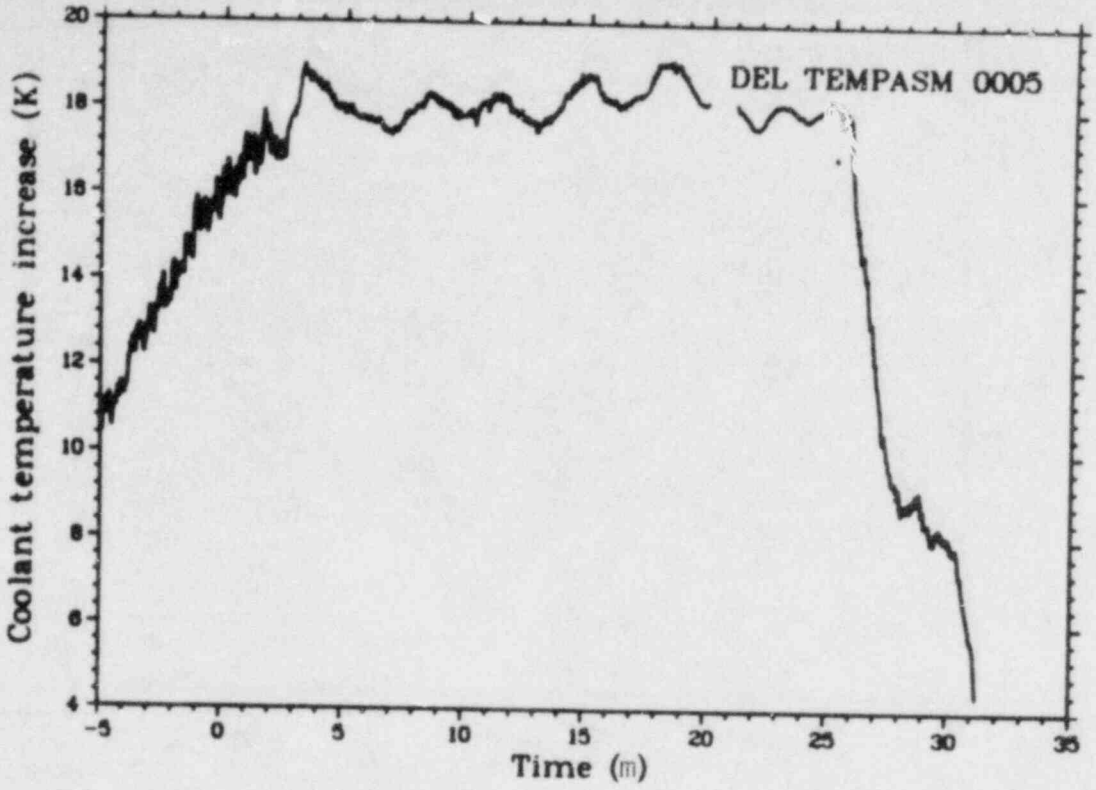
DEL TEMPASM 0005
Coolant temperature increase (K)
Time (m)

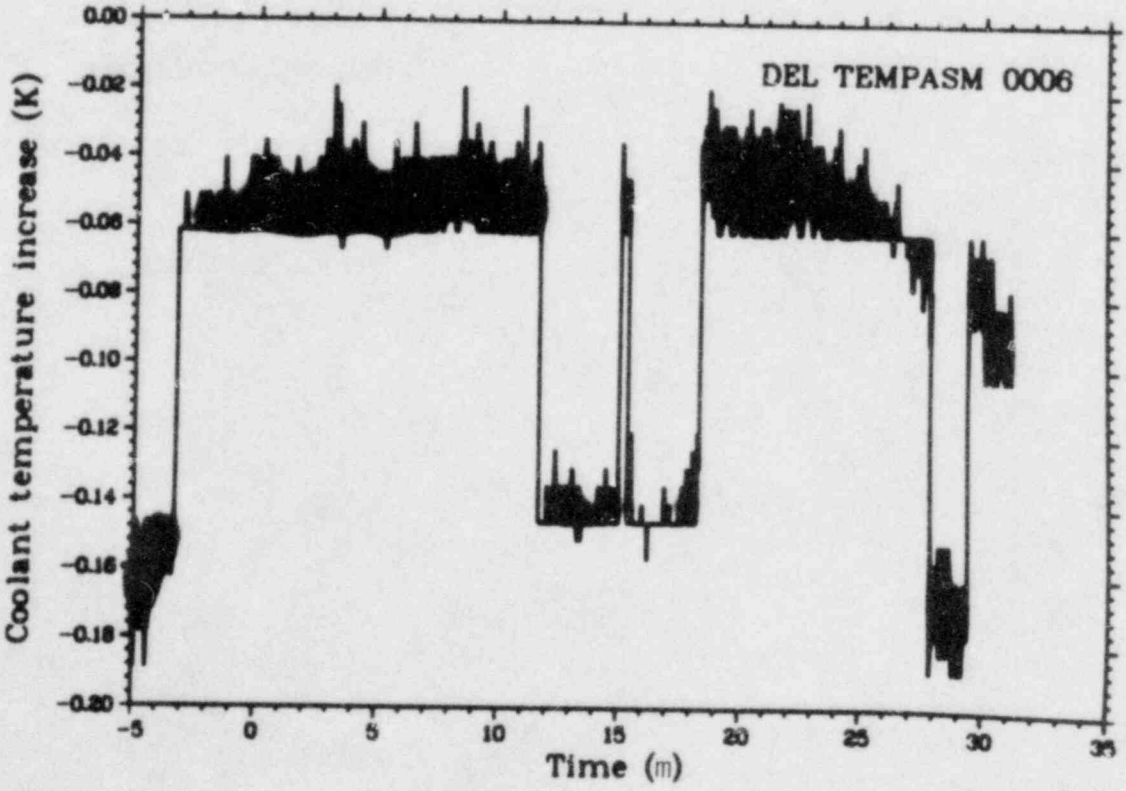
DEL TEMPASM 0006
Coolant temperature increase (K)
Time (m)

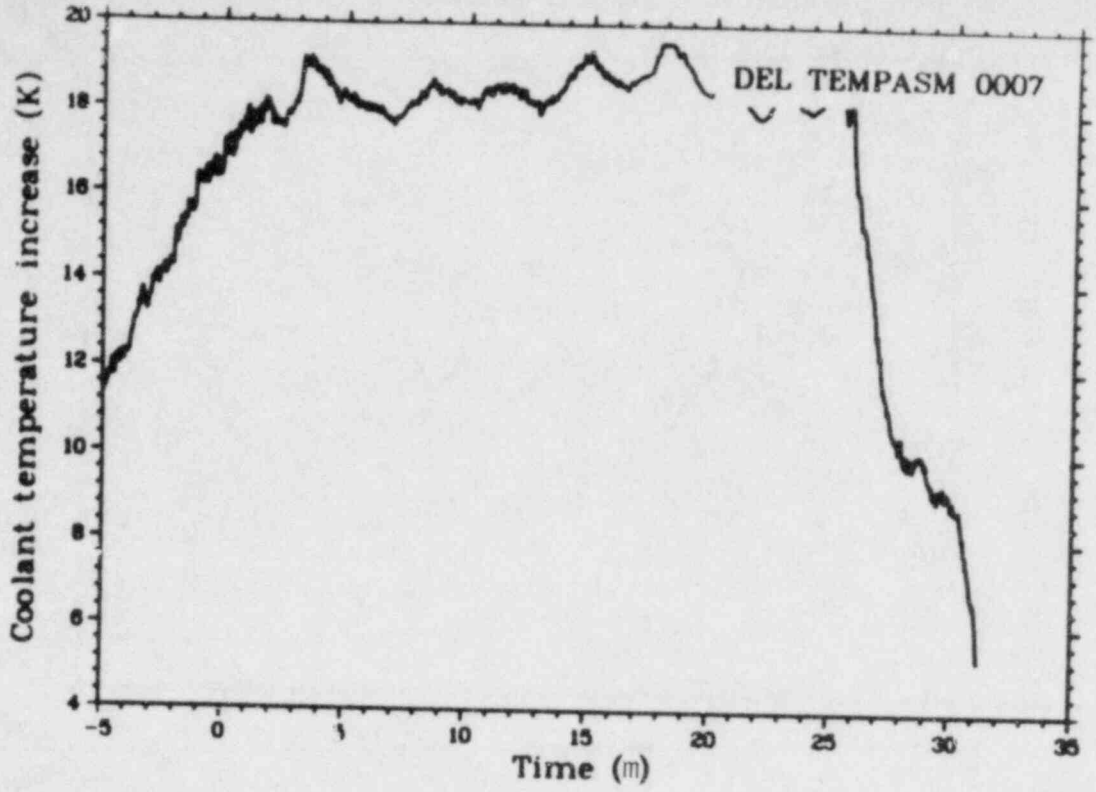
DEL TEMPASM 0007
Coolant temperature increase (K)
Time (m)

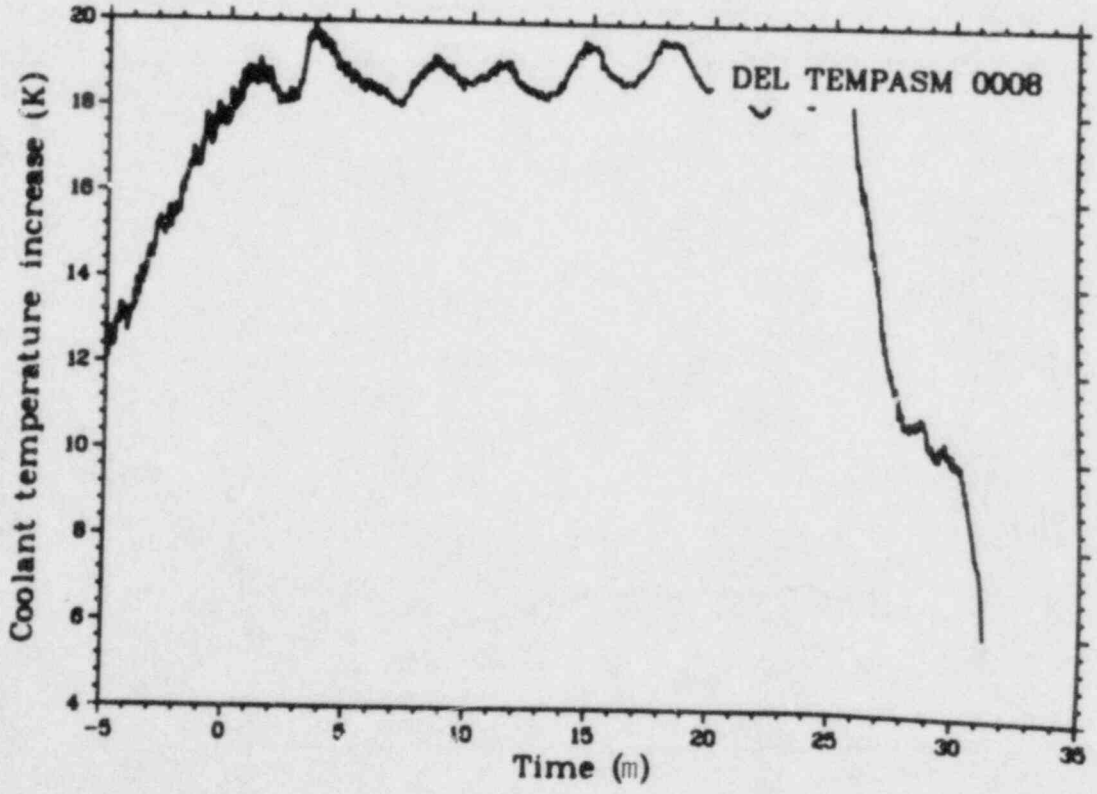
DEL TEMPASM 0008
Coolant temperature increase (K)
Time (m)

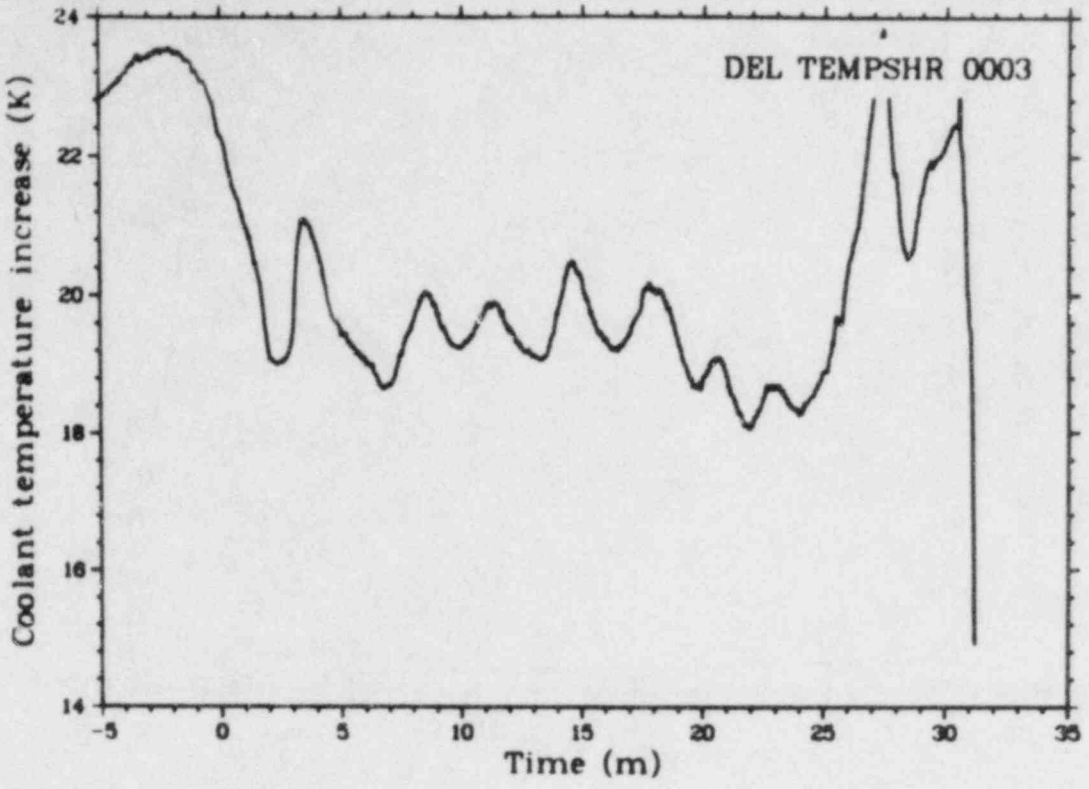
DEL TEMPSHR 0003
Coolant temperature increase (K)
24
22
20
18
16
14
-5
0
5
10
15
20
25
30
35
Time (m)

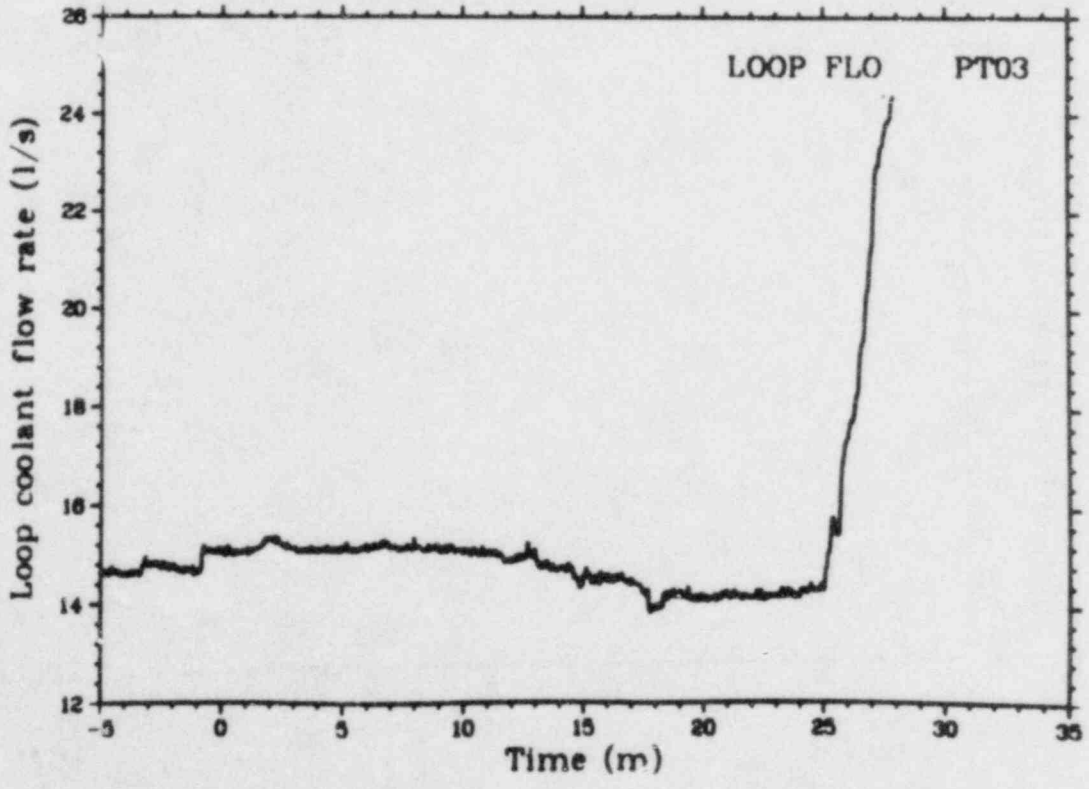
LOOP FLO PT03
Loop coolant flow rate (l/s)
26
24
22
20
18
16
14
12
-5
0
5
10
15
20
25
30
35
Time (m)

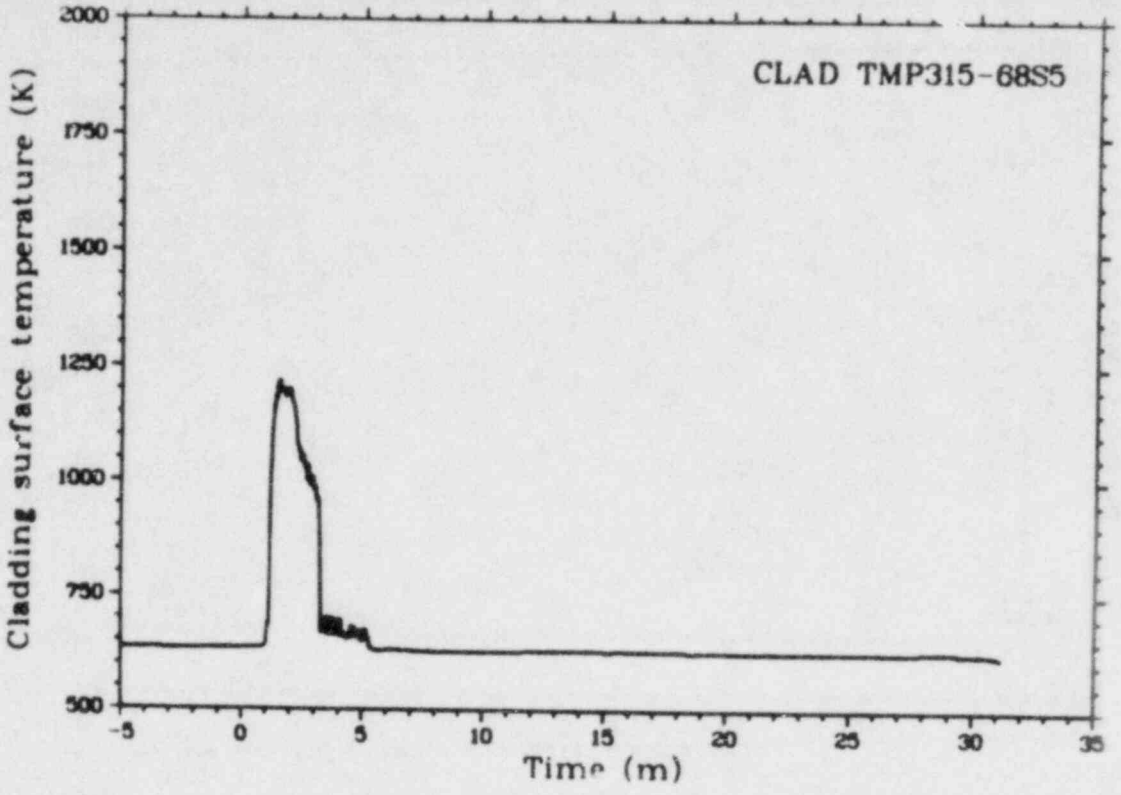
CLAD TMP315-68S5
Cladding surface temperature (K)
2000
1750
1500
1250
1000
750
500
-5
0
5
10
15
20
25
30
35
Time (m)

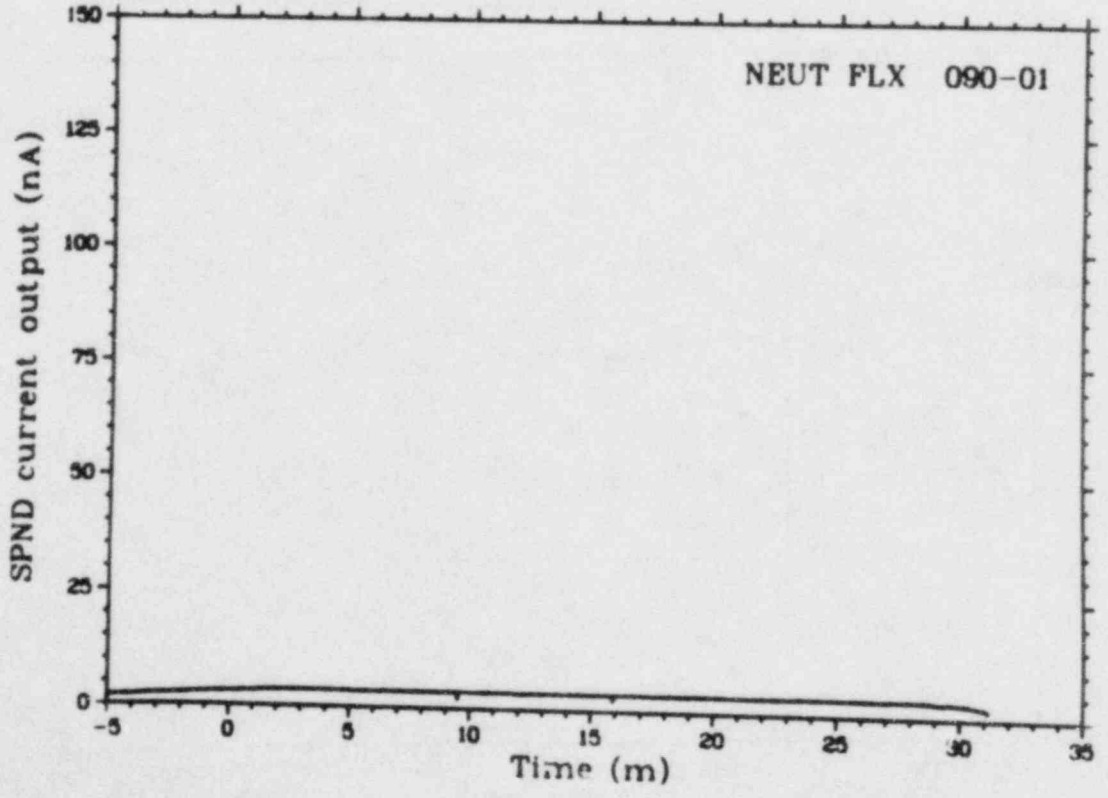
NEUT FLX 090-01
SPND current output (nA)
150
125
100
75
50
25
0
-5
0
5
10
15
20
25
30
35
Time (m)

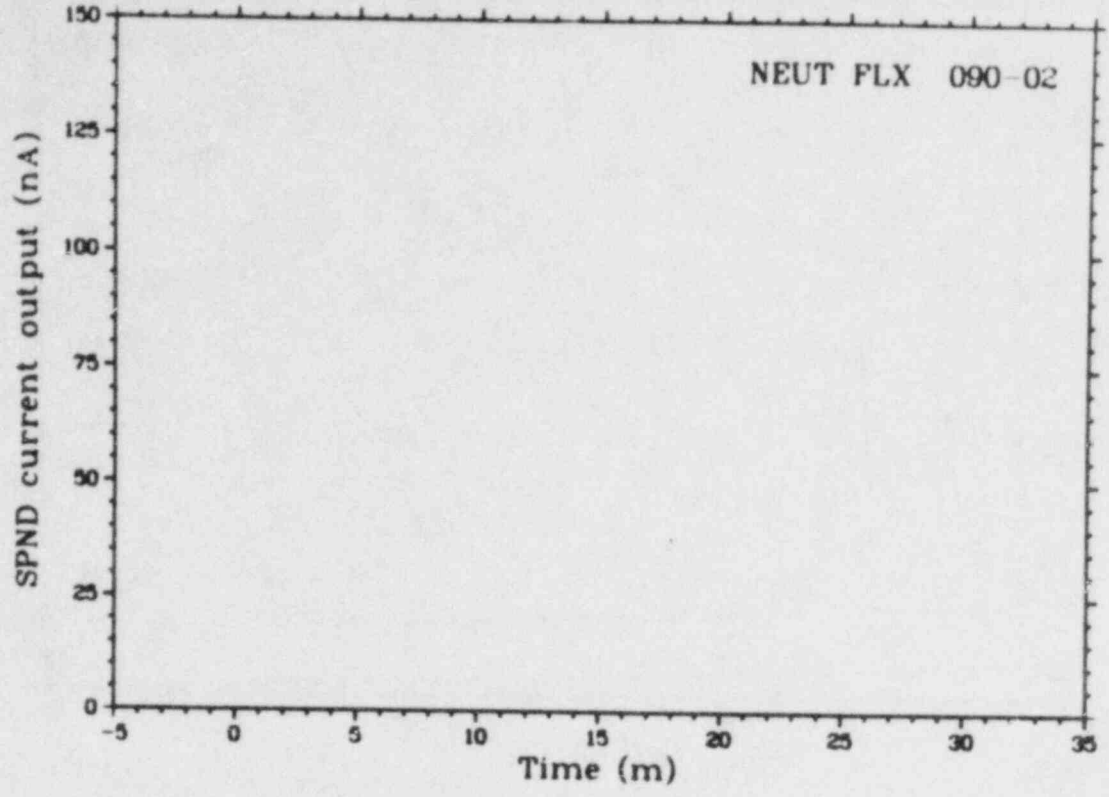
NEUT FLX 090-02
SPND current output (nA)
150
125
100
75
50
25
0
-5
0
5
10
15
20
25
30
35
Time (m)

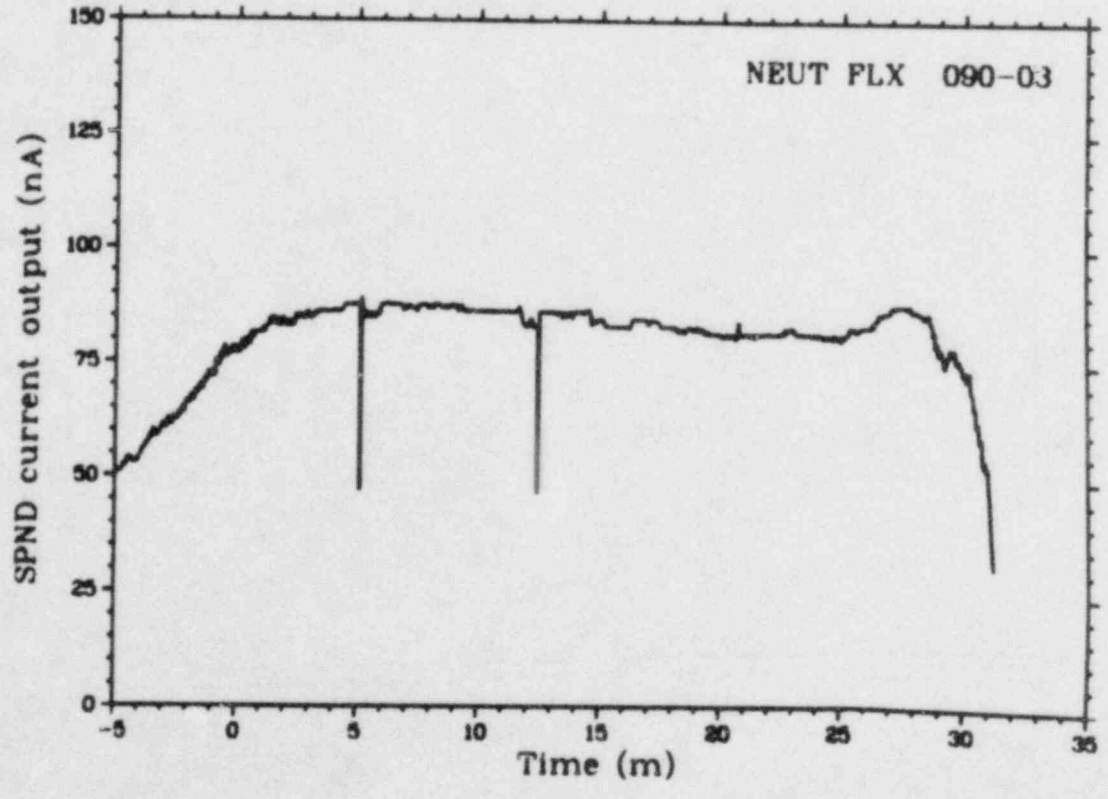
NEUT FLX 090-03
SPND current output (nA)
150
125
100
75
50
25
0
-5
0
5
10
15
20
25
30
35
Time (m)

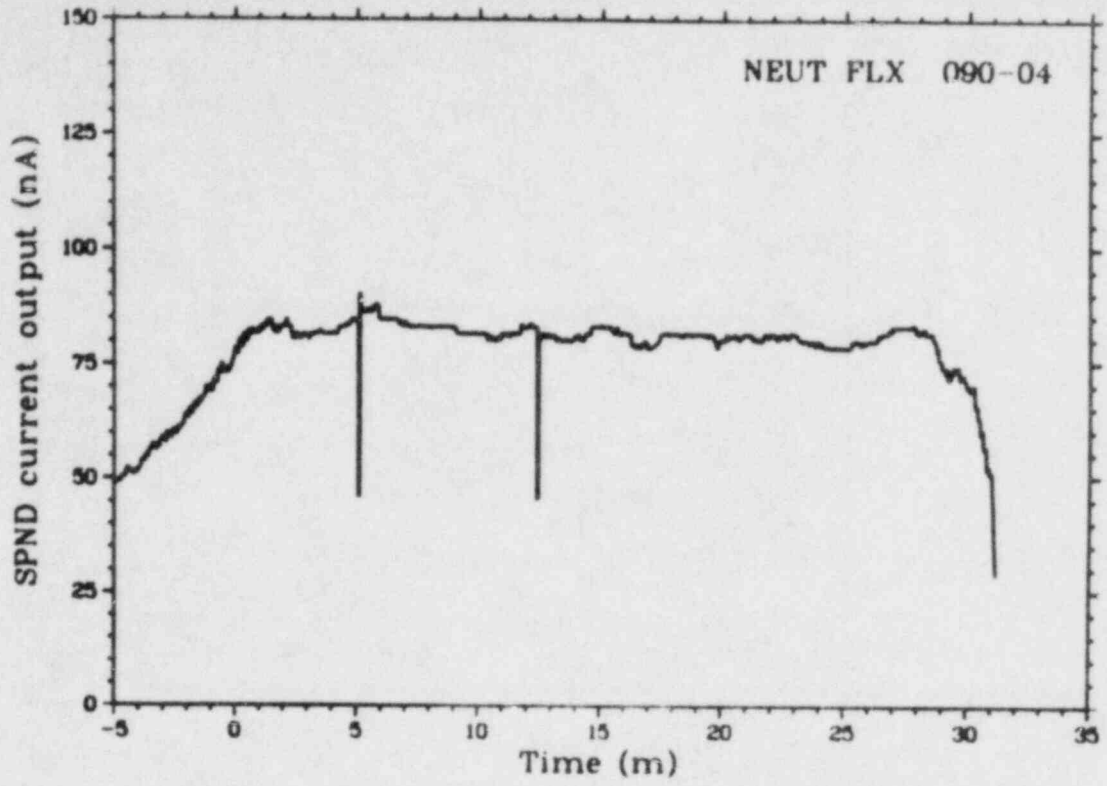
NEUT FLX 090-04
SPND current output (nA)
Time (m)
150
125
100
75
50
25
0
-5
0
5
10
15
20
25
30
35

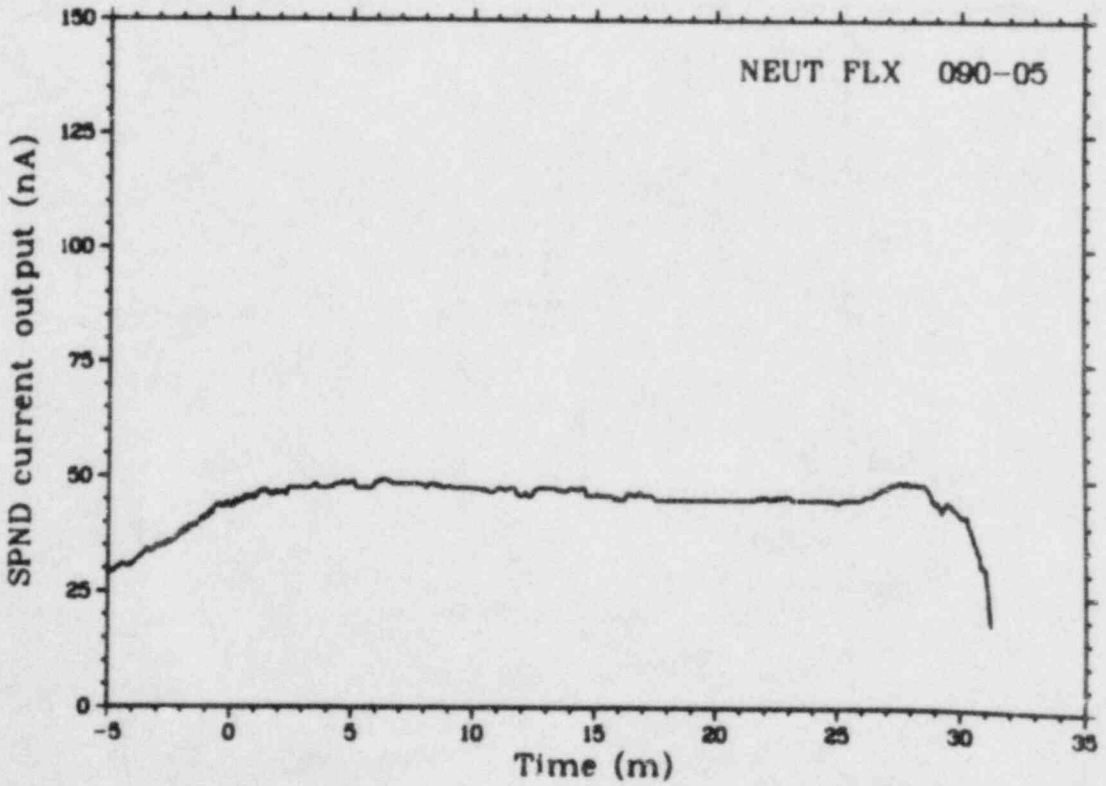
NEUT FLX 090-05
SPND current output (nA)
Time (m)
150
125
100
75
50
25
0
-5
0
5
10
15
20
25
30
35

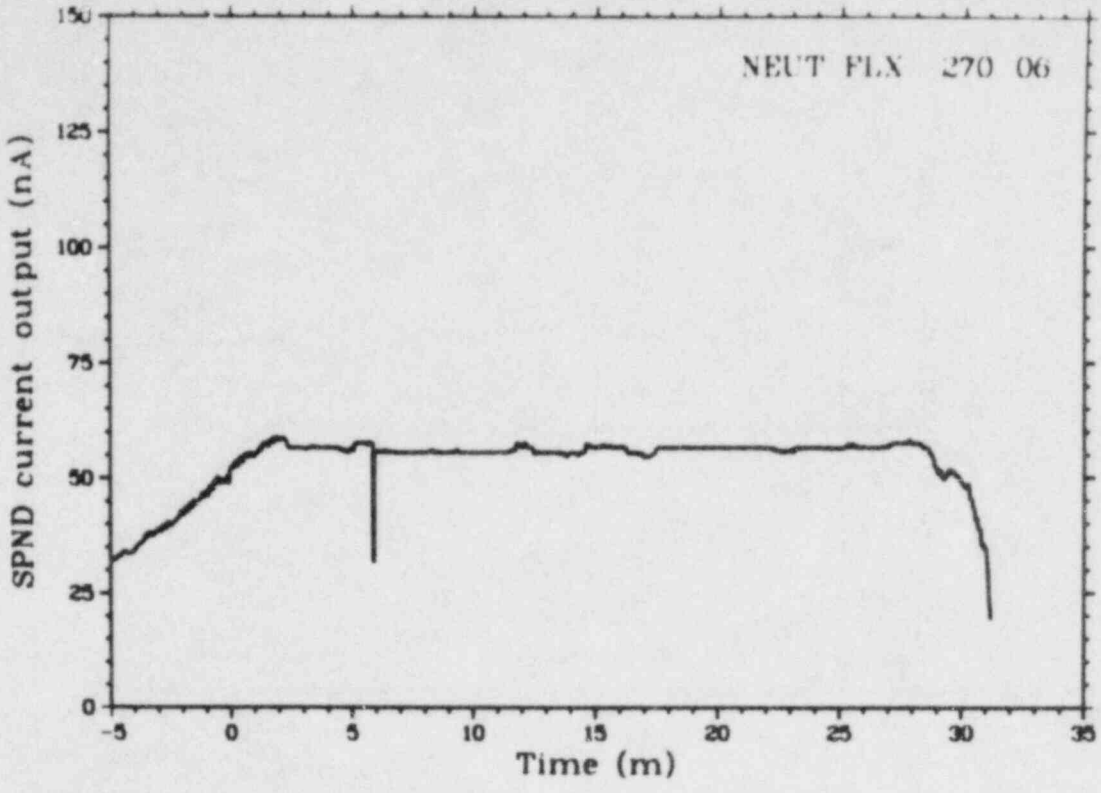
NEUT FLX 270 06
SPND current output (nA)
Time (m)
150
125
100
75
50
25
0
-5
0
5
10
15
20
25
30
35

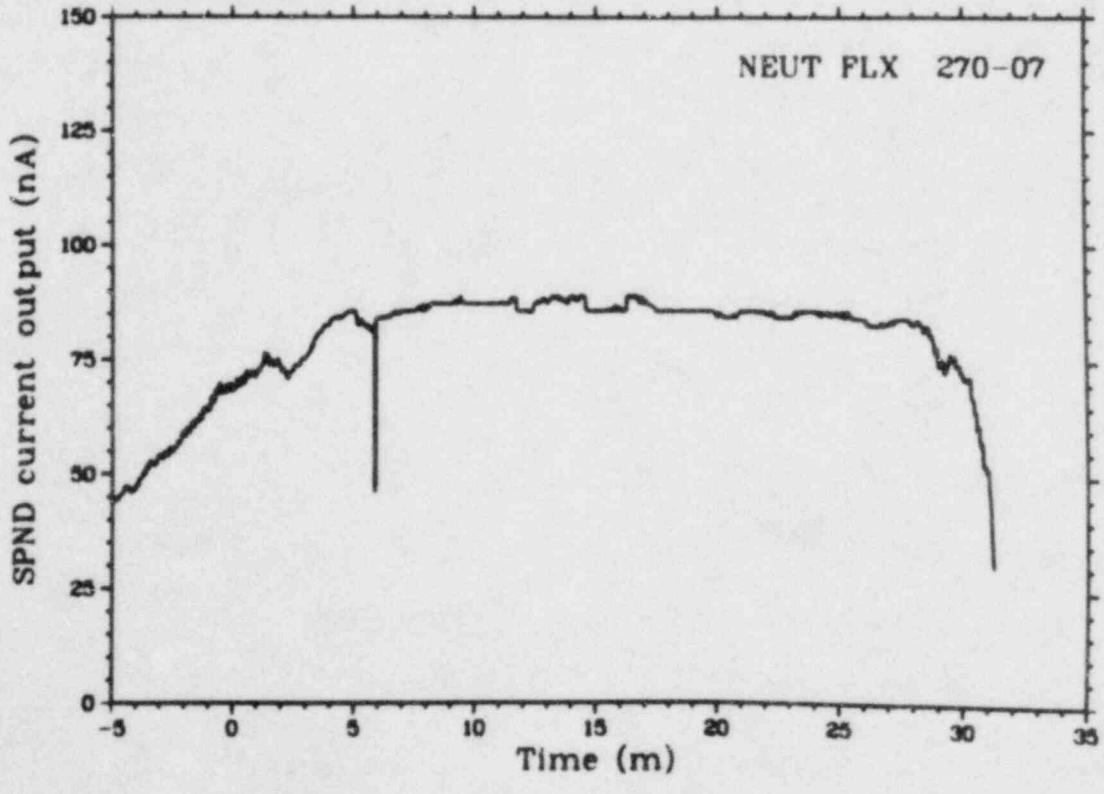
NEUT FLX 270-07
SPND current output (nA)
Time (m)
150
125
100
75
50
25
0
-5
0
5
10
15
20
25
30
35

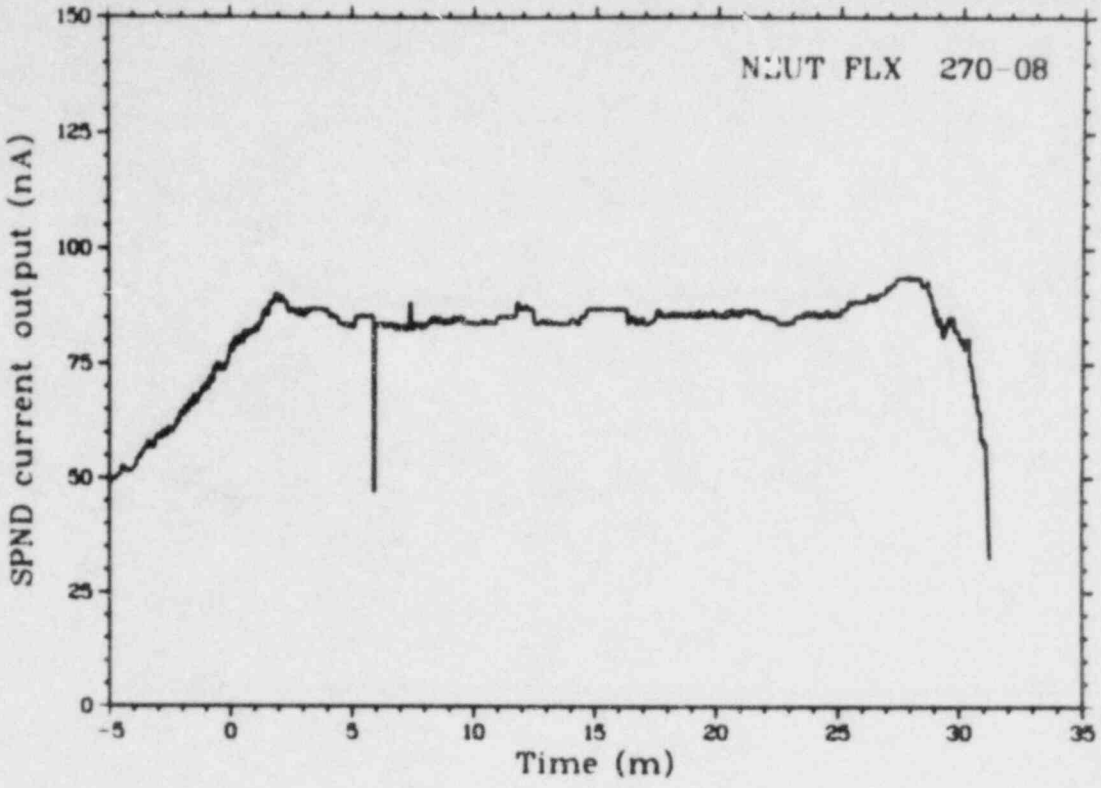
NEUT FLX 270-08
SPND current output (nA)
Time (m)
150
125
100
75
50
25
0
-5
0
5
10
15
20
25
30
35

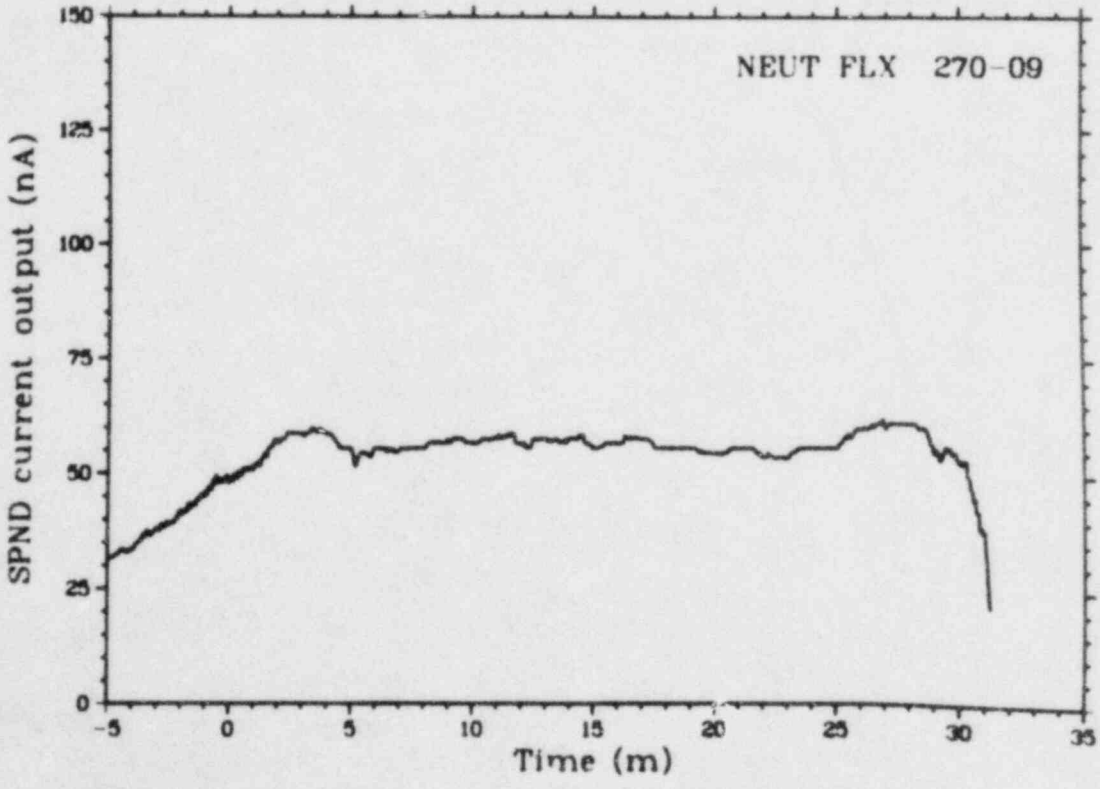
NEUT FLX 270-09
SPND current output (nA)
Time (m)
150
125
100
75
50
25
0
-5
0
5
10
15
20
25
30
35

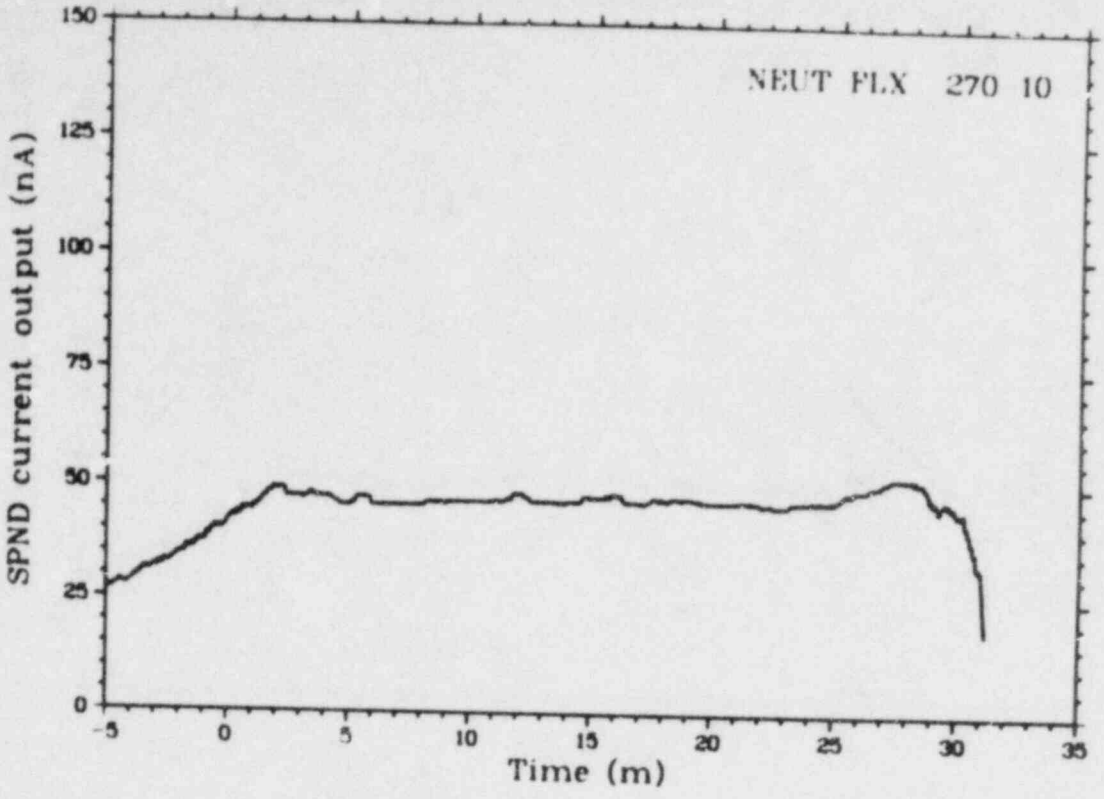
NEUT FLX 270 10
SPND current output (nA)
150
125
100
75
50
25
0
-5
0
5
10
15
20
25
30
35
Time (m)

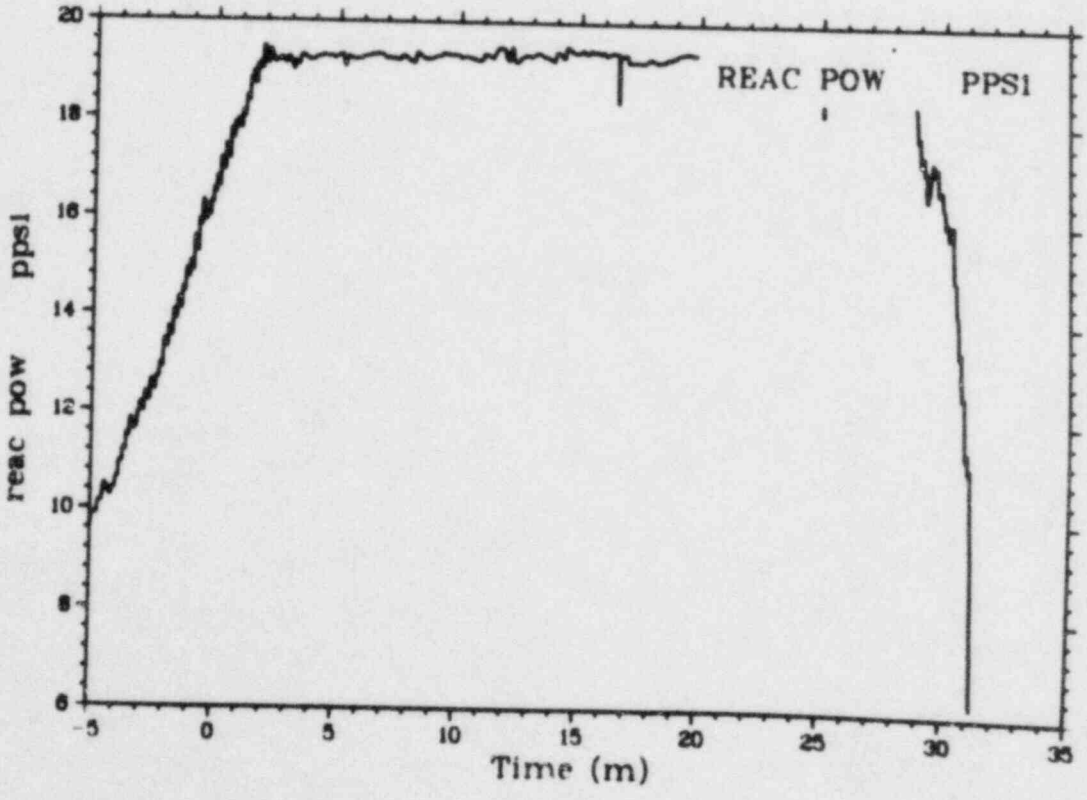
REAC POW PPS1
reac pow ppsl
20
18
16
14
12
10
8
6
-5
0
5
10
15
20
25
30
35
Time (m)

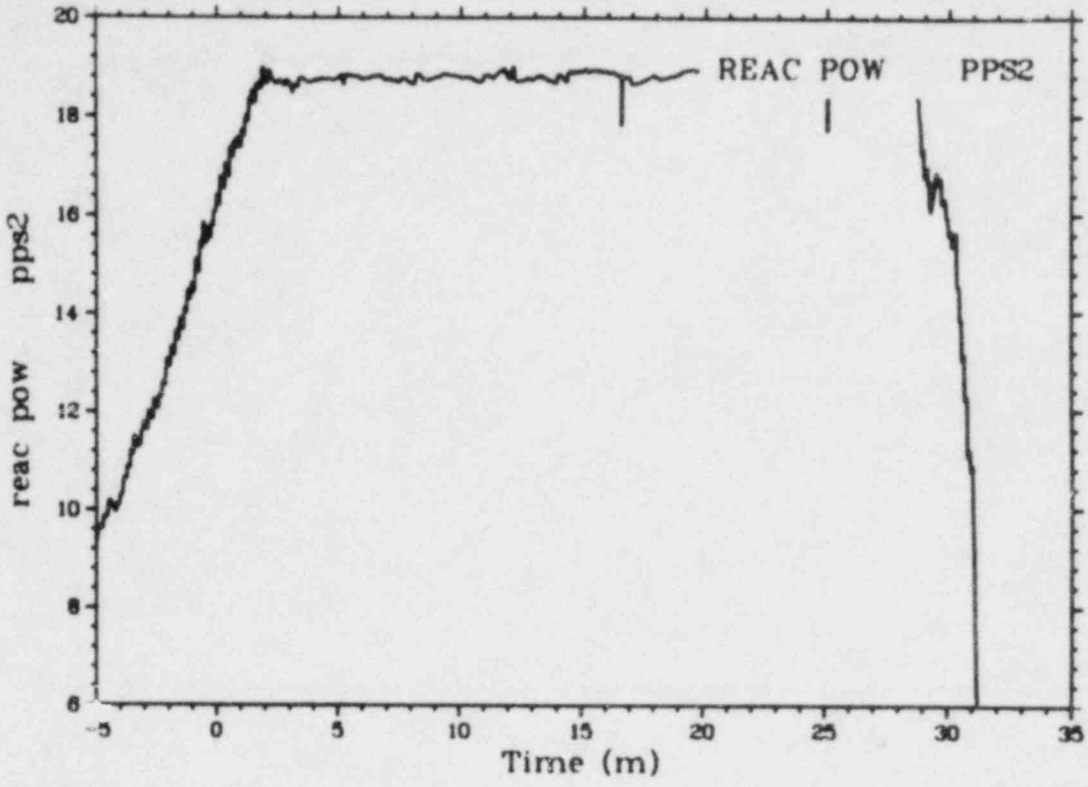
REAC POW
PPS2
reac pow pps2
Time (m)
20
18
16
14
12
10
8
6
-5
0
5
10
15
20
25
30
35